Intracellular Ca^{2+} content and phosphatidylserine exposure in human red blood cells

Kumulative Dissertation
zur Erlangung des Grades
des Doktors der Naturwissenschaften
der Naturwissenschaftlich-Technischen Fakultät III
Chemie, Pharmazie, Bio- und Werkstoffwissenschaften
der Universität des Saarlandes

vorgelegt von
Mauro Carlos Wesseling

Saarbrücken, 2016

Tag des Kolloquiums:	08.08.2016
Dekan:	Prof. Dr. Dirk Bähre
Berichterstatter:	Prof. Dr. Ingolf Bernhardt
	Prof. Dr. Claus Jacob
	Prof. Dr. Florian Lang
Vorsitz:	Prof. Dr. Marc Schneider
Akad. Mitarbeiter:	Dr. Frank Hannemann

Scientific contributions

This work is based on three original research papers reproduced in Chapter 2. The original manuscripts are printed with the kind permission from Cellular Physiology and Biochemistry (Wesseling et al (2016), Wesseling et al (2016), and Nguyen et al (2016)).

2.1 Wesseling et al. 2016a

The author planned and performed most of the experiments in cooperation with Lisa Wagner-Britz and Henry Huppert and wrote the manuscript. The project was supervised by Prof. Dr. Ingolf Bernhardt.

2.2 Wesseling et al. 2016b

The author planed and performed all experiments and wrote the manuscript. The project was supervised by Prof. Dr. Ingolf Bernhardt.

2.3 Nguyen et al. 2016

The author performed the part of the experiments concerning the flow cytometry and fluorescence microscope measurements, as well as some scanning electron microscope and atomic force microscope experiments. Furthermore, the author participated in writing the manuscript. The project was supervised by Prof. Dr. Ingolf Bernhardt.

2.4 Martens et al. 2016

Submitted manuscript to Open Biological Sciences Journal: The author planed and performed all the biological experiments. Furthermore, the author participated in writing the manuscript. The project was supervised by Prof. Dr. Ingolf Bernhardt.

2.5 Wesseling et al. 2016c, to be submitted

The manuscript is in the submission form. It will be submitted to Cellular Physiology and Biochemistry after the final comments of the co-author are obtained: The author planned and performed about half of the experiments, partly in cooperation with Lisa Wagner-Britz. Furthermore, the author wrote part of the manuscript. The project was supervised by Prof. Dr. Ingolf Bernhardt and PD Dr. Lars Kaestner.

2.6 Participation in international meetings with invited talks

19th Meeting of the „European Red Cell Society“ (ERCS), October 2013, IJmuiden, The Netherlands.

20th Meeting of the „European Red Cell Society“ (ERCS), April 2014, Roscoff, France.

Workshop „Living Fluids“, September 2015, Saarbrücken, Germany.

2.7 Participation in international meetings with poster presentation

Conference „Cell Physics“, September 2014, Saarbrücken, Germany.

Concerence of the „Red Cell Club“, October 2015, Yale University, New Haven, USA.

Content

Abstract

Ca^{2+} uptake as well as PS exposure in RBCs has been activated with different substances: lysophosphatidic acid (LPA), phorbol-12 myristate-13 acetate (PMA, activator of the PKC), and A23187 (Ca^{2+} ionophore, used as positive control). Measurement techniques included flow cytometry and live cell imaging (fluorescence or confocal microscopy).

PS exposure is not solely based on the increased intracellular Ca^{2+} content. Ca^{2+} activates the scramblase. In addition, we were able to show that the PKC as well as Ca^{2+}-activated K^+ channel play substantial role in the process of PS exposure.

Ca^{2+} uptake and PS exposure do not depend on the cell age. Quantitative discrepancies with respect to results obtained by different investigators and also with respect to the LPA batches used have been observed. In addition, we realized differences comparing the results of single and double labelling experiments (for Ca^{2+} and PS). The results are also affected by the fluorescent dye used.

The reason for existing RBCs showing PS exposure but without increased Ca^{2+} content is do to cell membrane damage and loss of Ca^{2+} and/or Ca^{2+} with fluorescent dye shortly before eryptosis. RBCs with increased Ca^{2+} content but without PS exposure is probably depending on the cell shape (echinocytes show significantly less PS exposure than discocytes or stomatocytes). This result suggests that the shape of the RBCs plays a substantial role for the PS exposure.

Zusammenfassung

Die Ca^{2+}-Aufnahme und die PS-Exposition in humanen roten Blutzellen (RBCs) wurde durch verschiedene Substanzen aktiviert: Lysophosphatidsäure (LPA), Phorbol-12 myristat-13 acetat (PMA, Aktivator der PKC) und A23187 (Ca^{2+}-Ionophor, Positivkontrolle). Die Messmethoden beinhalteten Durchflusszytometrie und Fluoreszenz- bzw. Konfokal-Mikroskopie.

Die PS-Exposition basiert nicht nur auf einer erhöhten intrazellulären Ca^{2+}-Konzentration. Ca^{2+} aktiviert die Scramblase. Zusätzlich konnten wir zeigen, dass sowohl die PKC als auch der Ca^{2+}-aktivierte K^+ Kanal eine substanzielle Rolle im Prozess der PS-Exposition spielen. Die Ca^{2+}-Aufnahme und die PS-Exposition hängen nicht vom Zellalter ab.

Quantitative Unterschiede von Messdaten, die von unterschiedlichen Experimentatoren und mit unterschiedlichen LPA-Chargen erzielt wurden, konnten erklärt werden. Zusätzlich konnten Unterschiede der Ergebnisse, die auf der Basis von Einzelfärbungs- und Doppelfärbungs-Experimenten (für Ca^{2+} und PS) erzielt wurden, aufgeklärt werden. Die Resultate werden auch durch die verwendeten Fluoreszenzfarbstoffe beeinflusst. Der Grund dafür, dass es einige RBCs gibt, die eine PS-Exposition aber keinen erhöhten Ca^{2+}-Gehalt aufweisen, basiert wahrscheinlich auf einer beginnenden Schädigung der Membran unmittelbar vor der Eryptose, was zu einem Verlust an Ca^{2+} und/oder Ca^{2+} mit Fluoreszenzfarbstoff führt. Die Existenz von RBCs mit erhöhtem Ca^{2+}-Gehalt, aber ohne PS-Exposition, basiert wahrscheinlich auf der Zellform (Echinozyten haben eine geringere PS-Exposition als Discozyten oder Stomatozyten). Dieses Ergebnis deutet darauf hin, dass die Form der RBCs eine substanzielle Rolle für die PS-Exposition spielt.

Abbreviations

APTL	Amino phospholipid translocase (flippase)
ATP	Adenosine triphosphate
DAG	Diacylglycerol
DIDS	4,4’-diisothiocyano-2,2’-stilbenedisulfonic acid
DMSO	Dimethyl sulfoxide
DNA	Deoxyribonucleic acid
EDTA	Ethylenediaminetetraacetic acid
EPO	Erythropoietin
EVs	Extracellular vesicles
FITC	Fluorescein isothiocyanate
G6PD	Glucose-6-phosphate dehydrogenase
HEPES	4-(2-hydroxyethyl)-1-piperazineethanesulfonic acid
LPA	Lysophosphatidic acid
MRP1	Multidrug resistance protein 1
MVs	Microvesicles
NMDA	N-Methyl-D-Aspartat
NSVDC	Non selective voltage dependent cation channel
PC	Phosphatidylcholine
PE	Phosphatidylethanolamine
PGE2	Prostaglandin E2
PI	Phosphatidylinositol
PKC	Protein kinase C
PMA	Phorbol 12-myristate 13-acetate
PS	Phosphatidylserine
RBC	Red blood cell
SCA	Sickle cell anaemia
SM	Sphingomyelin

1. Introduction

1.1 Red blood cells

Erythrocytes, also called red blood cells (RBCs), are by far the main component of human blood cells, with 25 % of the cells [1]. Humans have about 5-6 million RBCs per microliter (µl) of blood [2]. They have a diameter of about 7.5 µm and a thickness of 1.5 to 2 µm and have neither a nucleus nor organelles (mammals mature RBCs) and are unable therefore to synthesize proteins or gain energy from processes in mitochondria. Therefore, the energy demand is met by anaerobic glycolysis. They perform important tasks, such as various transport and regulatory mechanisms. The transport of oxygen (and thus also the CO_2 removal) is one of the main function of RBCs because the oxygen cannot be consumed from the RBCs by themselves. For oxygen transport the RBCs travel large distances, therefore they need to be very flexible and assume different shapes (Fig. 1) [3]. The oxygen is taken to the lungs by binding to haemoglobin, and in turn CO_2 is released [4]. In addition, the RBCs are important for wound healing. The consequent wear requires the degradation of the old, useless cells that achieve a maximum life. This is associated with a permanent new production of young cells [5].

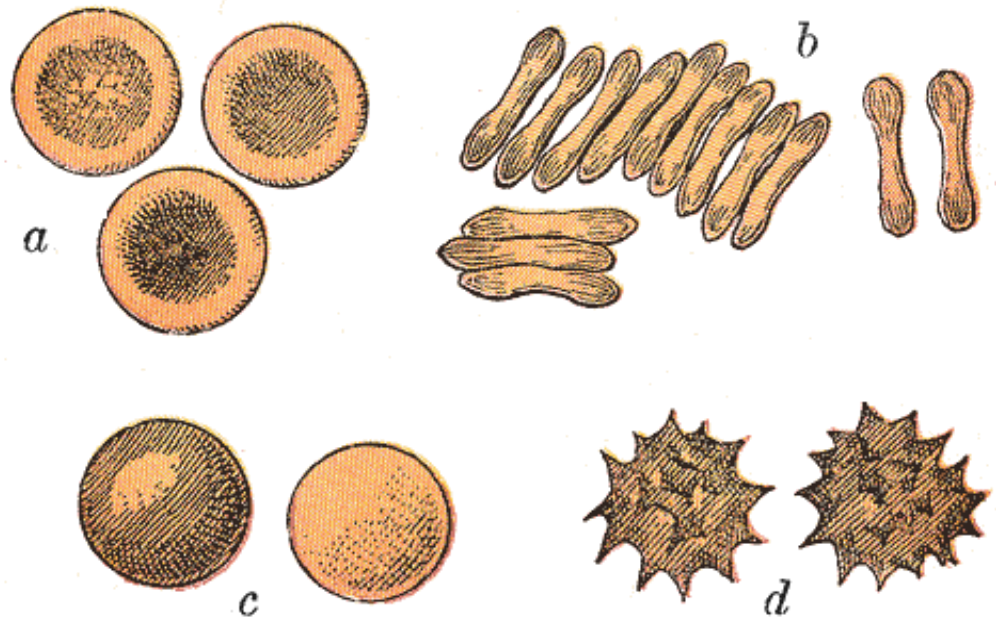

Figure 1: Typical Mammalian RBCs: (a) Seen from surface (b) In profile, forming rouleaux (c) rendered spherical by water (d) rendered crenate by salt. (c) and (d) do not normally occur in the body. Not all cell shapes are shown [3].

The RBC development (erythropoiesis) takes about seven days [6]. It takes place before birth in the yolk sac, liver, spleen and bone marrow, after birth only in the red marrow of the plates and short bone [7]. Initially, by lack of oxygen in the tissues (hypoxia) the kidney stimulates, by the hormone erythropoietin (EPO), the formation of new blood cells in the bone marrow [8]. A disorder of erythropoiesis leads to anaemia. From multipotent stem cells first emerge erythroblasts, which still have a nucleus. They already produce haemoglobin and store this on. After erythroblasts have reduced their nucleus and other organelles with the aid of enzymes, they are called reticulocytes. Reticulocytes migrate into the blood and mingle with the RBCs different cell ages, so that there is an approximate average age of 40 days. Once formed sets with them the aging process that will be affected only by a few factors, such as post-translational modification or mechanical stress. From the age of 7 days they can start carrying oxygen as mature RBCs. The lifespan of the RBCs is about 120 days [5].

1.2 Red blood cell membrane

The membrane of RBCs consists of a lipid bilayer (41 % of lipids) with embedded and superimposed proteins (52 %) and a small carbohydrate moiety (7%) [9]. In healthy cells, the distribution of the phospholipids is asymmetrical between the inner and outer leaflet of the cell membrane. In the inner membrane side are particularly phosphatidylserine (PS) and phosphatidylethanolamine (PE), whereas in the outside are predominantly sphingomyelin (SM) and phosphatidylcholine (PC) (Fig. 2) [10].

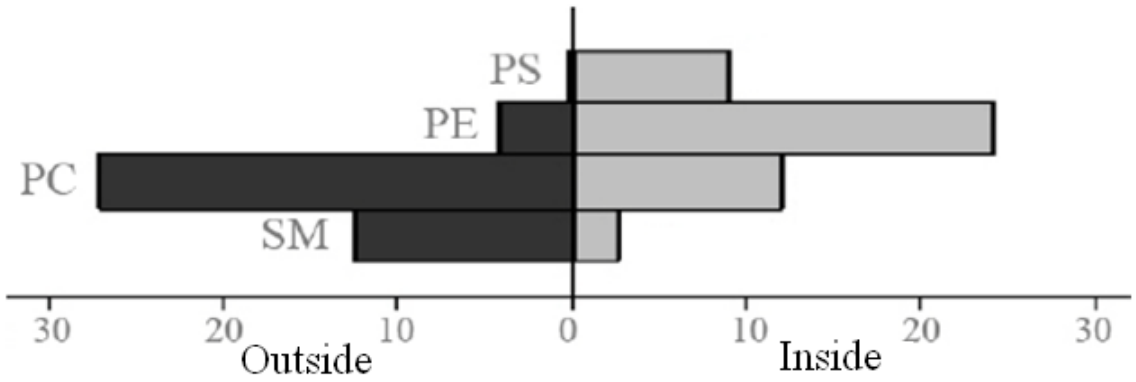

Figure 2: Distribution of the main membrane lipids between the outer and inner membrane leaflet of human RBCs [10].

This asymmetry is maintained by ATP-dependent lipid transporters [11, 12], the flippase also named aminophospholipid translocase (APLT) (transports very quickly PS to the membrane inside, against the concentration gradient and under ATP consumption) and the floppase (transports choline-containing and aminophospholipids of the membrane inside to the membrane outside) (Fig. 3) [13]. The structure and mechanism of the flippase has been published recently by Perez et al. [14]. The floppase belong to the family of ATP-binding cassette proteins (ABC transporters) and were identified as multidrug resistance protein 1 (MRP1) [15].

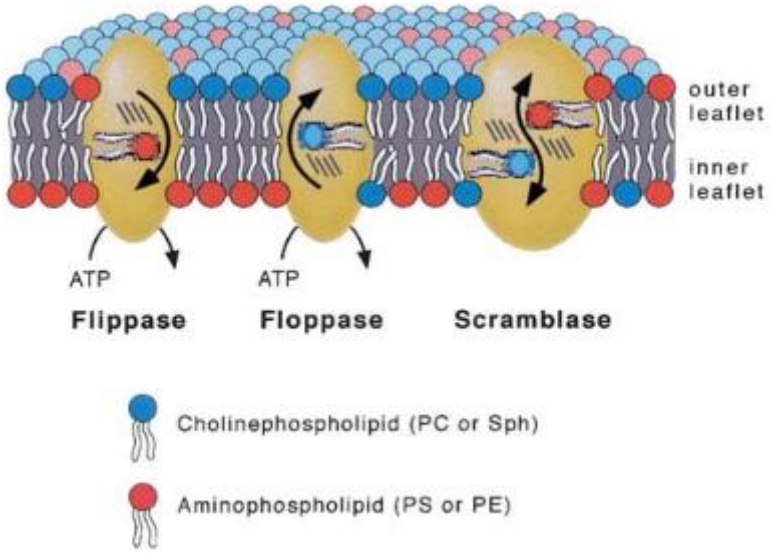

Figure 3: Transporter-controlled exchange of phospholipids between both lipid leaflets of the cell membrane. Unidirectional phospholipid transport by flippase is directed inward, whereas floppase promotes outward directed transport. Both transporters are ATP-dependent and frequently move phospholipids against their respective concentration gradients. Bidirectional phospholipid transport is catalyzed by a scramblase, activation of which may occur following Ca^{2+} influx or when cells go into apoptosis. Scramblase promotes collapse of membrane phospholipid asymmetry with appearance of PS at the cells' outer surface [13].

The asymmetric organization is important for cell functions such as cell signalling. After about 120 days, RBCs undergo eryptosis, an apoptosis-like process (a term introduced by Lang [16]), defining the suicidal death of RBCs. By stimulating the eryptosis in RBCs by an increase in intracellular Ca^{2+} levels, the lipid asymmetry may collapse. The signal of eryptosis is the movement of PS from the inner to the outer membrane leaflet [16, 17]. The aforementioned lipid transporters (flippase, floppase) are inhibited by Ca^{2+} [11]. Another consequence of the increased intracellular Ca^{2+} content is the outward-directed

transport of PS, realized by a protein termed “scramblase” [18-22]. This can lead to a stimulation of blood coagulation [23]. The identity of this protein has been identified only recently as a member of the TMEM16 or anoctamin family of proteins and the crystal structure was published [24]. The balance between lipid transporters and scramblase is crucial if a PS exposure at the outer membrane leaflet occurs [25].

1.3 Membrane transport

Proteins are responsible for a large part of the dynamic processes that occur on membranes (solute and ion transport, signal transduction, cell-cell contact, anchoring the cytoskeleton etc.). Membrane proteins in RBCs are expressed in early stage of cell maturation. Later on, they can be modified only by posttranslational modifications. Because the cell membrane is impermeable for big molecules (like glucose, sucrose) and charged ions and molecules (Na^+, K^+, Ca^{2+}, Cl^-), this substances must be transported through the membrane by special transporters. A distinction is made between simple electro-diffusion (residual or leak transport) and three different transport mechanisms. Possible transport mechanisms are: active transport (pumps), transport through channels, and carrier-mediated transport. A review on cation transport mechanisms in RBC membranes can be found in Bernhardt [26].

Important for the present work are ion channels, which are formed by protein subunits. In general, ion channels are more or less selective (they have a selectivity filter) and they posses a mechanism for opening and closing (gating mechanism). They allow the flow of ions along their electrochemical gradient. Their regulation (opening and closing) occur by one of four different possibilities: Regulation via (i) membrane potential, (ii) specific substances including Ca^{2+}, (iii) mechanical forces or stress, and (iv) light [26]. In human RBCs the following cation channels have been detected so far: Ca^{2+}-activated K^+ channel (Gardos channel) [27], non-selective voltage-dependent cation (NSVDC) channel [28-31], low conductance cation channel [32] (it is not even clear whether it is a substate of channels mentioned before, or if it has its own identity; no molecular date are available yet [33]), receptor-activated non-selective cation channel [34, 35], TRP C6 channel [36], NMDA-channel [37, 38], P-Type $Ca_V2.1$ [39, 40] channel. It has been speculated that the $Ca_V2.1$ is identical to the NSVDC channel [33]. From the electrophysiological

characterisation it is very hard to compare the data of the NSVDC channel in RBCs to the $Ca_V2.1$ channel since the channel properties are differentially affected by the co-expression level of particular ß-subunits as well as by alternative splicing of the α_{1A}-subunit [33]. There are also several anion channels present in the human RBC membrane, like the small conductance chloride channel and the voltage-dependent anion channel (VDAC) [41]. However, anion channels are not in the focus of the present work. A summary is given in the paper of Thomas et al., [41].

1.4 Signal cascade to induce phosphatidylserine exposure and the active participation of red blood cells in thrombus formation

Thrombus formation in consequence of an injury of the blood vessels is an essential and vital process, which can be found in all vertebrates. Formation and degradation of the thrombus constitute the protective mechanism which protects living beings against excessive blood loss. The process of wound healing by an injury in or on the body begins with the closure of the wound. Through an injury, blood flows out and the wound is closed by using the platelets, which release among other thrombin, which cleaves fibrinogen into fibrin and thus crucial contributes to the formation of a thrombus [42]. This process starts as soon as the surrounding tissue of the damaged blood vessel comes into contact with blood. On the other hand, the formation of blood clots may also be pathological. If it comes to the development of thrombosis (narrowing / blockage of a blood vessel by a thrombus), pulmonary embolism, heart attack and stroke may be the consequence [43-47]. For some time the role of RBCs in the thrombus formation has been discussed. In older literature, the RBCs were long considered only as passive oxygen transporters and also to serve as a buffering of the blood. The participation in thrombus formation has been described as a pure passive process which occurs coincidentally (RBCs attain into a thrombus only because of their large number) [48]. However, recent results suggested that RBCs not just adhere in the thrombus (in the fibrin network), but also play thereby an active role [42, 49] and certainly have a prothrombotic effect [50, 51].

In healthy cells, the distribution of the phospholipids is asymmetrical between the inner and outer side of the cell membrane (as explained in the previous section). Substances released from platelets, such as e.g. prostaglandin E_2 (PGE_2) and lysophosphatidic acid

(LPA) activate in RBCs a signalling cascade that leads to an increase in the intracellular Ca^{2+} concentration [34, 52]. The Ca^{2+}-activated protein scramblase then causes redistribution of the membrane lipids whereby the PS is moved from the inner to the outer membrane leaflet [12, 13, 16-19]. The exposure of PS forms a catalytic surface that promotes the blood clotting [50-53]. This contributes to increased intercellular adhesion and also serves as recognition side for macrophages, which can remove the RBCs from the blood stream [54-56]. After a Ca^{2+} uptake, the Gardos channel is simultaneously activated [57], which leads to an efflux of K^+ and Cl^-, and osmotically obliged H_2O loss, whereby the cells shrink. It has been assumed that possibly the interaction surface is increased for the adhesion process of the RBCs [9, 18, 52]. It has been demonstrated that PS exposure induced by LPA leads to cell-cell adhesion of human RBCs [52, 58]. Based on a correlation between decreased haematocrit and longer bleeding times [46] and experiments carried out by Andrews and Low [49], an active role of RBCs in thrombus formation has been proposed [49]. A detailed signalling cascade was published by Kaestner et al. [35]. A Ca^{2+}-independent pathway for PS exposure has been proposed by Chung et al. [51]. They demonstrated that LPA-induced activation of protein kinase Cζ (PKCζ, a Ca^{2+}-independent isoform of PKC present in human RBCs) leads to the exposure of PS even in the absence of Ca^{2+}.

Another possibility for the enhancement of the intracellular Ca^{2+} content is the activation of PKCα (a Ca^{2+}-dependent isoform of PKC present in human RBCs) by phorbol-12 myristate-13 acetate (PMA) leading to two independent Ca^{2+} entry processes [40]. The first is P-Type $Ca_V2.1$ channel independent and the second is associated with a likely indirect activation of $Ca_V2.1$ [40]. It leads to a secondary Ca^{2+} influx into RBCs. PMA is a powerful pharmacological tool that activates PKCα in terms of translocation from the cytosol to the plasma membrane. Once at the membrane, it can bind PS and moves to the outer membrane leaflet [19].

In addition, PS exposure in the outer membrane leaflet of the RBCs membrane is of importance for the adhesion of RBCs to the endothelium in certain diseases such as sickle cell disease, malaria, β-thalassemia, and diabetes (e.g. [59-63]). These diseases are either caused or complicated by the transition through Ca^{2+} induced, coupled with PS exposure, exchange between non-adherent to adherent state of RBCs [25, 64, 65]. It is of particular interest for thrombus formation. How exactly the complete process looks like, however, is not yet fully known.

1.5 Vesicle formation

Under stimulating conditions (e.g. with LPA or PMA), together with the PS exposure also a formation and release of vesicles has been observed in human RBCs [66]. Extracellular vesicles (EVs) are spherical fragments of cell membrane released from various cell types under physiological as well as pathological conditions. Based on their size and origin, EVs are classified as exosome, microvesicles (MVs) and apoptotic bodies [67]. The formation of the vesicles increases with increasing Ca^{2+} content of the cells [68].

Exosomes are small enclosed membrane vesicles of nearly uniform size from 30 to 100 nm already described by Johnstone during the *in vitro* culture of sheep reticulocytes [69]. They were also observed in a variety of cultured cells such as lymphocytes, dendritic cells, cytotoxic T cells, mast cells, neurons, oligodendrocytes, Schwann cells, and intestinal epithelial cells [70, 71]. In these cells, exosomes originate from the endosomal network that locates within large sacs in the cytoplasm. The release of exosomes to extracellular environment is carried out by the fusion of these sacs to the plasma membrane [70, 72, 73].

Recently, the release of MVs from human RBCs under different conditions has been reported [69]. Distinct from exosomes, the biogenesis of MVs arises through direct outward budding and fission of the plasma membrane following different kinds of cell activation or during early state of apoptosis [74]. Normally, MVs are larger compared to exosomes with size ranging from 50 to 1000 nm [74-76]. However, there is an overlapping of the size between exosomes and MVs. So far the mechanism of biogenesis is primarily used to distinguish MVs and exosomes [67, 75]. The formation and release of MVs is the result of dynamic processes of phospholipid redistribution and cytoskeletal protein breakdown [67].

A vast amount of literature dealing with the release mechanism of MVs in RBCs and their properties in response to A23187, ATP depletion, oxidative stress and storage has been reported (e.g. [77-83]). In addition, an increase of the levels of RBC-derived MVs in the circulating blood of patients with sickle cell anemia (SCA), thalassemia and glucose-6-phosphate-deficiency (G6PD) has been observed [84, 85]. Morphological transitions of RBCs stimulated by exogenous compounds, according to the bilayer-couple hypothesis, also result in the formation of MVs [78, 81, 86]. Furthermore, the reorganization of the

cell membrane such as loss of asymmetrical membrane phospholipid distribution leads to membrane blebbing and formation of MVs [87-90]. Recently, several studies have shown that an increase of the intracellular Ca^{2+} concentration by opening Ca^{2+} channels or activation of PKC leads to PS exposure and formation of MVs in many different cell types including human RBCs [40, 52, 88, 89].

In contrast, apoptotic bodies have been characterized as largest EVs with the size varying from 1 to 5 μm. Nucleated cells undergoing apoptosis pass through several stages, beginning with condensation of the nuclear chromatin, followed by membrane blebbing, and finally releasing EVs and apoptotic bodies [67]. However apoptotic cells are also known to release smaller vesicles (MV) in response to apoptosis induction and these MVs are known to stimulate innate immune responses [91]. Although mature human RBCs have no nucleus and organelles, however, they are able to undergo an apoptosis-like process (eryptosis, see above) with similar characteristics, e.g. membrane blebbing and formation of MVs [87, 88].

Although there is a number of reports about the formation of MVs in RBCs, investigations of the kinetics of this process as well the characterization of released MVs are still limited. By using different methods and techniques we investigated the kinetics of formation of MVs. In addition, the MVs released from human RBCs under different conditions were also isolated and characterized.

1.6 Correlation between increased intracellular Ca^{2+} content and phosphatidylserine exposure in human red blood cells

The Ca^{2+} influx in RBCs can be stimulated by various substances such as PGE2, LPA [52], or PMA [92], resulting in activation of the protein scramblase. This in turn leads to an increased PS exposure (see session 1.4). A further consequence of the Ca^{2+} influx is the activation of PKCα, which can phosphorylate other proteins [94]. Experiments show that Ca^{2+} influx and PS exposure are closely linked to protein phosphorylation and dephosphorylation [92]. The diacylglycerol (DAG), a PMA analogue, can activate the PKC in RBCs and cause its translocation from the cytosol to the cell membrane. Once at the membrane, it can bind DAG and PS and moves to the outer membrane leaflet [19]. Another, Ca^{2+}-independent, activation mechanism of the scramblase has been discussed

[51]. However, activation by LPA or PMA does not lead to the reaction of all RBCs. Two subpopulations can be detected, a reactive (with increased intracellular Ca^{2+} content) and a non-reactive (with no significant change of the intracellular Ca^{2+} content) [40]. Another way to increase the intracellular Ca^{2+} content in RBCs is given by the Ca^{2+} ionophore A23187. The ionophore A23187 does not activate proteins directly [94], but generate pores in the cell membrane. Ca^{2+} can flow into the cells through the pores. Thereby almost all RBCs have an increase in the intracellular Ca^{2+} content and thus serve as a positive control.

Inhibition of PKC by chelerythrine chloride results in a decreased Ca^{2+} influx after PMA stimulation [39]. Conversely, De Jong et al. [17] showed that the inhibition of PKC has no effect on the Ca^{2+} influx. Another way of increasing the intracellular Ca^{2+} concentration in RBCs doesn't exists since RBCs have no intracellular Ca^{2+} stores [39].

New results showed that the PS exposure on the outer side of the membrane and the Ca^{2+} influx do not always correlate [90]. In fluorescence microscopy experiments RBCs with increased PS exposure and very low intracellular Ca^{2+} content and *vice versa* RBCs with high intracellular Ca^{2+} content but without PS exposure could be visualized (Fig. 4).

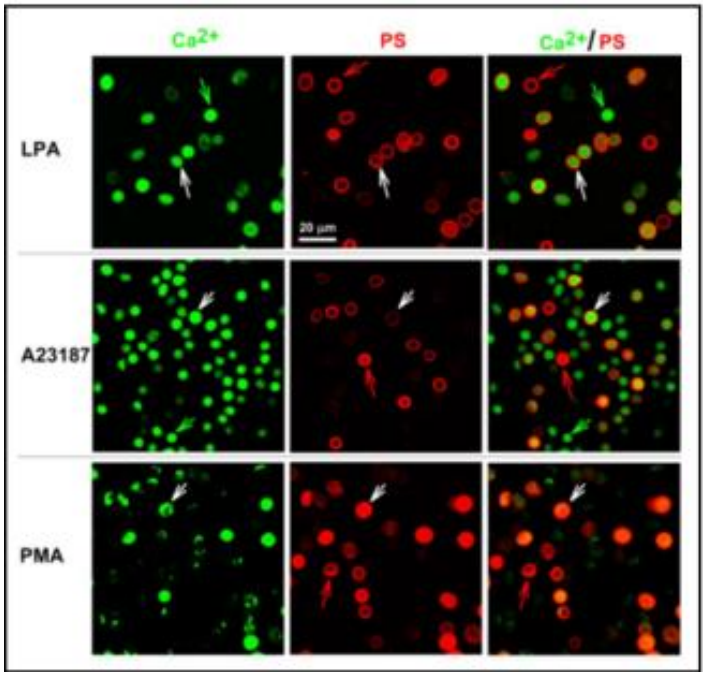

Figure 4: Human RBCs with fluo-4 and annexin V-Alexa double staining 568 after stimulation of a Ca^{2+} influx with 2.5 µM LPA, 2 µM A23187 or 6 µM PMA. White arrows indicate cells with increased intracellular Ca^{2+} and PS exposure, green arrows cells with increased Ca^{2+} concentration without PS exposure and red arrows cells with only PS exposure [89].

This finding raises the question of whether an increased Ca^{2+} content is essential for PS exposure, and/or whether a Ca^{2+} influx is the only factor responsible for the lipid redistribution (PS exposure). However, the kinetic of the two processes are unclear. The Ca^{2+}-dependent signalling pathways, and the externalization of PS, play a crucial role in eryptosis, haemolysis, as well as the active participation of RBCs in the thrombus formation. The contributing mechanisms are only partly understood and further research may lead to improved therapies for many diseases and for more effective storage of blood.

1.7 Red blood cell shape transformation

RBCs are primarily responsible for the gas exchange in the body. They transport O_2 from the lungs to the peripheral tissues and CO_2 from there to the lungs. The RBCs have to pass through capillaries, whose diameter is smaller than that of the RBCs themselves (7.5 µm) [3]. Therefore, the necessary deformability is ensured by the absence of organelles and a flexible plasma membrane. These properties allow the RBCs to take several different cell shapes. Starting from the classical biconcave discocyte shape, the RBCs are able to transform to either, echinocyte or stomatocyte shapes (see session 1.1), depending on a large variety of membrane and cytoplasmatic parameters [95-97]. The classical theory explaining the RBC shape is based on the bilayer-coupled hypothesis developed by Sheetz and Singer [86]. Changes of the membrane curvature (i.e. cell shape) are based on an expansion of the inner or outer membrane leaflet relative to the other one, since the two leaflets cannot separate from each other due to their coupling by hydrophobic interactions [86].

It has been demonstrated that an expansion of one of the leaflets can occur after the transversal redistribution of the membrane phospholipids or after an insertion of amphiphilic compounds intro the membrane. Both processes needs at least several minutes. On the other hand, a quickly transformation can occur due to conformational changes of integral membrane proteins. Such a process happens in a few seconds [97]. Echinocytosis can be induced by outer lipid leaflet expansion [97, 99] or inner leaflet contraction [97-100].

1.8 Aims and scope

In this work the influence of Ca^{2+} uptake with respect to the PS exposure of human RBCs has been investigated. Ca^{2+} uptake as well PS exposure in RBCs were activated with different stimulating substances (LPA, activator of the NSVDC channel), PMA (activator of the PKC) and A23187 (Ca^{2+} ionophore, used as a positive control). The experiments were carried out using a flow cytometer and a fluorescence microscope (in some cases also a confocal microscope).

The first question of the present work was to investigate some methodological issues. This is based on the findings that quantitative discrepancies with respect to results obtained by different investigators and also with respect to the LPA batches used have been observed. In addition, we realized differences comparing the results of single and double labelling experiments (for Ca^{2+} and PS). For this reason, single and double labelling experiments using a verity of fluorescent dyes were carried out to understand the challenge and to be able to compare results obtained by different research groups.

Another fundamental question was to study whether an increased Ca^{2+} content is solely the cause of PS exposure. It was also necessary to investigate the participation of the Ca^{2+} activated K^{+} channel in the PS exposure. Furthermore, it has to be clarified why exist some RBCs with increased intracellular Ca^{2+} content but no PS exposure and *vice versa* some RBCs showing PS exposure but no increased intracellular Ca^{2+} content.

To investigate this effect, RBCs separated by age were analyzed. In addition, the shape of the RBCs has to be taken into consideration.

2. Publication of the results

The results of this work here published in the articles listed below:

2.1 Phosphatidylserine exposure in human red blood cells depending on cell age
Mauro C. Wesseling, Lisa Wagner-Britz, Henri Huppert, Benjamin Hanf, Laura Hertz, Duc Bach Nguyen, Ingolf Bernhardt

2.2 Measurements of intracellular Ca^{2+} content and phosphatidylserine exposure in human red blood cells: Methodological issues
Mauro C. Wesseling, Lisa Wagner-Britz, Fatima Boukhdoud, Salome Asanidze, Duc Bach Nguyen, Lars Kaestner, Ingolf Bernhardt

2.3 Characterization of microvesicles released from human red blood cells
Duc Bach Nguyen, Thi Bich Thuy Ly, Mauro Carlos Wesseling, Marius Hittinger, Afra Torge, Andrew Devitt, Yvonne Perrie, Ingolf Bernhardt

2.4 Robust automated image analysis of activated red blood cells
Jan Martens, Mauro Carlos Wesseling, Joachim Weickert, Ingolf Bernhardt

2.5 Phosphatidylserine exposure in human red blood cells: Role of scramblase, protein kinase C, Gardos channel, and cell volume
Mauro C. Wesseling, Lisa Wagner-Britz, Nguyen Duc Bach, Salome Asanidze, Judy Mutua, Nagla Mohamed, Mira Türknetz, Benjamin Hanf, Mehrdad Ghashghaeinia, Lars Kaestner, Ingolf Bernhardt

2.1 Phosphatidylserine exposure in human red blood cells depending on cell age

Mauro C. Wesseling, Lisa Wagner-Britz, Henri Huppert, Benjamin Hanf, Laura Hertz, Duc Bach Nguyen, Ingolf Bernhardt

Cell Physiol Biochem, 2016 Mar, 38, 1376-1390
DOI: 10.1159/000443081

Cellular Physiology and Biochemistry

Cell Physiol Biochem 2016;38:1376-1390
DOI: 10.1159/000443081
Published online: March 24, 2016
Accepted: March 07, 2016

1421-9778/16/0384-1376$39.50/0
www.karger.com/cpb

Original Paper

Phosphatidylserine Exposure in Human Red Blood Cells Depending on Cell Age

Mauro C. Wesseling[a] Lisa Wagner-Britz[a] Henri Huppert[a] Benjamin Hanf[a]
Laura Hertz[a] Duc Bach Nguyen[b] Ingolf Bernhardt[a]

[a]Laboratory of Biophysics, Faculty of Natural and Technical Sciences III, Saarland University, Campus, Saarbrücken, Germany; [b]Department of Molecular Biology, Faculty of Biotechnology, Vietnam National University of Agriculture, Ngo Xuan Quang, Gia Lam, Hanoi, Vietnam

Key Words
Red blood cells • Red blood cell age • Ca^{2+} content • Phosphatidylserine exposure • Lysophosphatidic acid • Phorbol-12 myristate-13 acetate • Flow cytometry • Fluorescence imaging

Abstract
Background/Aims: The exposure of phosphatidylserine (PS) on the outer membrane leaflet of red blood cells (RBCs) serves as a signal for suicidal erythrocyte death or eryptosis, which may be of importance for cell clearance from blood circulation. PS externalisation is realised by the scramblase activated by an increase of intracellular Ca^{2+} content. It has been described in literature that RBCs show an increased intracellular Ca^{2+} content as well as PS exposure when becoming aged up to 120 days (which is their life span). However, these investigations were carried out after incubation of the RBCs for 48 h. The aim of this study was to investigate this effect after short-time incubation using a variety of stimulating substances for Ca^{2+} uptake and PS exposure. ***Methods:*** We separated RBCs by age in five different fractions by centrifugation using Percoll density gradient. The intracellular Ca^{2+} content and the PS exposure of RBCs with different age has been investigated after treatment with lysophosphatidic acid (LPA) as well as after activation of protein kinase C (PKC) using phorbol-12 myristate-13 acetate (PMA). For positive control RBCs were treated with 4-bromo-A23187. Measurement techniques included flow cytometry and live cell imaging (fluorescence microscopy). ***Results:*** The percentage of RBCs showing increased Ca^{2+} content as well as the PS exposure did not change significantly in dependence on cell age after short-time incubation in control experiments (without stimulating substances) or using LPA or PMA. However, we confirm findings reported that Ca^{2+} content and the PS exposure of RBCs increased after 48 h incubation. ***Conclusion:*** No significant differences of intracellular Ca^{2+} content and PS exposure can be seen for RBCs of different age in resting state or after stimulation of Ca^{2+} uptake at short-time incubation.

M.C. Wesseling and L. Wagner-Britz contributed equally.

Ingolf Bernhardt
Laboratory of Biophysics, Faculty of Natural and Technical Sciences III,
Saarland University, Campus, 66123 Saarbrücken (Germany)
Tel. +49 681 3026689, Fax +49 681 3026690, E-Mail i.bernhardt@mx.uni-saarland.de

KARGER

Introduction

In a population of human red blood cells (RBCs) one can find cells with different age. They have a life span of about 120 days. Depending on age, their density is different. Young cells have a lower density in comparison to old cells [1]. This makes it possible to separate them into fractions with different ages by density gradient centrifugation using Percoll [2, 3]. Which factors are crucial for the aging process and the mechanisms for the removal of damaged or old RBCs from the blood stream is not yet fully understood. It has been described that older RBCs have a higher intracellular Ca^{2+} content [4, 5] leading to an activation of the scramblase, which in turn results in a significant exposure of phosphatidylserine (PS) in the outer membrane leaflet [6-8]. However, the data of Romero and Romero [4] are in our opinion not completely reliable since they are based on fluorescence measurements using fura-2. It has been demonstrated that the fluorescence dye fura-2 is not applicable for Ca^{2+} content determinations in RBCs because of the absorption spectrum of haemoglobin ([9], see also [10]). Recently, Makhro et al. [11] reported that reticulocytes obtained from rat blood have a higher Ca^{2+} content than mature rat RBCs. Unfortunately the Ca^{2+} content has not been measured directly in these experiments. However, de Haro et al. [10] also found an enhanced intracellular Ca^{2+} concentration in human reticulocytes compared with mature RBCs. Furthermore, other authors have shown recently that PS exposure of human RBCs is independent of cell age [12]. Only after long-time incubation for 48 h in Ringer solution a significant increase in the intracellular Ca^{2+} content as well as PS exposure with cell age could be detected [13].

In previous papers we have shown several mechanisms leading to an enhanced intracellular Ca^{2+} content of RBCs. One possibility is the opening of the non-specific, voltage-dependent cation (NSVDC) channel by lysophosphatidic acid (LPA) or prostaglandin E_2 (PGE_2) [14, 15]. LPA and PGE_2 are local mediators released from platelets after their activation within the coagulation cascade. PGE_2 can be released also by RBCs under mechanical stress [16]. We were able to show that PS exposure induced by LPA lead to cell-cell adhesion of human RBCs [17, 18]. In addition, PS exposure in the outer membrane leaflet of the RBCs membrane is of importance for the adhesion of RBCs to the endothelium in certain diseases such as sickle cell disease, malaria, and diabetes (e.g. [19-23]). Based on a correlation between decreased haematocrit and longer bleeding times [24] and experiments carried out by Andrews and Low [25], an active role of RBCs in thrombus formation has been proposed [25]. A detailed signalling cascade was published by Kaestner et al. [15].

Another possibility for the enhancement of the intracellular Ca^{2+} content is the activation of protein kinase Cα (PKCα), e.g. by phorbol-12 myristate-13 acetate (PMA) leading to two independent Ca^{2+} entry processes. The first is P-Type $Ca_v2.1$ channel independent and the second is associated with a likely indirect activation of $Ca_v2.1$ [26]. PMA is a powerful pharmacological tool that activates PKCα in terms of translocation from the cytosol to the plasma membrane even in the absence of Ca^{2+} [27].

In all cases of LPA and PMA stimulation the increased intracellular Ca^{2+} content leads to an externalisation of PS. However, there was no clear correlation between the increased intracellular Ca^{2+} content and the PS exposure. Most cells with enhanced Ca^{2+} concentration clearly showed PS exposure. Interestingly, some cells could be found showing an increased intracellular Ca^{2+} content but no PS exposure, and, *vice-versa*, some cells that showed PS exposure but no enhanced Ca^{2+} content [28, 29].

To solve the mentioned discrepancies as well as to understand why not all RBCs after stimulation do not react equally with an increased intracellular Ca^{2+} content as wells as PS exposure, we performed short-time incubation experiments, comparable to the experiments carried out by Nguyen et al. [28], with RBCs separated in 5 fractions with different cell age according to the method of Lutz et al. [2], which was also used for the experiments reported by Ghashghaeinia et al. [13]. The intracellular Ca^{2+} content and PS exposure at the outer membrane leaflet of human RBCs has been investigated using ionophore A23187 (as positive control), LPA, and PMA.

Materials and Methods

Blood and solution

Human venous blood from healthy donors was obtained from the Institute of Sports and Preventive Medicine of Saarland University and the Institute of Clinical Haematology and Transfusion Medicine of Saarland University Hospital. EDTA or heparin was used as anticoagulants. Freshly drawn blood samples were stored at 4 °C and used within one day. Blood was centrifuged at 2,000 g for 5 min at room temperature and the plasma and buffy coat was removed by aspiration. Subsequently, RBCs were washed 3 times in HEPES-buffered physiological solution (HPS) containing (mM): NaCl 145, KCl 7.5, glucose 10, HEPES 10, pH 7.4 under the same conditions. After that the RBCs were separated by cell age in 5 different fractions using discontinuous Percoll density gradients according to the method described by Lutz et al. [2]. Finally, the 5 different RBC fractions were re-suspended in HPS and stored at 4 °C until the beginning of the experiment. The experiment was started immediately after resuspension of the 5 RBC fractions with random order of measurements of the fractions. The experiment of the last fraction was started not later than 3 h after the beginning of the experiment.

Single labelling experiments

Measurement of intracellular Ca^{2+} content: For fluorescent microscopy imaging single labelling experiments were carried out. Measurement of intracellular Ca^{2+} content: RBCs were loaded with 1 µM fluo-4 AM from a 1 mM stock solution in dimethyl sulfoxide (DMSO) in 1 ml HPS. The extracellular Ca^{2+} concentration was 2 mM, i.e. $CaCl_2$ was added to the HPS. Cells were incubated at a haematocrit of 0.1 % in the dark for 30 min at 37 °C with continuous shaking. Then the cells were washed again (16,000 g for 10 s), with an ice-cold HPS, re-suspended and measured as a control (at room temperature), or incubated with a substance to activate Ca^{2+} uptake (A23187 (2 µM) as positive control, LPA (2.5 µM), PMA (6 µM)) at 37 °C. Stock solutions for A23187 (1 mM), LPA (1 mM), and PMA (10 mM) were prepared in DMSO. The incubation time with one of the three substances was 30 min. After incubation the cells were washed again (16,000 g for 10 s) with an ice-cold HPS, re-suspended and measured at room temperature.

Measurement of PS exposure: The cells were prepared like for measurement of the Ca^{2+} content. To detect the PS exposure, annexin V-FITC at a concentration of 4.5 µM was used. Annexin binds to PS in the outer layer of the membrane and is coupled with a fluorescent dye (FITC), which can be measured by flow cytometry and fluorescence microscopy [30]. First a control measurement was performed. After that the substances to activate the Ca^{2+} uptake (A23187, LPA, PMA) were added. The cells were then incubated at 37 °C for 30 min. Then the cells were washed again (16,000 g for 10 s) with an ice-cold HPS and re-suspended. Finally, annexin V-FITC was added to the cells. The staining was performed at a haematocrit of 0.1% in HPS solution with the addition of 2 mM Ca^{2+} at room temperature for 10 min. The measurements were also performed at room temperature.

The procedure to prepare the RBCs for measurement of intracellular Ca^{2+} content as well as PS exposure is based on the protocol of Nguyen et al. [28]. The time intervals between various incubation steps were kept as short as possible.

Double labelling experiments

Although double labelling experiments are common in flow cytometry measurements, there are only few publications where such procedure is used for the investigation of Ca^{2+} content and PS exposure in RBCs. We followed the protocol developed by Nguyen et al. [28].

For double labelling experiments the same procedure was used as for single labelling experiments to measure the Ca^{2+} content, i.e. for Ca^{2+} loading the extracellular Ca^{2+} concentration was 2 mM. However, with double labelling experiments we performed kinetic investigations incubating the cells with the substances (A23187, LPA, PMA) for 1, 5, 10, 15, 20, and 30 min. After the last re-suspension of the RBCs for Ca^{2+} measurements (see above) annexin alexa 647 (4.5 µM) was added (to detect PS) and the cells incubated at room temperature for 10 min.

Fluorescence microscopy

The RBCs were monitored using an inverted fluorescence microscope (Eclipse TE2000-E, Nikon, Tokyo, Japan) as described by Nguyen et al. [28]. The diluted RBC samples (approximately 0.025% haematocrit)

were placed on a cover slip in a dark room at room temperature. Images were taken with an electron multiplication CCD camera (CCD97, Photometrics, Tucson, USA) using a 100x1.4 (NA) oil immersion lens with infinity corrected optics. From each RBC sample, 5 images from different positions of the cover slip randomly chosen were taken using the imaging software Metavue (Universal Imaging Corp., Marlow, UK). Each image consists of one transmitted light and one fluorescence (exposure time 1 s) shot. Fluo-4 and annexin V-FITC were excited with a xenon lamp-based monochromator (Visitron Systems, Puchheim, Germany) at a centre wavelength of 488 nm. Emission was recorded at 520/15 nm.

Flow cytometry

Intracellular free Ca^{2+} content as well as PS exposure was measured by flow cytometry (FACS Calibur and Cell Quest Pro software, Becton Dickinson Biosciences, Franklin Lakes, USA) as described by Nguyen et al. [28] as well as Kucherenko and Bernhardt [31]. Ca^{2+} was measured in the FL-1 channel (excitation at 488 nm, emission at 520/15 nm). PS exposure in case of annexin V-FITC (single labelling experiments) was detected also in the FL-1 channel. In both cases the positive gates were identified based on control experiments (without stimulating substances). In the control experiments, the maximum amount of cells in the positive gates was less than 1%. In case of double labelling experiments, PS exposure was determined using annexin alexa 647 with a xenon diode in the FL-4 channel (excitation at 633 nm, emission at 661/8 nm). Compensation was not necessary since there was no overlapping. The relative fluorescence intensity was analysed using the mean value of 30,000 cells from each blood sample. To compare the sizes of the RBCs of the different fractions (cp. preparation of RBCs of different cell age, see above) the forward scatter (FSC) signal of the flow cytometer was analysed. For each experiment at least three different blood samples were used.

Determination of the relative cell volume

The relative volume of the RBCs of the different fractions was determined using the dry weight method. RBCs from the same fractions obtained from 4 separation experiments using Percoll density gradient (see above) were pooled in a 1.5 ml Eppendorf tube. The haematocrit was adjusted to 10% by adding HPS. The samples were centrifuged at 20.000 g for 7 min at 4 °C. Then the Eppendorf tube was cut to get the part of the tube, which contains the RBC sediment only. The weight of this part was determined (wet weight) and subsequently this part was dried at 90 °C for 48 h (i.e. until constant weight was attained [32]). It was weighted again and the dry weight obtained. The relative cell volume can be easily calculated by: Relative volume (in arbitrary units) = (wet weight – dry weight) / dry weight.

Redox activity measurement

It is assumed that the plasma membrane redox system (PMRS) activity is changing with cell age [33]. To measure the activity of the PMRS in RBCs of different cell age (fractions 1 – 5), the ferrocyanide assay developed by Avron and Shavit [34] was used. Washed RBCs were re-suspended in ferrocyanide solution (obtained from Roth, Karlsruhe, Germany) at a haematocrit of about 1 % and incubated at 37 °C for 30 min. The cell suspension was then centrifuged and 0.9 ml of the supernatant was transferred in a reaction solution (0.3 ml sodium acetate, 0.3 ml citric acid, 0.15 ml $FeCl_3$, 0.15 ml 4,7-diphenyl-1,1-O-phenandrolin sulfonate solution). The probe was again incubated (23 °C, 10 min) in the dark. It was analysed at 535 nm using a photometer (UV mini 1240, Shimadzu, Japan). The obtained optical density was multiplied with factor 0.145 giving the ferrocyanide content of the probe (in µM) [34].

Reticulocyte determination

For reticulocyte determination 5 µl of RBCs from one of the 5 fractions were re-suspended and incubated in 1 ml retic-COUNT reagent (obtained from BD Biosciences, Heidelberg, Germany) at room temperature in the dark for 30 min. The cells were counted using a flow cytometer (see above) [35].

Determination of protein band 4.1a:4.1b ratio

The determination of protein band 4.1a:4.1b ratio has been performed according to the method of Mueller et al. [36]. This included the isolation of membrane proteins, determination of protein concentration as well as protein separation by gel electrophoresis. Finally, the gel was scanned in an image file and the band 4.1a:4.1b ratio was determined using the programme ImageJ (internet open source). To demonstrate that

the analyzed protein is identical in size with the band 4.1, a Western blot was done. For Western blotting, the gel was blotted on a PVDF membrane (70 V, 2 h). The membrane was then washed twice with phosphate buffered saline (PBS) and blocked in blocking solution (milk powder 1 g, 100 ml PBS with 0.1 % Tween 20) on a shaker over night at 4 °C. The incubation with antibodies followed: Primary antibody (erythroid membrane protein 4.1 (elliptocytosis 1, RH-linked (EPB41)), rabbit anti-human polyclonal antibody (1 µg/ml) (Catalog ID / Lot ID: LS-C80526 / 16044), epitope: N-terminus, commercially available from LifeSpan BioSciences Inc. (Seattle, USA), incubation at room temperature for 60 min. After washing 3 times in PBS with Tween (0.1 %) (room temperature, 5 min) the incubation with the secondary antibody (goat anti-rabbit IgG, horseradish peroxidase conjugate (Catalog ID 65-6120)), obtained from Invitrogen (Carlsbad, USA) (diluted 1 : 16,000) followed in analogy to the primary antibody. Finally, the membrane was treated with the ECL advanced Western blotting detection kit (from Amersham, UK).

Reagents

If not mentioned, all chemicals used were purchased from Sigma-Aldrich (Munich, Germany). Fluo-4 AM and annexin V-FITC were obtained from Molecular Probes (Eugene, USA) and annexin alexa 647 from Roche Diagnostics GmbH (Mannheim, Germany).

Statistical significance

Data are presented as mean values ± SD of at least 3 independent experiments. The significance of differences was tested by ANOVA. Statistical significance of the data was defined as follows: $p > 0.05$ (n.s.); $0.01 < p \leq 0.05$ (*); $0.001 < p \leq 0.01$ (**); $p \leq 0.001$ (***).

Results

One picture of a typical Percoll density gradient with RBCs separated in 5 fractions is presented in Fig. 1. To test the quality of the RBC separation by age, forward scatter (FSC) measurements of cells from fractions 1, 3, and 5 and for comparison of RBCs from whole blood have been carried out. In Fig. 2 one can see that RBCs in fraction 1 (young RBCs) are the biggest in size and that cells are becoming smaller with increasing age. In addition, RBCs from whole blood samples are comparable in size compared with cells of fraction 3 (middle aged RBCs). The statistical analysis is given in the figure legend. These data prove that the RBC separation was efficient. The control data, i.e. FSC of cells without activation, are shown at time zero. Directly after the addition of LPA, i.e. after 1 min, there is a slight but not significant reduction of cell sizes in all samples. The same tendency has been obtained after addition of other activators (A23187 and PMA, data not shown). Analysing the data of the fractions depending on time, only a significant difference of the value at time zero and at time 30 min for fraction 3 has been found.

In addition to the FCS measurements, the relative cell volume of the different fractions and of non-separated cells was obtained based on the determination of the RBC dry weight (see Methods, n = 4, in arbitrary units): non-separated cells = 1.83 ± 0.16, fraction 1 = 2.03 ± 0.13, fraction 2 = 1.87 ± 0.13, fraction 3 = 1.73 ± 0.10, fraction 4 = 1.59 ± 0.13, fraction 5 = 1.50 ± 0.12. Statistical analysis (ANOVA) revealed that the value of the non-separated cells is significantly different from the values of fraction 5 ($p \leq 0.05$). The value of fraction 1

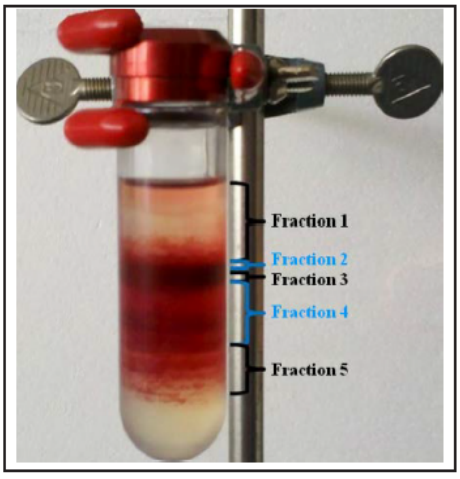

Fig. 1. The picture shows a typical Percoll density gradient with RBCs separated by age in 5 fractions.

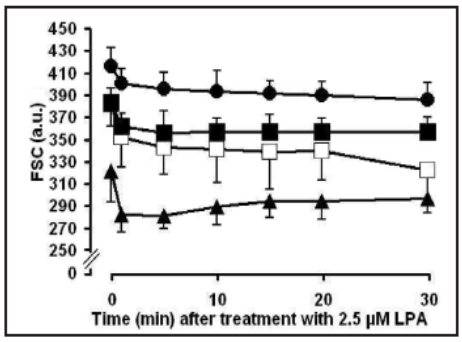

Fig. 2. Forward scatter (FSC) measurements of RBCs from different fractions (cells separated by age) after activation with LPA (2.5 µM) using flow cytometry depending on time. White square = non-separated RBCs; dark circle = young cells (fraction 1); dark square = middle aged cells (fraction 3); dark triangle = old cells (fraction 5). N = 3 (90,000 cells), error bars = S.D. (only half error bar is shown for convenience). Significant differences for fractions at a certain time, ANOVA ($0.01 < p \leq 0.05$ (*); $0.001 < p \leq 0.01$ (**); $p \leq 0.001$ (***)); for 0 min: * non-separated (n-s) vs. fraction (fr) 5, fr 3 vs. fr 5, ** fr 1 vs. fr 5; for 1 min: * n-s vs. fr 1, ** n-s vs. fr 5, fr 3 vs. fr 5, *** fr 1 vs. fr 5; for 5 min: * n-s vs. fr 1, n-s vs. fr 5, ** fr 3 vs. fr 5, *** fr 1 vs. fr 5; for 10 and 15 min: * fr 3 vs. fr 5, ** fr 1 vs. fr 5; for 20 min: ** fr 1 vs. fr 5; for 30 min: * n-s vs. fr 1, fr 3 vs. fr 5, ** fr 1 vs. fr 5. Significant differences of separate fractions depending on time: * only for fr 3: 0 min vs. 30 min (only differences between 0 min and 1 min vs. 30 min have been tested).

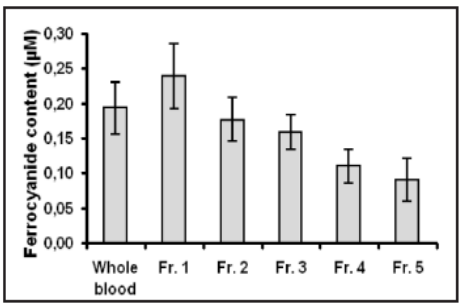

Fig. 3. Redox activity (ferrocyanide content) of RBCs from different fractions (cells separated by age) based on flow cytometry measurements. Error bars = S.D.. N = 5 (150,000 cells). Significant differences, ANOVA ($0.01 < p \leq 0.05$ (*); $0.001 < p \leq 0.01$ (**); $p \leq 0.001$ (***)): *fraction (fr) 2 vs. fr 4, fr 3 vs. fr 5, ** non-separated (n-s) vs. fr 4, fr 1 vs. fr 3, fr 2 vs. fr 5, *** n-s vs. fr 5, fr 1 vs. fr 4, fr 1 vs. fr 5.

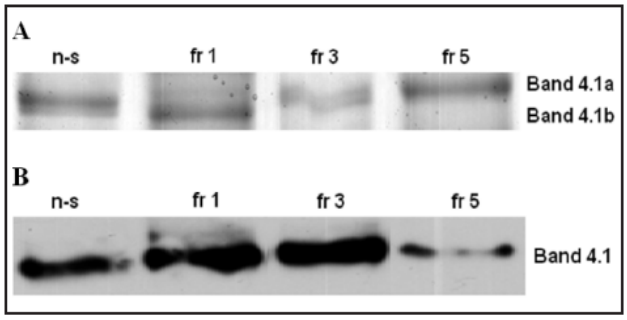

Fig. 4. (A) The picture shows the fragment of the Coomassie-stained gel containing the protein band 4.1a and b from RBCs of different fractions (cells separated by age) and non-separated (n-s) cells. (B) Corresponding Western blot showing the protein band 4.1.

is different from the value of fraction 3 ($p \leq 0.05$), and the value of fraction 1 is different from the value of fraction 5 ($p \leq 0.001$).

Another test was the determination of the amount of reticulocytes in the different fractions. The obtained results showed that reticulocytes are present in fraction 1 to a high amount (11.07 ± 6.38 %). For fraction 2, 3, 4, and 5, the corresponding values are 1.12 ± 0.47 %, 0.72 ± 0.58 %, 0.53 ± 0.33 %, and 0.62 ± 0.45 %, respectively. The value for the non-separated cells was 0.68 ± 0.30 %, (n = 4). Statistical analysis (ANOVA) revealed that only the value of fraction 1 is significantly different from the values of all other fraction ($p \leq 0.001$).

Furthermore, the redox activity of the RBCs of the different fractions has been measured and compared with data obtained for cells from whole blood. It can be clearly seen in Fig. 3 that the amount of ferrocyanide, i.e. the activity of the PMRS, is decreasing with increasing age of the RBCs.

Finally, the protein band 4.1a:4.1b ratio has been determined. Fig. 4A shows the Coomassie-stained gel containing the protein band 4.1a and b. An increasing value in the

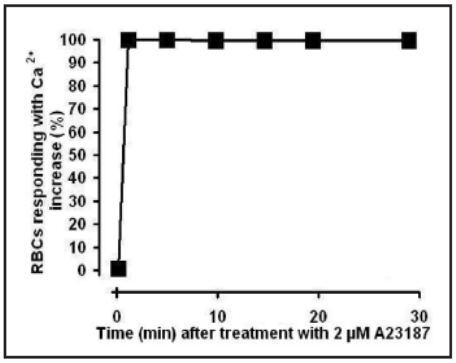

Fig. 5. Percentage of RBCs responding with increased intracellular Ca^{2+} content from different fractions (cells separated by age) after activation with A23187 (2 µM) using flow cytometry depending on time. Non-separated RBCs, young cells (fraction 1); middle aged cells (fraction 3); old cells (fraction 5) have been investigated. There were no significant differences between different fractions. Almost all RBCs of the fractions 1, 3, and 5 show increased intracellular Ca^{2+} content. That is why a discrimination of the different fractions is not possible (all data fit to the same symbol at different time points). N = 3 (90,000 cells), error bars = S.D. are smaller than symbols. There are no significant differences between the fractions, ANOVA, $p > 0.05$.

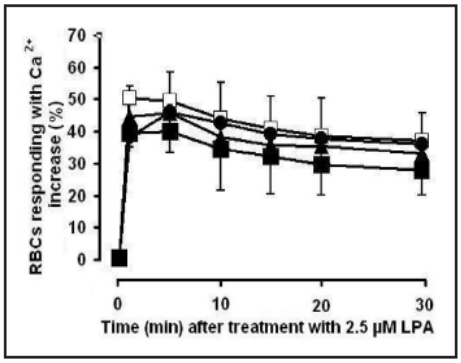

Fig. 6. Percentage of RBCs responding with increased intracellular Ca^{2+} content from different fractions (cells separated by age) after activation with LPA (2.5 µM) using flow cytometry depending on time. White square = non-separated RBCs; dark circle = young cells (fraction 1); dark square = middle aged cells (fraction 3); dark triangle = old cells (fraction 5). N = 3 (90,000 cells), error bars = S.D. (only half error bar is shown for convenience). There are no significant differences between the fractions, ANOVA, $p > 0.05$. Significant differences of separate fractions depending on time: ANOVA ($0.01 < p \leq 0.05$ (*)) only for fraction 1: 5 min vs. 30 min (only differences between 1 min and 5 min vs. 30 min have been tested).

Fig. 7. Percentage of RBCs responding with increased intracellular Ca^{2+} content from different fractions (cells separated by age) after activation with PMA (6 µM) using flow cytometry depending on time. White square = non-separated RBCs; dark circle = young cells (fraction 1); dark square = middle aged cells (fraction 3); dark triangle = old cells (fraction 5). N = 3 (90,000 cells), error bars = S.D. (only half error bar is shown for convenience). Significant differences, ANOVA ($0.01 < p \leq 0.05$ (*)) for 1 min: * fraction (fr) 1 vs. fr 3, fr 1 vs. fr 5. Significant differences of separate fractions depending on time: ANOVA ($0.01 < p \leq 0.05$ (*)) only for fraction 1: 1 min vs. 30 min, 5 min vs. 30 min (only differences between 1 min and 5 min vs. 30 min have been tested).

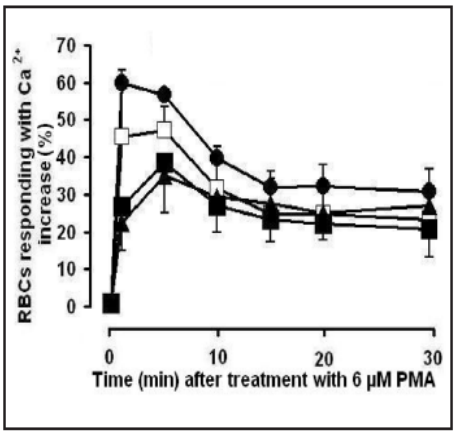

band 4.1a:4.1b ratio with increasing cell age has been determined. The values obtained are 0.179, 0.722, and > 3 for RBCs from fraction 1, 3 and 5, respectively. The Western blot showing the protein band 4.1 is displayed in Fig. 4B.

When the RBCs were stimulated with the Ca^{2+} ionophore A23187 (positive control) almost all cells show an increased intracellular Ca^{2+} content independent on the fraction (Fig. 5). By activation of the RBCs with LPA about 50 % of the cells react with an increased intracellular Ca^{2+} content (Fig. 6). The maximum of reacting RBCs is reached after 1 - 5 min incubation with LPA. After that a slight decrease can be seen (statistically significant only

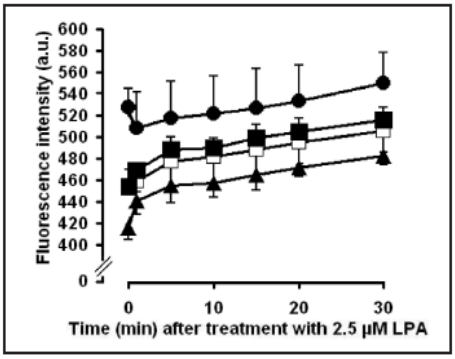

Fig. 8. Fluo-4 fluorescence intensity (arbitrary units) of RBCs from different fractions (cells separated by age) after activation with LPA (2.5 µM) using flow cytometry depending on time. White square = non-separated RBCs; dark circle = young cells (fraction 1); dark square = middle aged cells (fraction 3); dark triangle = old cells (fraction 5). N = 3 (90,000 cells), error bars = S.D. (only half error bar is shown for convenience). Significant differences, ANOVA ($0.01 < p \leq 0.05$ (*); $0.001 < p \leq 0.01$ (**); for 0 min: * non-separated (n-s) vs. fraction (fr) 1, fr 1 vs. fr 3, ** fr 1 vs. fr 5; for 1 min, 5 min, 10 min, 15 min, 20 min, 30 min: * fr 1 vs. fr 5. Significant differences of separate fractions depending on time: * for n-s: 0 min vs. 30 min, 1 min vs. 30 min, ** for fr 3 and fr 5: 0 min vs. 30 min, 1 min vs. 30 min (only differences between 0 min and 1 min vs. 30 min have been tested).

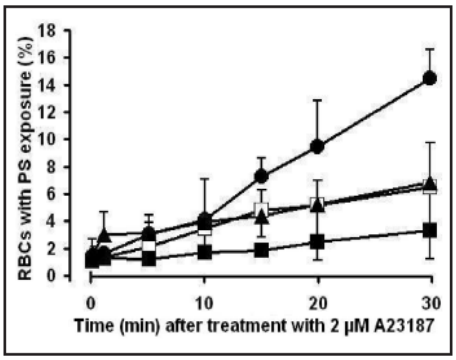

Fig. 9. Percentage of RBCs from different fractions (cells separated by age) showing increased PS exposure after activation with A23187 (2 µM) using flow cytometry depending on time. White square = non-separated RBCs; dark circle = young cells (fraction 1); dark square = middle aged cells (fraction 3); dark triangle = old cells (fraction 5). N = 3 (90,000 cells), error bars = S.D. (only half error bar is shown for convenience). Significant differences, ANOVA ($0.01 < p \leq 0.05$ (*); $0.001 < p \leq 0.01$ (**)) for 30 min: * non-separated vs. fraction (fr) 1, fr 1 vs. fr 5, ** fr 1 vs. fr 3.

for the fraction of the young RBCs (fraction 1)). However, there are no significant cell age dependent differences. Using PMA as activator, the same tendency for the increase of the intracellular Ca^{2+} content as in case of LPA stimulation occurred (Fig. 7). Only 1 min after addition of PMA RBCs of fraction 1 responded significantly more than cells from fractions 3 and 5. After PMA treatment of more than 1 min no significant cell age dependent differences could be detected.

The fluo-4 fluorescence intensity for RBCs from different fractions after treatment with LPA depending on time is shown in Fig. 8. Comparable results were obtained for A23187 and PMA stimulation (not shown). The statistical analysis is given in the figure legend. For non-separated cells as well as for cells from fraction 1, 3, and 5 there is a slight increase of the fluorescence intensity with time (statistically significant for values of non-separated cells and cells from fraction 3 and 5 at 0 min or 1 min tested *versus* 30 min). In addition, there are significant differences between fraction 1 and 5 over all time points and non-separated *versus* fraction 1 and fraction 1 *versus* fraction 3 at t = 0 min (Fig. 8).

Investigating the PS exposure after activation with A23187, LPA, or PMA (Figs. 9 - 11) one can see that in all 3 cases there is an increase of the amount of RBCs showing PS at the outer membrane surface with time. However, the amount of cells showing PS exposure after 30 min is different in all three cases, smallest with A23187 and highest with PMA activation. For all 3 activating substances no significant differences between cells from fractions 1, 3, and 5 as well as whole blood could be seen for most time points. Only in case of A23187 stimulation the youngest RBC population (fraction 1) showed a significantly higher amount of cells with PS exposure compared to the other fractions as well as to the non-separated cells after 30 min.

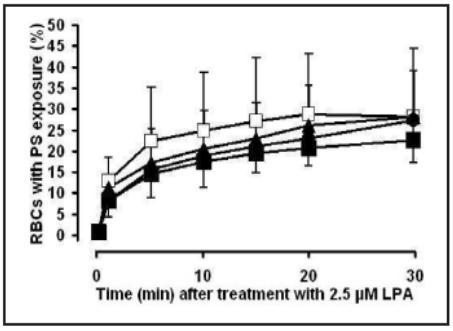

Fig. 10. Percentage of RBCs from different fractions (cells separated by age) showing increased PS exposure after activation with LPA (2.5 µM) using flow cytometry depending on time. White square = non-separated RBCs; dark circle = young cells (fraction 1); dark square = middle aged cells (fraction 3); dark triangle = old cells (fraction 5). N = 3 (90,000 cells), error bars = S.D. (only half error bar is shown for convenience). There are no significant differences between the fractions, ANOVA, $p > 0.05$.

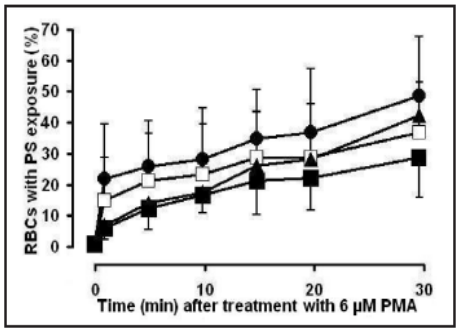

Fig. 11. Percentage of RBCs from different fractions (cells separated by age) showing increased PS exposure after activation with PMA (6 µM) using flow cytometry depending on time. White square = non-separated RBCs; dark circle = young cells (fraction 1); dark square = middle aged cells (fraction 3); dark triangle = old cells (fraction 5). N = 3 (90,000 cells), error bars = S.D. (only half error bar is shown for convenience). There were no significant differences between the fractions, ANOVA, $p > 0.05$.

Table 1. Percentage of RBCs from non-separated, fraction 1, 3, and 5 showing increased intracellular Ca^{2+} content as well as PS exposure at time zero, i.e. before stimulation with A23187, LPA or PMA (flow cytometry measurements). Data taken from Figs. 6, 10. Mean value ± S.D., N = 3 (90,000 cells). There are no significant differences between the fractions, ANOVA, $p > 0.05$

	Non-separated RBCs	Fraction 1	Fraction 3	Fraction 5
RBCs with increased Ca^{2+} (%)	0.80 ± 0.09	0.74 ± 0.20	0.90 ± 0.53	1.31 ± 0.69
RBCs showing PS exposure (%)	0.98 ± 0.15	0.77 ± 0.07	0.95 ± 0.31	1.52 ± 0.37

It can be seen for control measurements at time zero that there is a slight but not significant increase of the percentage of RBCs showing increased intracellular Ca^{2+} content as well as PS exposure with increasing age (Figs. 6, 10). The obtained values for intracellular Ca^{2+} content of RBCs from whole blood, fraction 1, 3, and 5 as well as the corresponding PS exposure is presented in Table 1.

In addition to flow cytometry investigations, images of the RBCs of different fractions after activation with A23187, LPA, or PMA were taken using a fluorescence microscope. In this case single labelling experiments for the detection of the increased intracellular Ca^{2+} content as well as the PS exposure have been performed. Fig. 12 shows the corresponding images for the LPA activation. No remarkable differences can be seen. This was also the case for A23187 and PMA stimulation (not shown).

Furthermore, from the obtained flow cytometry data the percentage of RBCs with an increased PS exposure but no increased intracellular Ca^{2+} level as well as with an increased intracellular Ca^{2+} content but no PS exposure after 30 min activation with A23187, LPA, and PMA has been determined. The results are presented in Table 2. No significant age-specific differences could be seen (data not shown).

Discussion

As one can see from various parameters of RBCs from different fractions (cell size, relative cell volume. reticulocyte content, redox activity, and protein band 4.1a:4.1b ratio)

Table 2. Percentage of RBCs with an increased PS exposure but no increased intracellular Ca^{2+} level as well as with an increased intracellular Ca^{2+} content but no PS exposure after 30 min activation with A23187 (2 µM), LPA (2.5 µM), and PMA (6 µM) (flow cytometry measurements). N = 3 (90,000 cells)

Activator	RBCs with PS exposure, but no increased Ca^{2+} content (%)	RBCs with increased Ca^{2+} content, but no PS exposure (%)
A23187	1 – 2	85 – 98
LPA	3 – 5	6 – 12
PMA	7 – 16	2 – 3

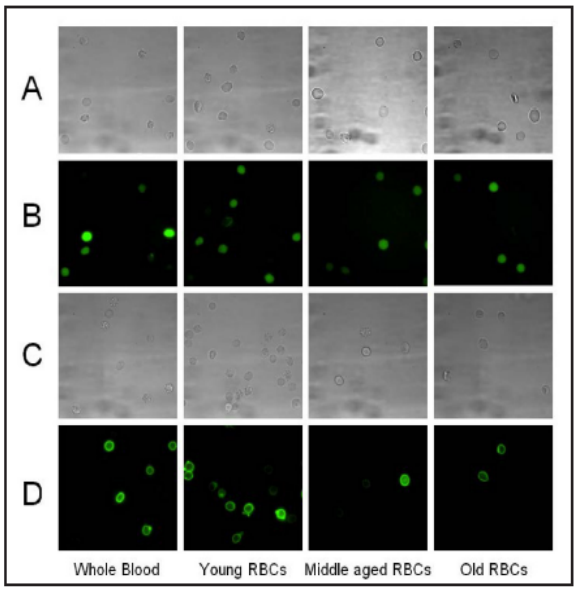

Fig. 12. Measurements of RBCs from different fractions (cells separated by age) showing transmitted light (A) and corresponding fluorescence image of RBCs with increased intracellular Ca^{2+} content (B) as well as transmitted light (C) and corresponding fluorescence image of RBCs with increased PS exposure (D) after 30 min activation with LPA (2.5 µM) using fluorescence microscopy (representative images). No significant differences of cells from different fractions could be observed. The figure shows one typical experiment out of 3.

the separation of RBCs by age was successful. The obtained results for these parameters are in agreement with literature data.

RBCs lose water with age and become denser, i.e. smaller (Fig. 2, and data of the relative cell volume) [1, 37]. Only shortly before eryptosis, sudden increase in cell volume can be observed [7]. However, the small amount of very old cells in the first fraction (containing the young cells) is negligible. The slight but not significant reduction of the FSC after 1 min is probably based on a shape change of the RBCs. In microscopy experiments we observed that there was a shape change from some discocytes to echinocytes directly after LPA activation (not shown).

Reticulocytes are the youngest RBCs in the bloodstream. They contain residues of RNA. Thiazole Orange (retic-COUNT) binds to RNA and can be analysed by flow cytometry [35]. The analysis of the reticulocyte count in the individual fractions revealed that the reticulocytes were almost exclusively in fraction 1. Our data also show that the contamination of the other fractions with reticulocytes does not play a substantial role.

The obtained data of the redox activity of RBCs of different age are in agreement with findings of Lawen et al. [33]. When the redox system is less active, less ferrocyanide is formed [38]. D'Alessandro et al. [39] showed a decrease of the anti-oxidant defence-related mechanisms when the RBCs becoming older. A higher Tyr-phosphorylation level of band 3 protein of old compared to young RBCs under hypertonic conditions has been described by Ciana et al. [40]. An overview and a discussion of a variety of markers of the redox activity of RBCs are presented in the review article written by Lutz and Bogdanova [41].

In addition, the observed increase of the protein band 4.1a:4.1b ratio with cell age is in agreement with findings reported in the literature [36, 42, 43].

The ionophore A23187 was used as positive control to produce an increase in the intracellular Ca^{2+} concentration. It is not surprising that almost all RBCs have an increased intracellular Ca^{2+} content under such conditions. Age-related differences could not be observed. In case of LPA and PMA treatment a maximum amount of RBCs responding with increased intracellular Ca^{2+} content is reached during the first minutes of stimulation (Figs. 6, 7). Thereafter, the percentage of RBCs with increased intracellular Ca^{2+} content is slightly decreasing (significant only for fraction 1). In case of PMA treatment younger RBCs (from fraction 1) respond with a higher amount of cells with increased intracellular Ca^{2+} content than old or middle-aged RBCs after 1 min of stimulation. It seem realistic to assume that the Ca^{2+} uptake pathways are less active in old RBCs compared to young ones, which is in agreement with findings of Romero [44] and Makhro et al. [11] showing that young RBCs have a higher Ca^{2+} uptake capacity than old RBCs. In fact in the paper of Makhro et al. [11] it has been demonstrated that the number of N-methyl-D-aspartate receptor (NMDAR), that contribute to the intracellular Ca^{2+} regulation, is higher in young cells compared with mature and senescent RBCs. However, it cannot be excluded completely that the old RBCs are less sensitive to PMA and therefore take up less Ca^{2+}. The differences in the decrease of the percentage of RBCs with enhanced intracellular Ca^{2+} content after the maximum is reached can be explained assuming a higher activity of the Ca^{2+} pump in young RBCs compared to old and middle-aged RBCs. Such an effect was also reported by Lew et al. [45] and Lucas et al. [46]. The situation is different in experiments with LPA stimulation. In this case there is no significant difference of the increase as well as the declining process between RBCs from different fractions. It should be mentioned that we realised in separate investigations using fluorescence microscopy that in case of LPA or PMA stimulation, some cells take up Ca^{2+} to such a high amount in a very short time that it leads to the damage of the cells (not shown). Therefore, it seems evident that these cells with high amount of intracellular Ca^{2+} (probably cells from fraction 1) are damaged already before the flow cytometry measurements started.

In all three cases of stimulation (A23187, LPA, PMA) there is a difference of the fluo-4 fluorescence intensity of the different fractions. For cells from fraction 1 the highest, and for fraction 5 the lowest fluorescence intensity was determined (for LPA see Fig. 8, data for A23187 and PMA are snot shown). Taking into consideration that RBCs from fraction 1 have a higher volume as RBCs from fraction 5 (Fig. 2 and determination of relative cell volume (see Results)), one can assume that the intracellular Ca^{2+} content of RBCs does not change substantially with cell age. A quantitative statement is not possible since the fluorescence intensity does not change linearly dependent with the Ca^{2+} concentration [9].

The Ca^{2+} content of RBCs from whole blood after 30 min activation with A23187, LPA, or PMA was investigated by our group and has been presented in a previous paper [47]. In this publication one can find representative histograms of flow cytometry analysis of intracellular Ca^{2+} content of RBCs for all 3 substances (Fig. 1 in [47]). In case of stimulation with LPA (Fig. 8) or PMA (not shown) the fluo-4 fluorescence intensity is increasing with time. In contrast, in case of A23187 treatment, the fluorescence intensity does not change significantly with time (measured over 30 min, not shown). This means that a small increase of the intracellular Ca^{2+} content occurs after LPA or PMA activation taking into consideration a constant or slightly reduced percentage of RBCs with increased intracellular Ca^{2+} content (Fig. 6).

Whether there is a difference of the intracellular Ca^{2+} concentration depending on the age of RBCs has been discussed for a long time. It has been described that older RBCs have a higher intracellular Ca^{2+} content than young RBCs [4, 5, 44]. In contrast, de Haro et al. [10] showed that the Ca^{2+} level in reticulocytes is higher than in mature RBCs. Assuming a higher intracellular Ca^{2+} concentration in old RBCs one could assume a higher amount of PS in the outer membrane leaflet of old RBCs compared to young once. On this basis it has been speculated that macrophages recognise old and senescent RBCs with a certain amount of PS in the outer membrane leaflet and remove them from the blood stream [12, 13, 27, 48-52].

Table 3. Percentage of RBCs responding with increased intracellular Ca^{2+} content and showing increased PS exposure from different fractions (cells separated by age) after 48 h incubation in Ringer solution containing glucose compared to control (0 h incubation). The experiments were carried out according to the experiments described by Ghashghaeinia et al. [13] (same solutions, only fluo-4 instead of fluo-3 was used). Non-separated RBCs, young cells (fraction 1), middle aged cells (fraction 3), and old cells (fraction 5) have been investigated using flow cytometry. Mean value ± S.D., N = 3 (90,000 cells). Significant differences for fractions, ANOVA ($0.01 < p \leq 0.05$ (*); $0.001 < p \leq 0.01$ (**)); for Ca^{2+} content, 48 h: * fraction (fr) 1 vs. fr 5, ** non-separated (n-s) vs. fr 5, fr 3 vs. fr 5; for PS exposure, 48 h: * n-s vs. fr 5, fr 1 vs. fr 5

Fraction	RBCs with increased intracellular Ca^{2+} content (%)		RBCs with PS exposure (%)	
	0 h	48 h	0 h	48 h
Non-separated	1.78 ± 0.83	4.14 ± 1.11	1.03 ± 0.17	5.44 ± 2.63
Fraction 1	3.28 ± 1.07	5.96 ± 0.31	1.05 ± 0.37	4.14 ± 2.10
Fraction 3	1.91 ± 1.03	4.13 ± 1.45	1.31 ± 0.97	6.56 ± 1.27
Fraction 5	1.45 ± 0.20	13.89 ± 4.79	1.18 ± 0.80	15.23 ± 6.03

Consistent with this idea it was shown that old RBCs responded with a higher increase of intracellular Ca^{2+} compared to young RBCs, based on flow cytometry measurements using the Ca^{2+}-sensitive dye fluo-3 [13], but interestingly only after a long incubation time of the RBCs (48 h). Such an effect is not surprising if it is taken into consideration that old RBCS have a lower Ca^{2+} transport rate (e.g. [45]). In addition, the ATP content of older RBCs is decreased faster [53]. We repeated the experiments of Ghashghaeinia et al. [13] carrying out long time incubation (48 h) of RBCs without activators (same experimental conditions, only fluo-4 instead of fluo-3 for Ca^{2+} measurements was used) and confirm a significant increase of the intracellular Ca^{2+} content as well as PS exposure in older cells (Table 3). One could think about a substantial role of ATP for the Ca^{2+} content and PS exposure in RBCs (see e.g. [54]). However, it has been demonstrated by ATP depletion experiments (2 h incubation in the presence of 10 mM inosine, 6 mM iodoacetamide, 5 mM sodium tetrathionate, resulting in an ATP content less than 2% of its normal level) that little or no ATP is required for the externalisation of PS [29].

Our data at time zero, i.e. before the stimulation (Table 1) show also a slightly higher percentage of older RBCs showing increased intracellular Ca^{2+} content and PS exposure compared to young ones. However, this effect is not significant and probably also not pronounced enough to explain the clearance of old RBCs from the blood stream on the basis of such mechanism. In the discussion of a possible increased intracellular Ca^{2+} content in old RBCs it was also proposed that such an increase might occur throughout RBC life in the circulation but this could be transient and rapidly reverted by the Ca^{2+} pump. Such an explanation was given based on observed increase in the products of Ca^{2+}-dependent proteolysis of phosphotyrosine phosphatases 1B (PTP1B) in old RBCs [40]. For a serious discussion of mechanisms tagging senescent RBCs for clearance in healthy humans we refer to the review article written by Lutz and Bogdanova [41].

The PS exposure is increasing with time in all cases of stimulation (A23187, LPA, PMA) (Figs. 9 - 11). There are no significant differences between the cells from different fractions in case of LPA and PMA stimulation (Figs. 9, 10). Only in case of the positive control (A23187 stimulation) a significant higher value was found for younger RBCs compared to non-separated, old, or middle-aged RBCs after 30 min stimulation. In case of A23187 stimulation nearly all cells contain a high amount of Ca^{2+} (see above). However, this effect could be due to a more efficient activation of the PKC and/or the scramblase in young RBCs. It has been described by Franco et al. [12] that older RBCs have a significantly lower aminophospholipid translocase (APLT) activity. However, the amount of cells showing PS exposure is smaller in the case of A23187 stimulation, which is in agreement with earlier findings [28]. It has been already discussed that the Ca^{2+} increase caused by A23187 does not lead to an activation of the PKC [28], which plays an important role in the mechanism of PS exposure (Ca^{2+}-independent

pathway) [28, 55]. Carrying out *in vivo* aging experiments, there was no evidence for elevated PS exposure of older RBCs [12]. It has also been discussed that a shrinkage of RBCs based on an increase of the intracellular Ca^{2+} content an subsequently activation of the Ca^{2+}-activated K^+ (Gardos) channel is partly responsible for the PS exposure in RBCs [56]. In this respect it has to be taken into consideration that it was found that the activity of the Gardos channel is reduced with cell aging [57].

Our findings question the idea that the removal of senescent RBCs from the blood stream is simply based on an increased PS exposure in the outer membrane leaflet. However, we are aware of limitations of the presented investigations such as lack of systemic environment, lack of shear stress, etc.

Conclusion

In summary, we were able to show that there are no significant differences in the intracellular Ca^{2+} content as well as PS exposure of RBCs of different age after stimulation of Ca^{2+} uptake and after short-time incubation. In addition, the findings of Nguyen et al. [28] and de Jong et al. [29], showing that some RBCs have an increased intracellular Ca^{2+} content but no enhanced PS exposure and that some other cells have an elevated PS exposure but no significant increase of the intracellular Ca^{2+} content cannot be explained assuming that this effect is depending on the age of the RBCs. The reason of the existence of RBCs with such characteristic features is still unclear and will be investigated in future work.

Acknowledgements

This research is funded by Vietnam National Foundation for Science and Technology Development (NAFOSTED) under grant number 106-YS.06-2013.16 for D. B. Nguyen and a grant from CNPq program "science without borders" to M. C. Wesseling, process number: 202426/2012-2 (Brasil).

Disclosure Statement

The authors declare no conflict of interest.

References

1 Piomelli S, Seaman C: Mechanism of red blood cell aging: relationship of cell density and cell age. Am J Hematol 1993;42:46-52.
2 Lutz HU, Stammler P, Fasler S, Ingold M, Fehr J: Density separation of human red blood cells on self-forming Percoll gradients: correlation with cell age. Biochim Biophys Acta 1992;1116:1-10.
3 Risso A, Ciana A, Achilli C, Minetti G: Survival and senescence of human young red cells in vitro. Cell Physiol Biochem 2014;34:1038-1049.
4 Romero PJ, Romero EA, Winkler MD: Ionic calcium content of light dense human red cells separated by Percoll density gradients. Biochim Biophys Acta 1997;1323:23-28.
5 Aiken NR, Satterlee JD, Galey WR: Measurement of intracellular Ca^{2+} in young and old human erythrocytes using F-NMR spectroscopy. Biochim Biophys Acta 1992;1136:155-160.
6 Woon LA, Holland JW, Kable EP, Roufogalis BD: Ca^{2+} sensitivity of phospholipid scrambling in human red cell ghosts. Cell Calcium 1999;25:313-20.
7 Lang KS, Lang PA, Bauer C, Duranton C, Wieder T, Huber SM, Lang F: Mechanisms of suicidal erythrocyte death. Cell Physiol Biochem 2005;15:195-202.

8 Lang F, Gulbins E, Szabo I, Leppel-Wienhues A, Huber SM, Duranton C, Lang KS, Lang PA, Wieder T: Cell volume and the regulation of apoptotic cell death. J Mol Recognit 2004;17:473-480.
9 Kaestner L, Tabellion W, Weiss E, Bernhardt I, Lipp P: Calcium imaging of individual erythrocytes: Problems and approaches. Cell Calcium 2006;39:13-19.
10 de Haro C, de Herreros AG, Ochoa S: Protein phosphorylation and translational control in reticulocytes: Activation of the heme-controlled translational inhibitor by calcium ions and phospholipid. Curr Top Cell Regul 1985;27:63-81.
11 Makhro A, Wang J, Vogel J, Boldyrev AA, Gassmann M, Kaestner L, Bogdanova A: Functional NMDA receptors in rat erythrocytes. Am J Physiol Cell Physiol 2010;299:1571-1573.
12 Franco RS, Puchulu-Campanella ME, Barber LA, Palascak MB, Joiner CH, Low PS, Cohen RM: Changes in the properties of normal human red blood cells during in vivo aging. Am J Hematol 2013;88:44-51.
13 Ghashghaeinia M, Cluitmans JC, Akel A, Dreischer D, Toulany M, Köberle M, Skabytska Y, Saki M, Biedermann T, Duszenko M, Lang F, Wieder T, Bosman GJ: The impact of erythrocyte age on eryptosis. Br J Haematol 2012;157:606-614.
14 Kaestner L, Bollensdorff C, Bernhardt I: Non-selective voltage-activated cation channel in the human red blood cell membrane. Biochim Biophys Acta 1999;1417:9-15.
15 Kaestner L, Tabellion W, Lipp P, Bernhardt I: Prostaglandin E2 activates channel-mediated calcium entry in human erythrocytes: an indicator for a blood clot formation supporting process. Thromb Haemost 2004;92:1269-1272.
16 Oonishi T, Sakashita K, Ishioka N, Suematsu N, Shio H, Uyesaka N: Production of prostaglandins E1 and E2 by adult human red blood cells. Prostaglandins Other Lipid Mediat 1998;56:89-101.
17 Steffen P, Jung A, Nguyen DB, Müller T, Bernhardt I, Kaestner L, Wagner C: Stimulation of human red blood cells leads to Ca^{2+}-mediated intercellular adhesion. Cell Calcium 2011;50:54-61.
18 Kaestner L, Steffen P, Nguyen DB, Wang J, Wagner-Britz L, Jung A, Wagner C, Bernhardt I: Lysophosphatidic acid induced red blood cell aggregation in vitro. Bioelectrochemistry 2012;87:89-95.
19 Closse C, Dachary-Progent J, Boisseau MR: Phosphatidylserine-related adhesion of human erythrocytes to vascular endothelium. Br J Haematol 1999;107:300-302.
20 Tiffert T., Bookchin RM, Lew VL: Calcium homeostasis in normal and abnormal human red cells. In Red cell membrane transport in health and disease; Bernhardt I, Ellory JC. Eds. Springer Verlag: Heidelberg, Germany, 2003; pp.373-405.
21 de Jong K., Larkin SK, Styles LA, Bookchin RM, Kuypers FA: Characterization of the phosphatidylserine-exposing subpopulation of sickle cells. Blood 2001;98:860-867.
22 Sherman IW, Prudhomme J, Tait JF: Altered membrane phospholipid asymmetry in plasmodium falciparum-infected erythrocytes. Parasitol. Today 1997;13:242-243.
23 Wali RK, Jaffe S, Kumar D, Kalra VK: Alterations in organization of phospholipids in erythrocytes as factor in adherence to endothelial cells in diabetes mellitus. Diabetes 1988;37:104-111.
24 Hellem AJ: The adhesiveness of human blood platelets in vitro. Scand J Clin Lab Invest 1960;12:1-117.
25 Andrews D, Low PS: Role of red blood cells in thrombosis. Curr Opin Hematol 1999;6:76-82.
26 Wagner-Britz L, Wang J, Kaestner L, Bernhardt I: Protein kinase Cα and P-type Ca^{2+} channel Cav2.1 in red blood cell calcium signalling. Cell Physiol Biochem 2013;31:883-891.
27 Klarl BA, Lang PA, Kempe DS, Niemoeller OM, Akel A, Sobiesiak M, Eisele K, Podolski M, Huber SM, Wieder T, Lang F: Protein kinase C mediates erythrocyte "programmed cell death" following glucose depletion. Am J Physiol Cell Physiol 2006;290:C244-53.
28 Nguyen DB, Wagner-Britz L, Maia S, Steffen P, Wagner C, Kaestner L, Bernhardt I: Regulation of phosphatidylserine exposure in red blood cells. Cell Physiol Biochem 2011;28:847-856.
29 de Jong K, Rettig MP, Low PS, Kuypers FA: Protein kinase C activation induces phosphatidylserine exposure on red blood cells. Biochemistry 2002;41:12562-12567.
30 Vermes I, Haanen C, Steffens-Nakken H, Reutelingsperger C: A novel assay for apoptosis. Flow cytometric detection of phosphatidylserine expression on early apoptotic cells using fluorescein labelled Annexin V. J Immunol Methods 1995;184:39-51.
31 Kucherenko YV, Bernhardt I: Natural antioxidants improve red blood cell "survival" in non-leukoreduced blood samples. Cell Physiol Biochem 2015;35:2055-2068.
32 Eisenmann AJ, Mackenzie LB, Peters JP: Protein and water of serum and cells of human blood, with a note on the measurement of red blood cell volume. J Biol Chem 1936;116:33-45.

33 Lawen A, Martinus RD, McMullen GL, Nagley P, Vaillant F, Wolvetang EJ, Linnane AW: The universality of bioenergetic disease: the role of mitochondrial mutation and the putative inter-relationship between mitochondria and plasma membrane NADH oxidoreductase. Mol Aspects Med 1994;15:s13-s27.
34 Avron M, Shavit N: A sensitive and simple method for determination of ferrocyanide. Anal Biochem 1963;6:549-554.
35 Lee L, Chen C, Chiu L: Thiazole Orange: a new dye for reticulocyte analysis. Cytometry 1986;7:508.
36 Mueller TJ, Jackson CW, Dockter ME, Morrison M: Membrane skeletal alterations in vivo mouse red cell aging. Increase in the band 4.1a:4.1b ratio. J Clin Invest 1987;79:492-499.
37 Waugh RE, Narla M, Jackson CW, Mueller TJ, Suzuki T, Dale GL: Rheologic properties of senescent erythrocytes: loss of surface area and volume with red cell age. Blood 1992;79:1351-1358.
38 Rizvi SI, Jha R, Maurya PK: Erythrocyte plasma membrane redox system in human aging. Rejuvenation Res 2006;9:470-474.
39 D'Alessandro A, Blasi B, D'Amici GM, Marrocco C, Zolla L: Red blood cell subpopulations in freshly drawn blood: Application of proteomics and metabolomics to a decades-long biological issue. Blood Transfus 2013;11:75-87.
40 Ciana A, Minetti G, Balduini C: Phosphotyrosine phosphatases acting on band 3 in human erythrocytes of different age: PTP1B processing during cell ageing. Bioelectrochemistry 2004;62:169-173.
41 Lutz HU, Bogdanova A: Mechanisms tagging senescent red blood cells for clearance in healthy humans. Front Physiol 2013;4:article 387.
42 Inaba M, Maede Y: Correlation between protein 4.1a/4.1b ratio and erythrocyte life span. Biochim Biophys Acta 1988;944:256-264.
43 Minetti G, Ciana A, Profumo A, Zappa M, Vercellati C, Zanella A, Arduini A, Brovelli A: Cell age-related monovalent cations content and density changes in stored human erythrocytes. Biochim Biophs Acta 2001;1527:149-155.
44 Romero PJ: Calcium and cell aging: the human red cell as a model. In: Advances in medicine and biology (ed. Bernhardt, LV). Volume 24, pp. 1-133, 2011. Nova Science Publishers, Inc.
45 Lew VL, Daw N, Etzion Z, Tiffert T, Muoma A, Vanagas L, Bookchin RM: Effects of age-dependent membrane transport changes on the homeostasis of senescent human red blood cells. Blood 2007;110:1334-1342.
46 Lucas M, Mata R, Romero A: Comparison of the active calcium extrusion, calcium buffering capacity and ATPase activity in rabbit reticulocytes and mature red cells. Biochim Biophys Acta 1988;942:65-72.
47 Wagner-Britz L, Wang J, Kaestner L, Bernhardt I: Protein kinase Cα and P-type Ca^{2+} channel $Ca_V2.1$ in red blood cell calcium signalling. Cell Physiol Biochem 2013;31:883-891.
48 de Jong K, Emerson RK, Butler J, Bastacky J, Mohandas N, Kuypers FA: Short survival of phosphatidylserine-exposing red blood cells in murine sickle cell anemia. Blood 2001;98:1577-1584.
49 Fadok VA, Bratton DL, Rose DM, Pearson A, Ezekewitz RA, Henson PM: A receptor for phosphatidylserine-specific clearance of apoptotic cells. Nature 2000;405:85-90.
50 Verhoeven B, Schlegel RA, Williamson P: Mechanisms of phosphatidylserine exposure, a phagocyte recognition signal, on apoptotic T lymphocytes. J Exp Med 1995;182:1597-1601.
51 Foeller M, Sopjani M, Mahmud H, Lang F: Vanadate-induced suicidal erythrocyte death. Kidney Blood Press Res 2008;31:87-93.
52 Bosman GJ, Were JM, Willekens FL, Novotný VM: Erythrocyte ageing in vivo and in vitro: structural aspects and implications for transfusion. Transfus Med 2008;18:335-347.
53 Vincenzi FF, Hinds TR: Decreased Ca pump ATPase activity associated with increased density in human red blood cells. Blood Cells 1988;14:139-159.
54 Lang F, Gulbins E, Lang PA, Zappulla D, Föller M: Ceramide in suicidal death of erythrocytes. Cell Physiol Biochem 2010;26:21-28.
55 Chung SM, Bae ON, Lim KM, Noh JY, Lee MY, Jung YS, Chung JH: Lysophosphatidic acid induces thrombogenic activity through phosphatidylserine exposure and procoagulant microvesicle generation in human erythrocytes. Arterioscler Thromb Vasc Biol 2007;27:414-421.
56 Maher AD, Kuchel PW: The Gardos channel: A review of the Ca^{2+}-activated K^+ channel in human erythrocytes. Int J Biochem Cell Biol 2003;35:1182-1197.
57 Tiffert T, Daw N, Etzion Z, Bookchin RM, Lew VL: Age decline in the activity of the Ca^{2+}-sensitive K^+ channel of human red blood cells. J Gen Physiol 2007;129:429-436.

2.2 Measurements of intracellular Ca^{2+} content and phosphatidylserine exposure in human red blood cells: Methodological issues

Mauro C. Wesseling, Lisa Wagner-Britz, Fatima Boukhdoud, Salome Asanidze, Duc Bach Nguyen, Lars Kaestner, Ingolf Bernhardt

Cell Physiol Biochem, 2016 Jun, 38, 2414-2425
DOI: 10.1159/000445593

Cellular Physiology and Biochemistry

Cell Physiol Biochem 2016;38:2414-2425
DOI: 10.1159/000445593
Published online: June 13, 2016
Accepted: May 17, 2016

1421-9778/16/0386-2414$39.50/0
www.karger.com/cpb

Original Paper

Measurements of Intracellular Ca^{2+} Content and Phosphatidylserine Exposure in Human Red Blood Cells: Methodological Issues

Mauro C. Wesseling[a] Lisa Wagner-Britz[a] Fatima Boukhdoud[a] Salome Asanidze[a] Duc Bach Nguyen[b] Lars Kaestner[c,d] Ingolf Bernhardt[a]

[a]Laboratory of Biophysics, Faculty of Natural and Technical Sciences III, Saarland University, Saarbrücken, Germany; [b]Department of Molecular Biology, Faculty of Biotechnology, Vietnam National Universityof Agriculture, Hanoi, Vietnam; [c]Institute for Molecular Cell Biology and Rearch Centre for Molecular Imaging and Screening, School of Medicine, Saarland University, Homburg, [d]Experimental Physics, Saarland University, Saarbrücken, Germany

Key Words
Red blood cells • Ca^{2+} content • Phosphatidylserine exposure • Lysophosphatidic acid • Flow cytometry • Fluorescence imaging

Abstract
Background/Aims: The increase of the intracellular Ca^{2+} content as well as the exposure of phosphatidylserine (PS) on the outer cell membrane surface after activation of red blood cells (RBCs) by lysophosphatidic acid (LPA) has been investigated by a variety of research groups. Carrying out experiments, which we described in several previous publications, we observed some discrepancies when comparing data obtained by different investigators within our research group and also between batches of LPA. In addition, we found differences comparing the results of double and single labelling experiments (for Ca^{2+} and PS). Furthermore, the results of PS exposure depended on the fluorescent dye used (annexin V-FITC *versus* annexin V alexa fluor® 647). Therefore, it seems necessary to investigate these methodological approaches in more detail to be able to quantify results and to compare data obtained by different research groups. ***Methods:*** The intracellular Ca^{2+} content and the PS exposure of RBCs separated from whole blood have been investigated after treatment with LPA (2.5 µM) obtained from three different companies (Sigma-Aldrich, Cayman Chemical Company, and Santa Cruz Biotechnology Inc.). Fluo-4 and x-rhod-1 have been used to detect intracellular Ca^{2+} content, annexin V alexa fluor® 647 and annexin V-FITC have been used for PS exposure measurements. Both parameters (Ca^{2+} content, PS exposure) were studied using flow cytometry and fluorescence microscopy. ***Results:*** The percentage of RBCs showing increased intracellular Ca^{2+} content as well as PS exposure changes significantly between different LPA manufacturers as well as on the condition of mixing of LPA with the RBC suspension. Furthermore, the percentage of RBCs showing PS exposure is reduced in double labelling compared to single labelling experiments and depends also on the fluorescent dye used. Finally, data on Ca^{2+} content are slightly affected whereas PS exposure data are not affected significantly by the measuring

Prof. Dr. Ingolf Bernhardt
Laboratory of Biophysics, Faculty of Natural and Technical Sciences III, Saarland University, Campus, 66123 Saarbrücken, (Germany)
Tel. +49 681 3026689, Fax +49 681 3026690, E-Mail i.bernhardt@mx.uni-saarland.de

KARGER

Cellular Physiology and Biochemistry
Cell Physiol Biochem 2016;38:2414-2425
DOI: 10.1159/000445593
Published online: June 13, 2016

method (flow cytometry, fluorescence microscopy). ***Conclusion:*** The LPA batch used and the mixing procedure of LPA and the RBC suspension has to be taken into consideration when comparing results of intracellular Ca^{2+} content and PS exposure of RBCs after LPA activation. In addition, one should consider that the results of single and double labelling experiments might be different depending on the fluorescent dyes used.

Introduction

In previous papers we have demonstrated that lysophosphatidic acid (LPA) or prostaglandin E_2 (PGE_2) open the non-specific, voltage-dependent cation (NSVDC) channel, which leads to an enhanced intracellular Ca^{2+} content of red blood cells (RBCs) [1, 2], although the molecular regulation mechanism of the Ca^{2+} entry still remains elusive. Both substances are local mediators released from platelets after their activation within the coagulation cascade. An increase of the intracellular Ca^{2+} content of RBCs can be also observed after activation of protein kinase Cα (PKCα), e.g. by phorbol-12 myristate-13 acetate (PMA). Two independent Ca^{2+} entry processes were reported, the first is P-Type $Ca_V2.1$ channel independent and the second is associated with a likely indirect activation of $Ca_V2.1$ [3]. A higher intracellular Ca^{2+} content leads to an activation of the scramblase, which in turn results in a significant exposure of phosphatidylserine (PS) in the outer membrane leaflet [4-6]. We also demonstrated that intracellular increase in Ca^{2+} induced by LPA leads to cell-cell adhesion of human RBCs [7, 8]. It has been reported that PS exposure in the outer membrane leaflet of the RBC membrane is of importance for the adhesion of RBCs to the endothelium in certain diseases (e.g. [9-12]). An active role of RBCs in thrombus formation has been proposed by Andrews and Low [13] whilst a correlation between decreased haematocrit and longer bleeding times has also been reported [14]. A signalling cascade was proposed by Kaestner et al. [2].

The increase of the intracellular Ca^{2+} content as well as the external presentation of PS after stimulation of RBCs by LPA or PMA has been investigated by many research groups [3, 7, 8, 15-23]. These investigations were mainly carried out to investigate physiological parameters affecting the PS exposure. Translocation of PS from the inner to the outer membrane leaflet of RBCs is a typical sign of eryptosis (a term introduced by Lang [24]), defining the suicidal death of RBCs. A large variety of physiological parameters as well as substances have been described to induce eryptosis (e.g., [25-31]).

The experiments on PS exposure performed in our research group have been carried out by several investigators. During these studies we observed quantitative discrepancies with respect to different investigators but also with respect to the LPA batches used. In addition, we realized differences comparing the results of double and single labelling experiments (for Ca^{2+} and PS). Furthermore, the results of PS exposure depended on the fluorescent dye used (annexin V-FITC *versus* annexin V alexa fluor® 647). We report here about the methodological approaches of the measurements of intracellular Ca^{2+} content as well as PS exposure to understand the challenge and to be able to compare results obtained by different research groups.

Material and Methods

Blood and solution

Human venous blood from healthy donors was obtained from the Institute of Sports and Preventive Medicine of Saarland University and the Institute of Clinical Haematology and Transfusion Medicine of Saarland University Hospital. EDTA or heparin was used as anticoagulants. Freshly drawn blood samples were stored at 4°C and used within one day. Blood was centrifuged at 2,000 g for 5 min at room temperature and the plasma and buffy coat was removed by aspiration. Subsequently, RBCs were washed 3 times in

HEPES-buffered physiological solution (HPS) containing (mM): NaCl 145, KCl 7.5, glucose 10, HEPES 10, pH 7.4 under the same conditions. Finally, the RBCs were re-suspended in HPS and stored at 4°C until the beginning of the experiment. The experiment was started immediately after resuspension of the RBCs.

Single labelling experiments

Measurement of intracellular Ca^{2+} content: RBCs were loaded with 1 µM fluo-4 AM or 1 µM x-rhod-1 AM from a 1 mM stock solution in dimethyl sulfoxide (DMSO) in 2 ml HPS. The extracellular Ca^{2+} concentration was 2 mM, i.e. $CaCl_2$ was added to the HPS. Cells were incubated at a haematocrit of 0.1 % in the dark for 30 min at 37°C with continuous shaking. Then the cells were washed again (16,000 g for 10 s), with an ice-cold HPS, re-suspended and measured as a control (at room temperature), or incubated with LPA (2.5 µM) at 37°C to activate Ca^{2+} uptake. Stock solutions for LPA from different companies (for comparison, 1 mM) were prepared in phosphate buffered saline. The incubation times with LPA were 1, 15 and 30 min. After incubation the cells were washed again (16,000 g for 10 s) with an ice-cold HPS, re-suspended and measured at room temperature.

Measurement of PS exposure: The cells were prepared as for measurement of the Ca^{2+} content. To detect the PS exposure, either annexin V-FITC or annexin V alexa fluor® 647, at a concentration of 4.5 µM was used. Annexin V binds to PS in the outer layer of the membrane and is coupled with a fluorescent dye (FITC or alexa fluor® 647), which can be measured by flow cytometry and fluorescence microscopy [32]. First a control measurement without LPA was performed. After that, LPA (2.5 µM) was added to activate the Ca^{2+} uptake. The cells were then incubated at 37°C for 1, 15 and 30 min. After incubation the cells were washed again (16,000 g for 10 s) with an ice-cold HPS and re-suspended. Finally, annexin V-FITC or annexin V alexa fluor® 647 was added to the cells. The staining was performed at a haematocrit of 0.1% in HPS solution with the addition of 2 mM Ca^{2+} at room temperature for 10 min. The measurements were also performed at room temperature.

The procedure to prepare the RBCs for measurement of intracellular Ca^{2+} content as well as PS exposure is based on the protocols of Nguyen et al. [15] and Wesseling et al. [16]. The time intervals between various incubation steps were kept as short as possible.

Double labelling experiments

For double labelling experiments we followed the protocols developed by Nguyen et al. [15] and Wesseling et al. [16]. The combinations of the fluorescent dyes applied were: (i) fluo-4 and annexin V alexa fluor® 647 or (ii) x-rhod-1 and annexin V-FITC to detect Ca^{2+} and PS, respectively.

For double labelling experiments the same procedure was used as for single labelling experiments to measure the Ca^{2+} content, i.e. for Ca^{2+} loading the extracellular Ca^{2+} concentration was 2 mM. The cells were stimulated with LPA and incubated at 37°C for 1, 15 and 30 min. After the last re-suspension of the RBCs for Ca^{2+} measurements (see above) annexin V-FITC or annexin V alexa fluor® 647 (4.5 µM) was added to detect PS and the cells incubated at room temperature for 10 min. Each sample has been measured first using flow cytometry and subsequently using fluorescence microscopy.

Flow cytometry

Intracellular free Ca^{2+} content as well as PS exposure was measured by flow cytometry (FACS Calibur and Cell Quest Pro software, Becton Dickinson Biosciences, Franklin Lakes, USA) as described before [15, 16, 33]. Ca^{2+} was measured in the FL-1 channel (excitation at 488 nm, emission at 520/15 nm) for fluo-4 and in the FL-2 channel (excitation at 550 nm, emission at 585/42 nm) for x-rhod-1. PS exposure in case of annexin V-FITC was detected also in the FL-1 channel. In case of annexin V alexa fluor® 647 it was detected in the FL-4 channel (excitation at 633 nm, emission at 661/16 nm) with a xenon diode. In all cases the negative and positive gates were identified based on control experiments (without stimulating substances) and A23187 (2 µM), respectively. Compensation was not necessary since there was no overlapping. The relative fluorescence intensity was analysed using the mean value of 30,000 cells from each blood sample. For each condition at least three different blood samples were used.

Fluorescence microscopy

The RBCs were monitored using an inverted fluorescence microscope (Eclipse TE2000-E, Nikon, Tokyo, Japan) as described before [15, 16]. The diluted RBC samples (approximately 0.025% haematocrit)

were placed on a cover slip in a dark room at room temperature. Images were taken with an electron multiplication CCD camera (CCD97, Photometrics, Tucson, USA) using a 100x1.4 (NA) oil immersion lens with infinity corrected optics. From each RBC sample, 5 images from different positions of the cover slip randomly chosen were taken using the imaging software VisiView (Visitron Systems, Puchheim, Germany). Each image consists of one transmitted light (exposure time 200 ms) and one (for single labelling) or two (for double labelling) fluorescence shot (exposure time 4 s). Fluo-4 and annexin V-FITC were excited with a xenon lamp-based monochromator (Visitron Systems, Puchheim, Germany) at a centre wavelength of 488 nm. Emission was recorded at 520/15 nm. X-rhod-1 and annexin V alexa fluor® 647 were excited at a centre wavelength of 543 nm and 661 nm, respectively. Emission was recorded at 610/20 nm for x-rhod-1 and 660/20 nm for annexin V alexa fluor® 647.

Reagents

If not mentioned otherwise, all chemicals used were purchased from Sigma-Aldrich (Munich, Germany). LPA was obtained from Sigma-Aldrich, Cayman Chemical Company (Ann Arbor, USA), and Santa Cruz Biotechnology Inc. (Heidelberg, Germany). Fluo-4 AM and annexin V-FITC were obtained from Molecular Probes (Eugene, USA) and annexin V alexa fluor® 647 from Roche Diagnostics GmbH (Mannheim, Germany).

Statistical significance

Data are presented as mean values ± SD of at least 3 independent experiments. The significance of differences was tested by ANOVA. Statistical significance of the data was defined as follows: $p > 0.05$ (n.s.); $0.01 < p \leq 0.05$ (*); $0.001 < p \leq 0.01$ (**); $p \leq 0.001$ (***).

Results and Discussion

Comparison of RBC activation using LPA from different companies

In our experiments described in previous papers [3, 15, 16, 21] we realised that RBC stimulation with LPA from different batches obtained from Sigma-Aldrich led to significant different results of the intracellular Ca^{2+} content as well as PS exposure. To investigate this phenomenon in more detail we performed experiments with LPA from 4 different batches, 2 from Sigma-Aldrich, one from Cayman Chemical Company, and one from Santa Cruz Biotechnology Inc. All 4 LPA probes were freshly ordered, re-frozen only once and were applied to the same blood on the same day and using the same HPS. In addition, all experiments were carried out by the same investigator using identical experimental conditions (see below). The results for double labelling measurement of intracellular Ca^{2+} content (with x-rhod-1) and PS exposure (with annexin V-FITC) in RBCs at LPA incubation times of 1 min, 15 min and 30 min using flow cytometry are shown in Fig. 1. The control data, i.e. Ca^{2+} content and PS exposure of RBCs without LPA activation, are shown at time zero. In all cases of LPA activation there is a significant increase in the percentage of RBCs showing increased intracellular Ca^{2+} content (Fig. 1A) and PS exposure (Fig. 1B) compared to control. Interestingly, there are significant differences in the percentages of RBCs responding with increased intracellular Ca^{2+} content as well as PS exposure depending on the LPA batch used. The highest LPA activation was obtained using one batch from Sigma-Aldrich (batch 1) and from Cayman Chemical Company (not significantly different) followed by a batch from Santa Cruz Biotechnology Inc. (significantly different from the two batches mentioned before). LPA from the second batch from Sigma-Aldrich (batch 2) resulted in much less stimulation (significantly different from all others) at any time point measured. In addition, we found that the LPA activation efficiency within a single batch decreased with the number of times the LPA stock solution was frozen and thawed. After 3 times thawing, the activation efficiency for Ca^{2+} measurements decreased by about 37% and 26% for fluo-4 and x-rhod-1, respectively. At the same time the activation efficiency for PS exposure decreased by 55%, both for annexin V-FITC and annexin V alexa fluor® 647. The findings are of importance comparing results of RBC activation with LPA from different batches of Sigma-Aldrich as

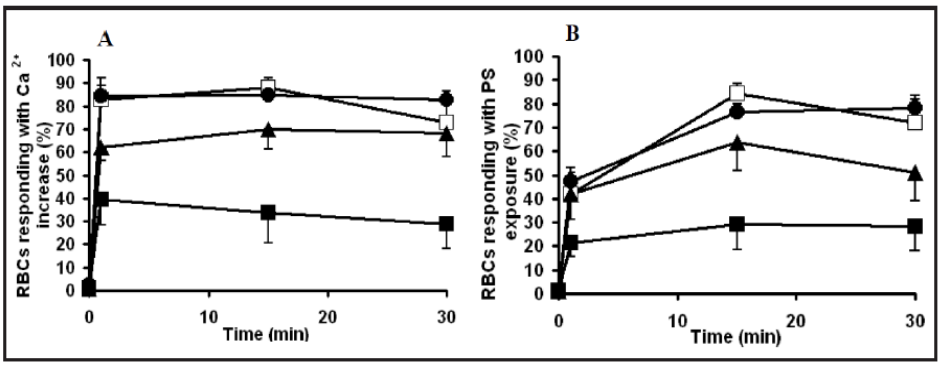

Fig. 1. Percentage of RBCs (A) responding with increased intracellular Ca^{2+} content (measured using x-rhod-1) and (B) responding with increased PS exposure (measured using annexin V-FITC) after activation with LPA (2.5 µM) obtained from different companies depending on time using flow cytometry. White square: LPA from Sigma-Aldrich (batch 1); dark square: LPA from Sigma-Aldrich (batch 2); dark circle: LPA from Cayman Chemical Company; dark triangle: LPA from Santa Cruz Biotechnology Inc. N = 3 (90,000 cells), error bars = S.D. (only half error bar is shown for convenience). Significant differences for LPA batches at a certain time, ANOVA ($0.01 < p \leq 0.05$ (*); $0.001 < p \leq 0.01$ (**); $p \leq 0.001$ (***)); for Ca^{2+} content, time point 1 min: * Cayman and Sigma 2 vs. Santa Cruz, *** Cayman and Sigma 1 vs. Sigma 2; time point 15 min: ** Santa Cruz vs. Sigma 2, *** Cayman vs. Sigma 2, Sigma 1 vs. Sigma 2; time point 30 min: ** Santa Cruz vs. Sigma 2, Sigma 1 vs. Sigma 2, *** Cayman vs. Sigma 2; for PS exposure, time point 1 min: * Cayman vs. Sigma 2; time point 15 min: ** Santa Cruz vs. Sigma 2, *** Cayman vs. Sigma 2, Sigma 1 vs. Sigma 2; time point 30 min: * Cayman vs. Santa Cruz, ** Sigma 1 vs. Sigma 2, *** Cayman vs. Sigma 2. Significant differences for LPA batches for PS exposure depending on time: LPA from Sigma 1: * 1 min vs. 30 min, ** 1 min vs. 15 min; LPA from Cayman: *** 1 min vs. 15 min and 30 min.

well as from different companies. For our investigations reported in the present paper we divided the obtained LPA into aliquots to avoid repeated thawing.

Comparison of RBC activation using LPA with different mixing conditions

To study a possible effect of the experimenter on the results obtained, we performed experiments with two different ways of mixing the RBC suspensions after LPA activation. Double labelling experiments for Ca^{2+} content (using x-rhod-1) and PS exposure (using annexin V-FITC) after activation of RBCs with LPA obtained from Cayman Chemical Company were compared following simple shaking by hand and with vortexing the RBC suspensions (both in Eppendorf tubes, 5 s each). The results are presented in Fig. 2. One can observe a significant higher percentage of RBCs responding with increased intracellular Ca^{2+} content as well as PS exposure when the suspension is vortexed after addition of LPA compared with simple shaking by hand. Similar relationships were obtained when the fluorescent dye combination fluo-4 (to detect Ca^{2+}) and annexin V alexa fluor® 647 (to detect PS) has been used (data not shown). These results suggest that a mechanosensitive channel, like the recently reported Piezo1, may contribute to the LPA-induced Ca^{2+} entry ([34] and references therein).

Comparison of RBC activation using LPA between single and double labelling. Effect of different fluorescent dyes

The intracellular Ca^{2+} content and the PS exposure of RBCs can be measured on the basis of single as well as double labelling experiments. Furthermore, different fluorescent dyes are available for the detection of either parameter. It was shown that fura-2 cannot be used for Ca^{2+} measurement in RBCs because of the haemoglobin absorption [35]. Commonly used for the Ca^{2+} and PS measurements are fluo-4 (or fluo-3) and annexin V-FITC, respectively [36-39]. However, for double labelling experiment the combination of these

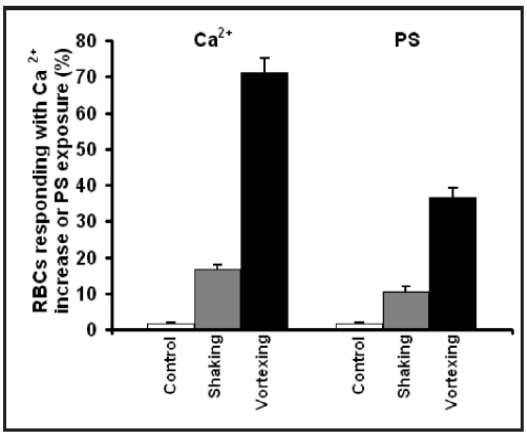

Fig. 2. Percentage of RBCs responding with increased intracellular Ca^{2+} content (detected with x-rhod-1) as well as PS exposure (detected with annexin V-FITC) after activation with LPA obtained from Cayman Chemical Company (2.5 µM) for 1 min with and without shaking by hand or vortexing the RBC suspensions using flow cytometry. Left 3 columns: RBCs with increased intracellular Ca^{2+} content. Right 3 columns: RBCs with increased PS exposure: White bars: control measurements (without LPA activation), grey bars: shaking the RBC suspensions by hand for 5 s, black bars: vortexing the RBC suspensions for 5 s. N = 3 (90,000 cells), error bars = S.D. (only half error bar is shown for convenience). Significant differences, ANOVA ($0.01 < p \leq 0.05$ (*); $0.001 < p \leq 0.01$ (**); $p \leq 0.001$ (***)); for Ca^{2+} content: ** control vs. LPA with shaking by hand, LPA with shaking by hand vs. LPA with vortexing, *** control vs. LPA with vortexing. For PS exposure: * control vs. LPA with shaking by hand, ** LPA with shaking by hand vs. LPA with vortexing, *** control vs. LPA with vortexing.

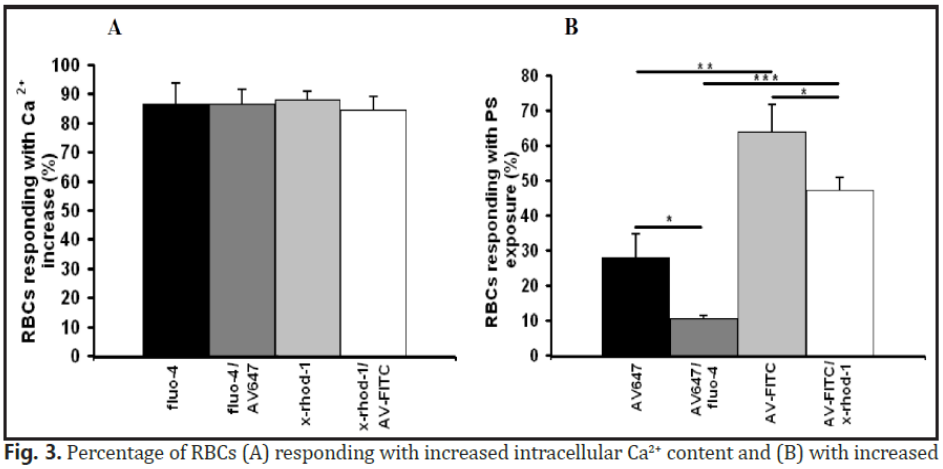

Fig. 3. Percentage of RBCs (A) responding with increased intracellular Ca^{2+} content and (B) with increased PS exposure after 1 min activation with LPA (2.5 µM) obtained from Cayman Chemical Company using flow cytometry. Comparison between single labelling (SL) and double labelling (DL) experiments using x-rhod-1 and fluo-4 for Ca^{2+} detection and annexin V-FITC and annexin V alexa fluor® 647 for PS detection. All experiments were done with vortexing the RBC suspensions. (A): Black column: SL, fluo-4, dark grey column: DL, fluo-4 and annexin V alexa fluor® 647 (AV647), light grey column: SL, x-rhod-1, white column: DL, x-rhod-1 and annexin V-FITC (AV-FITC). (B): Black column: SL, annexin V alexa fluor® 647 (AV647), dark grey column: DL, annexin V alexa fluor® 647 (AV647) and fluo-4, light grey column: SL, annexin V-FITC (AV-FITC), white column: DL, annexin V-FITC (AV-FITC) and x-rhod-1. N = 3 (90,000 cells), error bars = S.D. (only half error bar is shown for convenience). Significant differences, ANOVA ($0.01 < p \leq 0.05$ (*); $0.001 < p \leq 0.01$ (**); $p \leq 0.001$ (***)) are shown in the figure.

dyes is not suitable since they are both derivatives of fluorescein and thus their absorption and emission spectra are similar. Therefore, we compared results obtained on the basis of single labelling (fluo-4 and x-rhod-1 for Ca^{2+}, annexin V alexa fluor® 647 and annexin V-FITC for PS) and double labelling experiments using a combination of fluo-4 (for Ca^{2+}) / annexin V alexa fluor® 647 (for PS) and x-rhod-1 (for Ca^{2+}) / annexin V-FITC (for PS). The data after 1 min LPA activation are shown in Fig. 3. For these experiments LPA from Cayman Chemical Company was used. Fig. 3A indicates that for intracellular Ca^{2+} content there is no significant

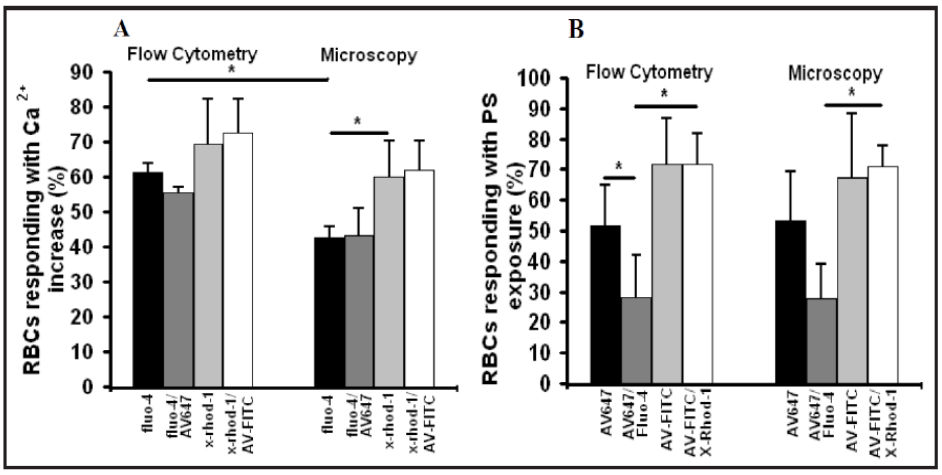

Fig. 4. Percentage of RBCs (A) responding with increased intracellular Ca^{2+} content and (B) with increased PS exposure after 30 min activation with LPA (2.5 µM) obtained from Sigma-Aldrich (batch 1). Comparison between flow cytometry (left 4 columns) and fluorescence microscopy (right 4 columns) measurements based on single labelling (SL) and double labelling (DL) experiments using x-rhod-1 and fluo-4 for Ca^{2+} detection and annexin V-FITC and annexin V alexa fluor® 647 for PS detection. All experiments were done with vortexing the RBC suspensions. (A): Black column: SL, fluo-4, dark grey column: DL, fluo-4 and annexin V alexa fluor® 647 (AV647), light grey column: SL, x-rhod-1, white column: DL, x-rhod-1 and annexin V-FITC (AV-FITC). (B): Black column: SL, annexin V alexa fluor® 647 (AV647), dark grey column: DL, annexin V alexa fluor® 647 (AV647) and fluo-4, light grey column: SL, annexin V-FITC (AV-FITC), white column: DL, annexin V-FITC (AV-FITC) and x-rhod-1. N = 3 (90,000 cells), error bars = S.D. (only half error bar is shown for convenience). Significant differences, ANOVA ($0.01 < p \leq 0.05$ (*); $0.001 < p \leq 0.01$ (**); $p \leq 0.001$ (***)) are shown in the figure.

difference between single and double labelling experiments. In addition, the results do not depend on the fluorescent dye (or the combination of the fluorescent dyes) used. The values for PS exposure are illustrated in Fig. 3B. It can be seen that the values of double labelling experiments are significantly lower for both fluorescent dyes (annexin V-FITC and annexin V alexa fluor® 647 (for PS), in combination with x-rhod-1 and fluo-4 (for Ca^{2+}), respectively) compared to single labelling experiments (annexin V-FITC or annexin V alexa fluor® 647 alone (for PS)). In addition, the amount of RBCs showing PS exposure is also significantly different in single labelling experiments when the cells were stained with annexin V-FITC in comparison to annexin V alexa fluor® 647 as well as in the corresponding double labelling experiments. Therefore, the combination of x-rhod-1 (to detect Ca^{2+} content) and annexin V-FITC (to detect PS exposure) seems to be more efficient than the combination of fluo-4 and annexin V alexa fluor® 647 in double labelling experiments. However, it should be taken into consideration that the PS data obtained in double labeling experiments are only hardly to compare with data obtained from single labeling measurements, because of the Ca^{2+} buffering by the Ca^{2+} fluorophor (see below).

In another set of experiments we investigated the intracellular Ca^{2+} content and PS exposure of RBCs after 30 min LPA activation. For these experiments LPA from one batch obtained from Sigma-Aldrich (batch 1) has been used. Results of single and double labelling experiments using different fluorescent dyes can be seen in Fig. 4. Figure 4A and 4B present data of Ca^{2+} and PS measurements, respectively, in which on the left side flow cytometry data and on the right side data obtained using fluorescence microscopy are shown (for analysing fluorescence microscopy images see below).

Similar to the results obtained after 1 min LPA activation, there are no significant differences in the Ca^{2+} content measured in single labelling experiments (fluo-4 and x-rhod-1

for Ca^{2+}) and the corresponding double labelling experiments using a combination of fluo-4 (for Ca^{2+}) / annexin V alexa fluor® 647 (for PS) and x-rhod-1 (for Ca^{2+}) / annexin V-FITC (for PS). In addition, the results of the experiments using fluo-4 and x-rhod-1 are also not significantly different (Fig. 4A, left). Comparing the data after 1 min and 30 min LPA activation (Figs. 3A and 4A), one can see in all cases a decrease of the Ca^{2+} content after 30 min. Such behaviour has been reported and explained in a recent publication [16]. For PS exposure, nearly the same tendency after 30 min compared to 1 min LPA activation can be seen (Fig. 4B, left). The results of single as well as double labelling experiment using annexin V alexa fluor® 647 for PS detection are again lower compared to the experiments where annexin V-FITC has been used (but only the double labelling data are significantly different). In addition, as for the 1 min LPA activation experiments, the amount of RBCs showing PS exposure is also significantly lower in double labelling compared to single labelling experiments when the cells were stained with annexin V alexa fluor® 647. Comparing the data after 1 min and 30 min LPA activation (Figs. 3B and 4B), one can see in all cases of measurement an increase of the PS exposure after 30 min. Such behaviour has been reported and explained in a recent publication [16].

The reasons for the differences in single labelling *versus* double labelling experiments as presented in Figs. 3 and 4 are multifactorial and can be explained by three major effects: (i) the Ca^{2+} buffering capacities of the Ca^{2+} fluorophores, (ii) the properties of the fluorescent dyes, and (iii) the temporal development of the Ca^{2+} signals.

(i) Fluo-4 and x-rhod-1 have *in vitro* dissociation constants K_d for Ca^{2+} of 345 nM and 700 nM, respectively [40]. In living cells these K_d's are, dependent on their cellular localisation, and are usually increased [41]. Especially when taking the low resting Ca^{2+} concentration in RBCs of around 60 nM [42] into account, the buffering capacity of the Ca^{2+} fluorophors loaded into the cells is high. The variety of the cellular responses [21] may add to the observed effects. Although the EC_{50} of the scramblase (30-70 µM) compared to the *in vivo* K_d of fluo-4 (1 µM) [43] is several fold higher, there are observations suggesting that scrambling may actually require much less Ca^{2+} [44], and therefore the buffering of the Ca^{2+} is the most likely explanation for a lower PS exposure in the double labelled cells as depicted in Figs. 3B and 4B. The relative decrease in PS exposure of the double labelling compared the single labelling is much higher for fluo-4 compared to x-rhod-1 (Fig. 3B). This observation is also in agreement with the K_d´s of the two fluorophors (see above) and hence their buffering properties.

(ii) Other aspects that may contribute to the differences between FITC and alexa fluor® 647 results are the photophysical properties of the dyes. Assuming that the fluorescence quantum yield of a cyanine dye (alexa fluor® 647) may change when the surrounding conditions are changed, e.g. in RBC haemoglobin close to the plasma membrane could be a factor influencing alexa fluor® 647. Isomerisation of double bonds of cyanine dyes is well known [45, 46]. Such changes in combination with wavelength dependencies of the detectors may account, at least partly, for the differences observed for PS detection based on FITC and alexa fluor® 647. Differences in incubation times for single and double labelling experiments as well as the solvent DMSO can be ruled out as sources for different results (we tested this by incubating the RBCs for 30 min in DMSO but without fluo-4, data not shown).

(iii) Apart from the different LPA batches, measurements between Fig. 3 and Fig. 4 differ in their measurement time after LPA stimulation (1 min *versus* 30 min, respectively). After 30 min LPA stimulation, the PS exposure, which is a cumulative process, reaches in the presence of x-rhod-1 the same value as that in the absence of x-rhod-1. As mentioned before, due to its K_d, x-rhod-1 buffers the Ca^{2+} at a higher level compared to fluo-4. This Ca^{2+} level allows a basal scramblase activity, which in combination with the temporal aspects explains the differences observed between Fig. 3B and Fig. 4B.

Furthermore, it is worthwhile to mention that de-esterification of the Ca^{2+} fluorophores may generate formaldehyde and thus affect RBC behaviour, namely by ATP-depletion [47], which can be prevented by the addition of pyruvate [48].

Comparison of RBC activation using LPA between flow cytometry and fluorescence microscopy measurements

In addition to flow cytometry investigations of intracellular Ca^{2+} content and PS exposure of RBCs, the same parameters were estimated from RBCs images of the same samples using fluorescence microscopy. The results obtained are presented for comparison in Fig. 4A and 4B (right). The percentage of RBCs after LPA activation showing an evaluated intracellular Ca^{2+} content is slightly lower when measured using fluorescence microscopy. This is in contrast to previous investigations, where a loss of high Ca^{2+} cells in flow cytometry due to their increased fragility was reported [49]. However, considering the hypothesis mentioned above, that a mechanosensitive channel contributes to the LPA-induced Ca^{2+} entry, the shear stress and pressure in flow cytometers could explain a higher Ca^{2+} content in flow cytometry compared to microscopy [50, 51]. Although there is such a tendency for all conditions measured, only for fluo-4 and single labelling experiments the difference is significant. For PS exposure no differences between flow cytometry and fluorescence microscopy measurements can be seen.

Conclusion

We were able to show that the results of measurements of the Ca^{2+} content as well as PS exposure of RBCs after LPA activation significantly depend on the LPA batches most probably due to the substance stability. We propose to handle that issue by limiting quantitative comparisons of data to those obtained with the same LPA batch. Nevertheless qualitative comparisons cross LPA batches and cross laboratories should still be possible.

We propose that differences in results due to the method of mixing LPA with the RBC suspension are caused by mechanosensitive ion channels. This hypothesis requires further investigations.

In addition, we demonstrated that annexin V-FITC is more sensitive in comparison to annexin V alexa fluor® 647 for the quantification of PS exposure both in single as well as double labelling experiments.

Furthermore, the percentage of RBCs showing PS exposure is reduced in double labelling compared to single labelling experiments, which is most probably caused by the Ca^{2+} buffering capacities of the Ca^{2+} indicators. It is an example how the measurement itself disturbs the process being investigated. It is an almost unavoidable side effect but should be taken into consideration.

Finally, data of Ca^{2+} content are slightly affected by the measuring method (flow cytometry *versus* fluorescence microscopy). Although compared to the issues discussed above, these are minor differences.

Acknowledgements

This research is funded by Vietnam National Foundation for Science and Technology Development (NAFOSTED) under grant number 106-YS.06-2013.16 for D. B. Nguyen, a grant from CNPq program "science without borders" to M. C. Wesseling, process number: 202426/2012-2 (Brasil) and from the European Union's Seventh Framework Programme for research, technological development and demonstration under grant agreement No 602121 (CoMMiTMenT) and the EU Framework Programme for Research and Innovation Horizon 2020, Maria Curie Innovative Training Network project under grant agreement No 675115 (RELEVANCE) to L. Kaestner. The authors are grateful for the discussion of the differences of the fluorescence intensities comparing the single and double labelling experiments to Prof. Gregor Jung, Department of Physical Chemistry, Saarland University. The authors thank Jörg Riedel for technical support.

Disclosure Statement

The authors declare no conflict of interest.

References

1 Kaestner L, Bollensdorff C, Bernhardt I: Non-selective voltage-activated cation channel in the human red blood cell membrane. Biochim Biophys Acta 1999;1417:9-15.
2 Kaestner L, Tabellion W, Lipp P, Bernhardt I: Prostaglandin E2 activates channel-mediated calcium entry in human erythrocytes: an indicator for a blood clot formation supporting process. Thromb Haemost 2004;92:1269-1272.
3 Wagner-Britz L, Wang J, Kaestner L, Bernhardt I: Protein kinase Cα and P-type Ca^{2+} channel CaV2.1 in red blood cell calcium signalling. Cell Physiol Biochem 2013;31:883-891.
4 Lang F, Qadri SM: Mechanisms and significance of eryptosis, the suicidal death of erythrocytes. Blood Purif 2012;33:125-130.
5 Föller M, Huber SM, Lang F: Critical Review. Erythrocyte programmed cell death. IUBMB Life 2008;60:661-668.
6 Woon LA, Holland JW, Kable EP, Roufogalis BD: Ca^{2+} sensitivity of phospholipid scrambling in human red cell ghosts. Cell Calcium 1999;25:313-320.
7 Steffen P, Jung A, Nguyen DB, Müller T, Bernhardt I, Kaestner L, Wagner C: Stimulation of human red blood cells leads to Ca^{2+}-mediated intercellular adhesion. Cell Calcium 2011;50:54-61.
8 Kaestner L, Steffen P, Nguyen DB, Wang J, Wagner-Britz L, Jung A, Wagner C, Bernhardt I: Lysophosphatidic acid induced red blood cell aggregation *in vitro*. Bioelectrochemistry 2012;87:89-95.
9 Closse C, Dachary-Progent J, Boisseau MR: Phosphatidylserine-related adhesion of human erythrocytes to vascular endothelium. Br J Haematol 1999;107:300-302.
10 De Jong K, Larkin SK, Styles LA, Bookchin RM, Kuypers FA: Characterization of the phosphatidylserine-exposing subpopulation of sickle cells. Blood 2001;98:860-867.
11 Sherman IW, Prudhomme J, Tait JF: Altered membrane phospholipid asymmetry in plasmodium falciparum-infected erythrocytes. Parasitol Today 1997;13:242-243.
12 Wali RK, Jaffe S, Kumar D, Kalra VK: Alterations in organization of phospholipids in erythrocytes as factor in adherence to endothelial cells in diabetes mellitus. Diabetes 1988;37:104-111.
13 Andrews D, Low PS: Role of red blood cells in thrombosis. Curr Opin Hematol 1999;6:76-82.
14 Hellem AJ: The adhesiveness of human blood platelets *in vitro*. Scand J Clin Lab Invest 1960;12:1-117.
15 Nguyen DB, Wagner-Britz L, Maia S, Steffen P, Wagner C, Kaestner L, Bernhardt I: Regulation of phosphatidylserine exposure in red blood cells. Cell Physiol Biochem 2011;28:847-856.
16 Wesseling MC, Wagner-Britz L, Huppert H, Hanf B, Hertz L, Nguyen DB, Bernhardt I: Phosphatidylserine exposure in human red blood cells depending on cell age. Cell Physiol Biochem 2016;38:1376-1390.
17 Andrews DA, Yang L, Low PS: Phorbol ester stimulates a protein kinase C-mediated agatoxin-TK-sensitive calcium permeability pathway in human red blood cells. Blood 2002;100:3392-3399.
18 De Jong K, Retting MP, Low PS, Kuypers FA: Protein kinase C activation induces phosphatidylserine exposure on red blood cells. Biochem 2002;41:12562-12567.
19 Tang F, Ren Y, Wang R, Lei X, Deng X, Zhao Y, Chen D, Wang X: Ankyrin exposure induced by activated protein kinase C plays a potential role in erythrophagocytosis. Biochim Biophys Acta 2016;1860:120-128.
20 Neidlinger NA, Larkin SK, Bhagat A, Victorino GP, Kuypers FA: Hydrolysis of phosphatidylserine-exposing red blood cells by secretory phospholipase A2 generates lysophosphatidic acid and results in vascular dysfunction. J Biol Chem 2006;281:775-781.
21 Wang J, Wagner-Britz L, Bogdanova A, Ruppenthal S, Wiesen K, Kaiser E, Tian Q, Krause E, Bernhardt I, Lipp P, Philipp SE, Kaestner L: Morphologically homogeneous red blood cells present a heterogeneous response to hormonal stimulation. PLoS ONE 2013;8:e67697.
22 Siegl C, Hamminger P, Jank H, Ahting U, Bader B, Danek A, Gregory A, Hartig M, Hayflick S, Hermann A, Prokisch H, Sammler EM, Yapici Z, Phrohaska R, Salzer U: Alterations of red cell membrane properties in Nneuroacanthocytosis. PLoS ONE 2013;8:e76715.

23 Chung SM, Bae ON, Lim KM, Noh JY, Lee MY, Jung YS, Chung JH: Lysophosphatidic acid induces thrombogenic activity through phosphatidylserine exposure and procoagulant microvesicle generation in human erythrocytes. Arterisoscler Thromb Vasc Biol 2007;27:414-421.
24 Lang KS, Lang PA, Bauer C, Duranton C, Wieder T, Huber SM, Lang F: Mechanisms of suicidal erythrocyte death. Cell Physiol Biochem 2005;15:195-202.
25 Peter T, Bissinger R, Enkel S, Alzoubi K, Oswald G, Lang F: Programmed erythrocyte death following *in vitro* Treosulfan treatment. Cell Physiol Biochem 2015;35:1372-80.
26 Faggio C, Alzoubi K, Calabrò S, Lang F: Stimulation of suicidal erythrocyte death by PRIMA-1. Cell Physiol Biochem 2015;35:529-40.
27 Zhang R, Xiang Y, Ran Q, Deng X, Xiao Y, Xiang L, Li Z: Involvement of calcium, reactive oxygen species, and ATP in hexavalent chromium-induced damage in red blood cells. Cell Physiol Biochem 2014;34:1780-91.
28 Arnold M, Bissinger R, Lang F: Mitoxantrone-induced suicidal erythrocyte death. Cell Physiol Biochem 2014;34:1756-67.
29 Tesoriere L, Attanzio A, Allegra M, Cilla A, Gentile C, Livrea MA: Oxysterol mixture in hypercholesterolemia-relevant proportion causes oxidative stress-dependent eryptosis. Cell Physiol Biochem 2014;34:1075-89.
30 Lupescu A, Bissinger R, Warsi J, Jilani K, Lang F: Stimulation of erythrocyte cell membrane scrambling by gedunin. Cell Physiol Biochem 2014;33:1838-48.
31 Jacobi J, Lang E, Bissinger R, Frauenfeld L, Modicano P, Faggio C, Abed M, Lang F: Stimulation of erythrocyte cell membrane scrambling by mitotane. Cell Physiol Biochem 2014;33:1516-26.
32 Vermes I, Haanen C, Steffens-Nakken H, Reutelingsperger C: A novel assay for apoptosis. Flow cytometric detection of phosphatidylserine expression on early apoptotic cells using fluorescein labelled Annexin V. J Immunol Methods 1995;184:39-51.
33 Kucherenko YV, Bernhardt I: Natural antioxidants improve red blood cell "survival" in non-leukoreduced blood samples. Cell Physiol Biochem 2015;35:2055-68.
34 Kaestner L: Channelizing the red blood cell: molecular biology competes with patch-clamp. Front Mol Biosci 2015;2:46.
35 Kaestner L, Tabellion W, Weiss E, Bernhardt I, Lipp P: Calcium imaging of individual erythrocytes: Problems and approaches. Cell Calcium 2006;39:13-19.
36 Ghashghaeinia M, Cluitmans JC, Akel A, Dreischer P, Toulany M, Köberle M, Skabytska Y, Saki M, Biedermann T, Duszenko M, Lang F, Wieder T, Bosman GJ: The impact of erythrocyte age on eryptosis. Br J Haematol 2012;157:606-614.
37 Ghashghaeinia M, Cluitmans JC, Toulany M, Saki M, Köberle M, Lang E, Dreischer P, Biedermann T, Duszenko M, Lang F, Bosman GJ, Wieder T: Age sensitivity of NFκB abundance and programmed cell death in erythrocytes induced by NFκB inhibitors. Cell Physiol Biochem 2013;32:801-813.
38 Lang E, Bissinger R, Fajol A, Salker MS, Singh J, Zelenak C, Ghashghaeinia M, Gu S, Jilani K, Lupescu A, Reyskens KMSE, Ackermann TF, Föller M, Schleicher E, Sheffield WP, Arthur JSC, Lang F, Qadri SM: Accelerated apoptotic death and *in vivo* turnover of erythrocytes in mice lacking functional mitogen- and stress-activated kinase MSK1/2. Sci Reports 2015;5:17316.
39 Klarl BA, Lang PA, Kempe DS, Niemoeller OM, Akel A, Sobiesiak M, Eisele K, Podolski M, Huber SM, Wieder T, Lang F: Protein kinase C mediates erythrocyte "programmed cell death" following glucose depletion. Am J Physiol Cell Physiol 2006;290:C244-253.
40 Haugeland RP: Handbook of fluorescent probes and research products, ed 9. Molecular Probes Inc, 2002.
41 Lipp P, Kaestner L: Detecting calcium in cardiac muscle: fluorescence to dye for. Am J Physiol Heart Circ Physiol 2014;307:H1687–1690.
42 Tiffert T, Bookchin RM, Lew VL: Calcium homeostasis in normal and abnormal human red cells; In Bernhardt I, Ellory JC (eds): Red cell membrane transport in health and disease. Heidelberg, Springer Verlag, 2003, pp 373-405.
43 Bogdanova A, Makhro A, Wang J, Lipp P, Kaestner L: Calcium in red blood cells - a perilous balance. Int J Mol Sci 2013;14:9848–9872.
44 Weiss E, Cytlak UM, Rees DC, Osei A, Gibson JS: Deoxygenation-induced and Ca^{2+} dependent phosphatidylserine externalisation in red blood cells from normal individuals and sickle cell patients. Cell Calcium 2012;51:51–56.
45 Widengren J, Schwille P: Characterization of photoinduced isomerization and back-isomerization of the cyanine dye Cy5 by fluorescence correlation spectroscopy. J Phys Chem 2000;104:6416-6428.

46 Zanetti-Domingues LC, Tynan CJ, Rolfe DJ, Clarke DT, Martin-Fernandez M: Hydrophobic fluorescent probes introduce artifacts into single molecule tracking experiments due to non-specific binding. PLoS ONE 2013;8:e74200.
47 Tiffert T, García-Sancho J, Lew VL: Irreversible ATP depletion caused by low concentrations of formaldehyde and of calcium-chelator esters in intact human red cells. Biochim Biophys Acta 1984;773:143–156.
48 García-Sancho J: Pyruvate prevents the ATP depletion caused by formaldehyde or calcium-chelator esters in the human red cell. Biochim Biophys Acta 1985;813:148–150.
49 Minetti G, Egée S, Mörsdorf D, Steffen P, Makhro A, Achilli C, Ciana A, Wang J, Bouyer G, Bernhardt I, Wagner C, Thomas S, Bogdanova A, Kaestner L: Red cell investigations: art and artefacts. 2013;27:91–101.
50 Bouchy M, Donner M, Andre JC: Erythrocyte membranes alteration in a shear stress measured by fluorescence anisotropy. Cell Biophys 1990;17:213-225.
51 Lakowicz JR: Principles of fluorescence spectroscopy, ed 3. New York, Springer Science + Business Media, LLC, 2006.

2.3 Characterization of microvesicles released from human red blood cells

Duc Bach Nguyen, Thi Bich Thuy Ly, Mauro Carlos Wesseling, Marius Hittinger, Afra Torge, Andrew Devitt, Yvonne Perrie, Ingolf Bernhardt

Cell Physiol Biochem, 2016 Mar, 38, 1085-1099
DOI: 10.1159/000443059

Cellular Physiology and Biochemistry

Cell Physiol Biochem 2016;38:1085-1099
DOI: 10.1159/000443059
Published online: March 04, 2016
Accepted: February 10, 2016

1421-9778/16/0383-1085$39.50/0
www.karger.com/cpb

Original Paper

Characterization of Microvesicles Released from Human Red Blood Cells

Duc Bach Nguyen[a] Thi Bich Thuy Ly[b] Mauro Carlos Wesseling[c] Marius Hittinger[d] Afra Torge[e] Andrew Devitt[f] Yvonne Perrie[g] Ingolf Bernhardt[c]

[a]Department of Molecular Biology, Faculty of Biotechnology, Vietnam National University of Agriculture, Ngo Xuan Quang, Trau Quy, Gia Lam, Hanoi, [b]Institute of Biotechnology, Vietnam Academy of Science and Technology, Hanoi, Vietnam; [c]Laboratory of Biophysics, Faculty 8, Saarland University, Saarbruecken, [d]PharmBioTec GmbH, Saarbruecken, Germany and Helmholtz-Institute for Pharmaceutical Research Saarland, Saarbruecken, [e]Department of Pharmacy, Biopharmaceutics and Pharmaceutical Technology, Saarland University Saarbruecken, Germany; [f]School of Life & Health Sciences, Aston University, Aston Triangle, Birmingham, [g]Aston Pharmacy School, Aston University, Aston Triangle, Birmingham, UK

Key Words
Red blood cells • Microvesicles • Phosphatidylserine • Fluorescence imaging • Cell adhesion

Abstract
Background/Aims: Extracellular vesicles (EVs) are spherical fragments of cell membrane released from various cell types under physiological as well as pathological conditions. Based on their size and origin, EVs are classified as exosome, microvesicles (MVs) and apoptotic bodies. Recently, the release of MVs from human red blood cells (RBCs) under different conditions has been reported. MVs are released by outward budding and fission of the plasma membrane. However, the outward budding process itself, the release of MVs and the physical properties of these MVs have not been well investigated. The aim of this study is to investigate the formation process, isolation and characterization of MVs released from RBCs under conditions of stimulating Ca^{2+} uptake and activation of protein kinase C. ***Methods:*** Experiments were performed based on single cell fluorescence imaging, fluorescence activated cell sorter/flow cytometer (FACS), scanning electron microscopy (SEM), atomic force microscopy (AFM) and dynamic light scattering (DLS). The released MVs were collected by differential centrifugation and characterized in both their size and zeta potential. ***Results:*** Treatment of RBCs with 4-bromo-A23187 (positive control), lysophosphatidic acid (LPA), or phorbol-12 myristate-13 acetate (PMA) in the presence of 2 mM extracellular Ca^{2+} led to an alteration of cell volume and cell morphology. In stimulated RBCs, exposure of phosphatidylserine (PS) and formation of MVs were observed by using annexin V-FITC. The shedding of MVs was also observed in the case of PMA treatment in the absence of Ca^{2+}, especially under the transmitted bright field illumination. By using SEM, AFM and DLS the morphology and size of stimulated RBCs, MVs were characterized. The sizes of the two populations of MVs were 205.8 ± 51.4 nm and 125.6 ± 31.4 nm, respectively. Adhesion of stimulated RBCs and MVs was observed. The zeta potential

Duc Bach Nguyen

Department of Molecular Biology, Faculty of Biotechnology, Vietnam National University of Agriculture, Ngo Xuan Quang, Trau Quy, Gia Lam, Hanoi, (Vietnam)
Tel. +84 983 926497, E-Mail ndbach@vnua.edu.vn, E-Mail ndbach@gmail.com

Cellular Physiology and Biochemistry
Cell Physiol Biochem 2016;38:1085-1099
DOI: 10.1159/000443059
Published online: March 04, 2016

www.karger.com/cpb

of MVs was determined in the range from - 40 mV to - 10 mV depended on the solutions and buffers used. ***Conclusion:*** An increase of intracellular Ca^{2+} or an activation of protein kinase C leads to the formation and release of MVs in human RBCs.

Introduction

Under physiological as well as pathological conditions, various cell types release small spherical fragments called membrane vesicles or extracellular vesicles (EVs). So far many different terms for these EVs such as ectosomes, microvesicles (MVs), shedding vesicles, apoptosomes or microparticles have been used in a number of reports [1-5]. Recently, based on their size and origin of formation, EVs have been classified as exosomes, MVs and apoptotic bodies [6-10].

Exosomes are small enclosed membrane vesicles of nearly uniform size from 30 to 100 nm already described by Johnstone during the *in vitro* culture of sheep reticulocytes [11]. They were also observed in a variety of cultured cells such as lymphocytes, dendritic cells, cytotoxic T cells, mast cells, neurons, oligodendrocytes, Schwann cells, and intestinal epithelial cells [12, 13]. In these cells, exosomes originated from the endosomal network that locates within large sacs in cytoplasm. The release of exosomes to extracellular environment is carried out by the fusion of these sacs to the plasma membrane [7, 12, 14].

Distinct from exosomes, the biogenesis of MVs arises through direct outward budding and fission of the plasma membrane following different kinds of cell activation or during early state of apoptosis [15]. Normally, MVs are larger compared to exosomes with the size ranging from 50 to 1000 nm [15-17]. However, there is an overlapping of the size between exosomes and MVs. So far the mechanism of biogenesis is primarily used to distinguish MVs and exosomes [4, 6, 16]. The formation and release of MVs is the result of dynamic processes of phospholipid redistribution and cytoskeletal protein breakdown [6].

A vast amount of literature dealing with the release mechanism of MVs in RBCs and their properties in response to A23187, ATP depletion, oxidative stress and storage has been reported (e.g. [18-24]). In addition, an increase of the levels of RBC-derived MVs in the circulating blood of patients with sickle cell anemia (SCA), thalassemia and glucose-6-phosphate-deficiency (G6PD) has been observed [25, 26]. Morphological transitions of RBCs stimulated by exogenous compounds, according to the bilayer-couple hypothesis, also result in the formation of MVs [19, 22, 27]. Furthermore, the reorganization of the cell membrane such as loss of asymmetrical membrane phospholipid distribution leads to membrane blebbing and formation of MVs [28-31]. Recently, numbers of studies have shown that an increase of the intracellular Ca^{2+} concentration by opening Ca^{2+} channels or activation of protein kinase C (PKC) leads to PS exposure and formation of MVs in many different cell types including human RBCs [29, 30, 32, 33].

In contrast, apoptotic bodies have been characterized as largest EVs with the size varying from 1 to 5 µm. Nucleated cells undergoing apoptosis pass through several stages, beginning with condensation of the nuclear chromatin, followed by membrane blebbing, and finally releasing EVs and apoptotic bodies [6]. However apoptotic cells are also known to release smaller vesicles (MV) in response to apoptosis induction and these MVs are known to stimulate innate immune responses [34]. Although mature human RBCs have no nucleus and organelles, however, they are able to undergo an apoptosis-like process (also called eryptosis [28, 29]) with similar characteristics, e.g. membrane blebbing and formation of MVs [28, 29].

Although there is a number of reports about the formation of MVs in RBCs, investigations of the kinetics of this process as well the characterization of released MVs are still limited. By using different methods and techniques we investigated the kinetics of formation of MVs. In addition, the MVs released from human RBCs under different conditions were also isolated and characterized. The study may contribute for understanding the role of MVs in normal biological process and diseases.

Cellular Physiology and Biochemistry
Cell Physiol Biochem 2016;38:1085-1099
DOI: 10.1159/000443059
Published online: March 04, 2016

www.karger.com/cpb

Materials and Methods

Blood and solutions

Fresh human venous blood from healthy donors was obtained from the Institute of Sports and Preventive Medicine (Saarland University, Saarbruecken) and from the Institute of Clinical Haematology and Transfusion Medicine (Saarland University Hospital, Homburg). Blood was withdrawn by venipuncture into citrate-coated tubes or with heparin as anticoagulant, stored at 4°C and used within one day. Freshly whole blood was centrifuged at 2,000 g for 5 min at room temperature and the plasma and buffy coat was removed by aspiration. Subsequently, RBCs were washed 3 times in HEPES buffered physiological solution (HPS) containing (mM): NaCl 145, KCl 7.5, glucose 10, HEPES 10, pH 7.4. Finally, RBCs were re-suspended in HPS and kept at 4°C for experiments.

For experiments, RBCs were used at 0.05% haematocrit in HPS containing additionally 2 mM$CaCl_2$ and incubated with Ca^{2+} inonophore 4-bromo-A23187 (positive control, further abbreviated as A23187) or LPA or PMA. After 2 h incubation at 37°C cells were washed in HPS. The concentrations of A23187, LPA, and PMA chosen in the present study are in accordance with previous investigations showing an optimal effect [30, 35].

Kinetic study of the formation and release of microvesicles

The formation and shedding of MVs was investigated by using an inverted fluorescence microscope (Eclipse TE2000-E, Nikon, Tokyo, Japan) under both transmitted bright field illumination and fluorescence modes. The exposure of phosphatidylserine (PS) in the outer layer of the plasma membrane and in MVs can be displayed by annexin V-FITC with excitation and emission wavelength at 488 nm and 512 nm, respectively. RBCs were prepared in HPS in the presence of 2 mM $CaCl_2$and 5 µl of annexin V-FITC (0.05% haematocrit). The suspension was transferred to a cover slip (previously coated with poly-L-lysine 0.01%). When the cells were settled on the surface of the cover slip, an imaging procedure for the kinetics of MVs formation was recorded immediately after adding A23187 at final concentration of 2 µM or PMA at 6 µM. For experiment with LPA, the substance was added before the addition of Ca^{2+} (to avoid the influence of Ca^{2+} on the solubility of this moiety [36]). Experiments in the presence of A23187, LPA, or PMA were also carried out in the absence of extracellular Ca^{2+} by adding 2 mM EGTA. For controls, ethanol or DMSO was added.

To take into consideration a possible effect of the intracellular glutathione (GSH) level, bright field imaging experiments were performed with RBCs pre-incubated with N-Acetyl-L-Cysteine (NAC) for 1 h and then stimulated with PMA under 4 different conditions: without NAC, treated with NAC (1 mM), PMA, and NAC plus PMA. All these experiments were carried out in HPS with and without Ca^{2+}.

Our experimental approach was designed to provide a real-time assessment of the formation of MVs, while maintaining identical imaging parameters under all conditions. This was accomplished by taking images with an electron multiplication CCD camera (CCD97, Photometrics, Tucson, USA) using a 100×1.4 (NA) oil immersion lens with infinity corrected optics. An image was taken every 20 s for 120 min using the imaging software VisiView (Visitron Systems GmbH, Puchheim, Germany). Exposure time was 4000 ms for fluorescence and 100 ms for bright field transmitted light. Experiments were performed at room temperature in a dark room.

Stimulation of RBCs and isolation of MVs

RBCs were treated with LPA, PMA or A23187 as stated before for stimulating the formation of EVs. RBCs were suspended in HPS solution at 0.05% haematocrit in the presence of 2 mM $CaCl_2$. Subsequently, A23187 or LPA or PMA was added at concentrations of 2 µM, 2.5 µM or 6 µM, respectively (LPA was added before the addition of Ca^{2+}). After incubation for 2 h at 37°C with occasionally shaking, cell suspensions were subjected to differential centrifugation. First, a centrifugation step at 1,500 g for 10 min was applied followed by centrifugation at 3,000 g for 15 min twice to remove intact cells, cell debris, and apoptotic blebs. The supernatants were collected and further centrifuged at 25,000 g for 1 h at 4°C to harvest large size MVs. Subsequently, the collected supernatants were transferred to new tubes and ultra-centrifuged at 35,000 rpm (corresponding to about 200,000 g) for 2 h at 4°C for the isolation of small size MVs (Beckman Coulter, Swinging Bucket rotor SW40 Ti, k-factor 137).

To obtain all MVs, after removing intact cells, cell debris, and apoptotic blebs, the supernatants were directly subjected to ultra-centrifuge at 200,000 g for 2 h at 4ºC. Pellets obtained after each centrifugation step were re-suspended in Milli-Q water (ultra-pure) for morphological, size and zeta potential measurements.

Flow cytometry

Samples were analyzed using a FACScalibur Flow Cytometer (Becton Dickinson Biosciences, Franklin Lakes, USA) and BD CellQuest™ Pro Software 5.2.1. All acquisition and analysis were done using log mode. The parameters were set up using standard calibration kit (BD Calibrite™, BD Calibrite 3 Beads, BD Biosciences). Parameters of both forward and side scatter were adjusted to remove instrument noise (dust). The gating process was done by using a combination of sheath fluid (blank), samples of stimulated RBCs, isolated MVs stained with fluorescence dyes annexin V-FITC for PS and Dil as lipophilic tracer.

Morphological analysis using SEM and AFM

Stimulated RBCs under conditions mentioned above were fixed with 2% glutaraldehyde at room temperature for 10 min and washed in phosphate buffered saline, pH 7.4 (PBS-TWEEN® Tablets, 1 tablet per litre, Calbiochem - Merck, Darmstadt, Germany) by centrifugation at 5,000 g for 5 min at room temperature to remove glutaraldehyde. The pellets were re-suspended in Milli-Q water and immediately applied on glass slides and air-dried for 1 h. The slides were dipped quickly and gently washed stepwise with ethanol from 50, 70, 90 to 100% for dehydration. For SEM analysis, the prepared slides were sputtered with a gold layer of 15 nm thickness prior to SEM imaging (Sputter coater: Quorum Q150R ES, Quorum Technologies Ltd, East Grinstead, UK) and kept in a closed box at room temperature.

To prepare samples of MVs for SEM analysis, these particles were fixed with 2% glutaraldehyde for 10 min at room temperature. Subsequently the samples were washed in phosphate buffered saline by an ultra-centrifuge step at 200,000 g for 30 min at 4°C. Further steps were performed similar to the preparation of stimulated RBCs described above.

For SEM imaging (EVO HD15, Carl Zeiss Microscopy GmbH, Jena, Germany), several randomly selected frames from each sample were captured for morphological observation and statistical purpose. SEM imaging was carried out using 5 kV acceleration voltage and secondary electron (SE) detector.

AFM equipment (Bioscope IV, Veeco Instruments, Santa Barbara, USA) was used for topographical imaging. Glutaraldehyde-fixed samples of stimulated RBCs, MVs were scanned in air by tapping-mode. The cantilever OMCL-AC160TS series (Olympus) was used with nominal spring constant of 26 N/m, tip radius less than 10 nm and reflective side coated with Al. Data of height, amplitude and phase modes were recorded simultaneously. The images were scanned at the resolution of 256 × 256 pixels, scanning rate in the range from 0.3 to 0.75 Hz. Topographical images were analyzed and displayed using NanoScope Analysis 1.5 software (Brucker Corporation).

Size and zeta potential measurement

A Zetasizer Nano ZS (Malvern, Worcestershire, UK) was used for MVs size and zeta potential measurement. Uniform polystyrene particles of 100, 200 and 400 nm diameter (Bangs Laboratories, Fishers, USA) at 001% in phosphate buffered saline (PBS) were used to verify instrument operation. For size measurement, the MVs samples were diluted in Milli-Q water (attenuator index position in the range from 7 to 9) and analyzed using the standard operation procedure (SOP) as follows: sample refractive index 1.43 (phospholipid liposomes), dispersant refractive index 1,33 (water), system temperature at 25°C and sample equilibration time for 60 s. One ml of each sample was measured in disposable polystyrene (DTS0012, Malvern Instruments) with a path length of 10 mm. Observed populations of particles were characterized by associated Z-average size (nm) and polydispersity index (PdI).

For zeta potential measurement, the disposable capillary cell DTS1070 (Malvern Instruments) was used. Samples were measured in different solutions and buffers: Milli-Q water, NaCl 5 mM or 10 mM, and Tris-HCl 5 mM or 10 mM, pH 7.0. The SOP was set up similar as described above. Each sample was measured 3 times with maximum 100 runs in automatic mode. Observed populations of particles were characterized by associated phase (rad) and zeta potential (mV).

The Malvern Zetasizer software v7.03 was used to collect and analyze the data. The error bars displayed on the DLS graphs were presented by the standard deviation (SD) of three measurements of the same sample.

Reagents

A23187, LPA, PMA and NAC were purchased from Sigma-Aldrich (St. Louis, USA). Annexin V-FITC and Dil stain (DiIC18(3)) were obtained from Life Technologies (Carlsbad, USA). In this study, A23187 was

dissolved in absolute ethanol at 1 mM. LPA and PMA were dissolved in DMSO at 1 mM and stored at -20°C. NAC was prepared as 0.5 M stock solution in water placed in a heating block for 1 h. Glutaraldehyde (for electron microscopy), and all other chemicals were at analytical grade and purchased from Sigma-Aldrich.

Statistics

Data are presented as the mean values ± S.D. of at least 3 experiments of different blood samples. Statistical analysis was performed using Student's t-test when Gaussian distributed. The values were taken as significant difference when $p \leq 0.05$ or $p \leq 0.01$. Otherwise, a Mann-Whitney test was performed.

Results

Kinetic formation of microvesicles

It has been shown that treatment of human RBCs with A23187, LPA, or PMA in the presence of extracellular Ca^{2+} leads to an increase of intracellular Ca^{2+} and exposure of PS in the outer cell membrane leaflet [30, 32, 37]. In our recent publication we mentioned that after treatment of human RBCs with these substances MVs have been observed [30]. However, this observation was not in the focus of that paper. Therefore, in this paper we investigated the process of membrane blebbing and formation of MVs and characterized these particles in more detail. Figure 1 shows the kinetics of the formation and the outward budding process of MVs in human RBCs after stimulation with A23187, LPA or PMA. The lag time before the formation of MVs started was different among different substances used for stimulation.

Treatment with A23187 resulted in a reduction of cell volume already after 5 min (not shown but can be seen in [30, 35]). The formation of MVs can be clearly seen after 15 min (small spots on the surface of RBCs and in the solution). The MVs were formed and subsequently released into the medium. The exposure of PS can be observed also after 15 min. After 2 h almost all cells show PS exposure and MVs on the cell membrane (Fig. 1, upper row).

In case of LPA treatment, after 10 min, there was an alteration in the morphology of RBCs from the echinocyte or discocyte to a spherical shape (not shown). Subsequently, MVs begin to appear on the cell surface. Although the process of PS exposure on the outer leaflet

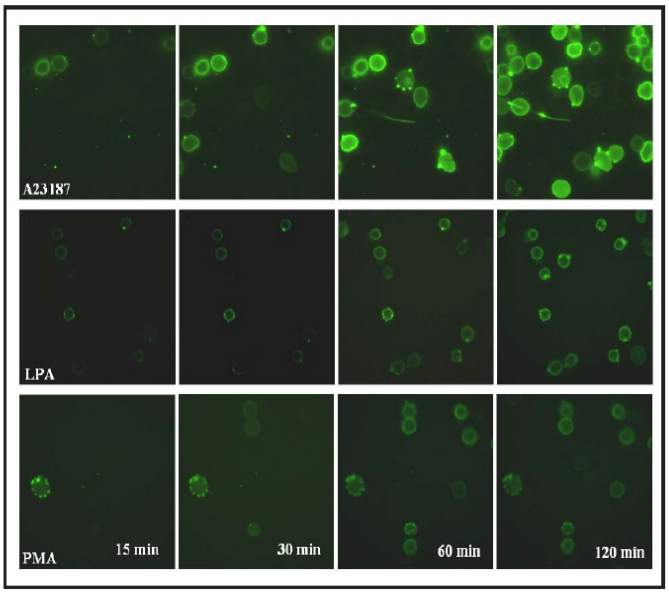

Fig. 1. Fluorescence imaging of the formation of MVs in human RBCs depending on time (up to 120 min) stimulated with 2 µM A23187 (upper row), 2.5 µM LPA (middle row) and 6 µM PMA (lower row) in the presence of 2 mM $CaCl_2$. Annexin V-FITC has been used for PS staining. The images of time zero (0 min) were not presented because of the completely absence of fluorescence signal. One typical experiment out of 10 is shown.

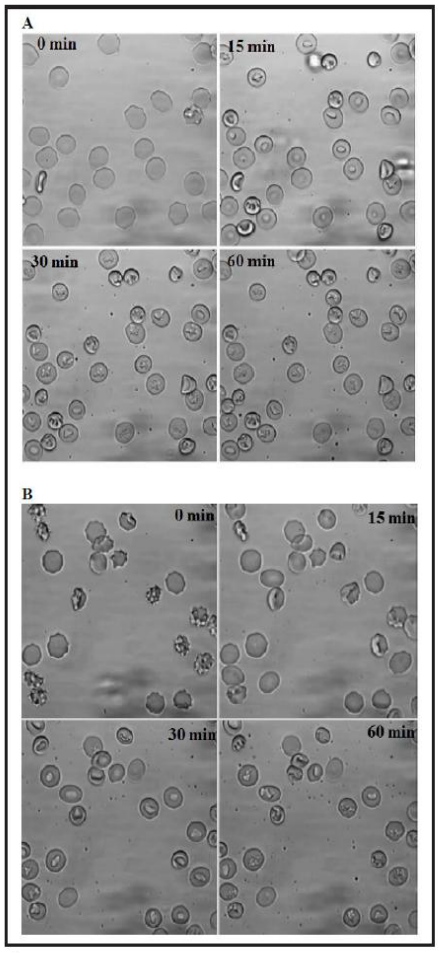

Fig. 2. Bright field imaging of the formation of MVs in human RBCs depending on time (up to 60 min) stimulated by 6 μM PMA in the absence of $CaCl_2$ (with 2 mM EGTA) (A) or in the presence of 2 mM $CaCl_2$ (B). One typical experiment out of 6 is shown.

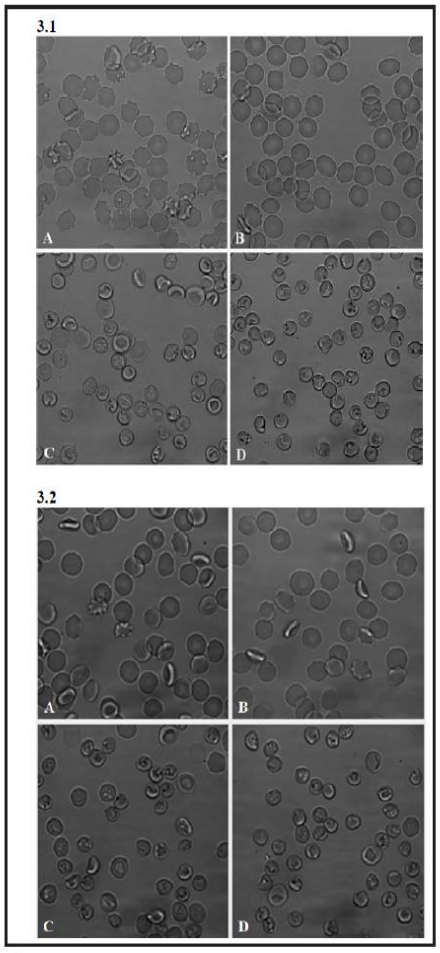

Fig. 3. Bright field imaging of the shape and the formation of MVs in human RBCs in the absence of $CaCl_2$ (with 2 mM EGTA) (Fig. 3.1) or in the presence of 2 mM $CaCl_2$ (Fig. 3.2). A: RBCs in HPS without NAC; B: RBCs treated with 1 mM NAC for 1 h; C: RBCs treated with 6 μM PMA in the absence of NAC for 1 h; D: RBCs treated with 6 μM PMA and 1 mM NAC for 1 h. One typical experiment out of 3 is shown.

of cell membrane was faster in comparison to the case of A23187 treatment, the number of cells showing a positive annexin V- FITC signal was about 60% of the cells only (Fig. 1, middle row).

In the presence of PMA, RBCs with echinocyte or discocyte shape showed a tendency to change their morphology to stomatocytes after 10 min of treatment. The stomatocyte shape was unchanged over time and coupled with the formation and shedding of MVs (Figs. 2 and 3.1) after 15 min of treatment. The exposure of PS in the outer leaflet of the cell membrane could be observed in about 70% of the cells after 2 h of treatment (Fig. 1, lower row).

Under all experimental conditions, the exposure of PS in the outer cell membrane leaflet and the formation of MVs were observed. However, the fluorescence signal of annexin V-FITC in case of PMA is significant lower in comparison to LPA or A23187 (Fig. 1).

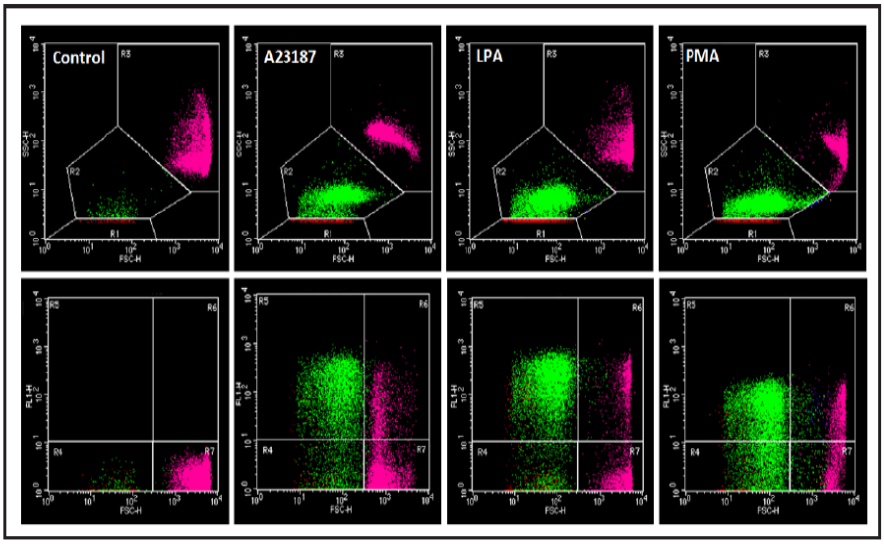

Fig. 4. Flow cytometry analysis of stimulated RBCs stained with annexin V-FITC. RBCs were stimulated with A23187, LPA or PMA for 2 h. The dot plots display the characteristics of the RBCs and MVs, the SSC *vs.* FSC (upper row) and the FL1 *vs.* FSC (lower row). Gates R1: instrument noise; R2: MVs and exosomes; R3: intact RBCs; R4: negative populations of small particles, MVs and exosomes; R5: positive population of MVs and exosomes; R6: positive population of RBCs; R7: negative population of RBCs.

Fluorescence imaging using annexin V-FITC for PS staining (Fig. 1) showed that under all stimulating conditions (A23187, LPA, PMA) only a small but more or less identical amount of MVs could be observed. However under bright-field imaging much more MVs can be seen in case of PMA treatment compared to fluorescence imaging (cp. Figs. 1, 2B) and compared to bright field imaging of cells and MVs after A23187 and LPA treatments (not shown). Furthermore, with bright field imaging, the formation of MVs was also clearly observed when RBCs were treated with PMA in the absence of Ca^{2+} (Fig. 2A).

Treatment of RBCs with NAC (1 mM) did not lead to changes of cell morphology in the presence or absence of extracellular Ca^{2+} (Fig. 3.1 A, B and Fig. 3.2 A, B). In addition, no significant difference in cell morphology between PMA-treated and NAC- plus PMA-treated cells in the presence or absence of extracellular Ca^{2+} could be observed (Fig. 3.1 C, D and Fig. 3.2 C, D). In all cases no significant differences in the formation of MVs were seen. There was also no PS exposure when RBCs were treated with NAC (data not shown).

Flow cytometry analysis

The formation of MVs was also analyzed by flow cytometry. In the controls (freshly washed RBCs) only a very small amount of MVs was observed (Fig. 4). For stimulated RBCs, the distribution of MVs was gated in R2 regions (Fig. 4). There was an overlapping of MVs with instrument noise but this was not significant. By staining with annexin V-FITC, the fractions of MVs showing PS on the outer surface were clearly separated from the noise. In addition, the fluorescent dye DiI was applied to stain MVs, RBCs and all particles derived from cell membrane. By using DiI, based on its lipophilic properties, we were able to separate RBCs, MVs, and instrument noise due to the high fluorescence signal of DiI bound to phospholipid components (Fig. 5).

All released MVs from stimulated RBCs were analyzed by flow cytometer (Fig. 6). The FSC *vs.* SSC dot plots displayed the distribution of MVs in the region R2. By staining with annexin V-FITC almost all MVs showed PS on their surfaces (gate R5). In case of LPA stimulation, more than 85% MVs showed positive signal of annexin V-FITC and about 15%

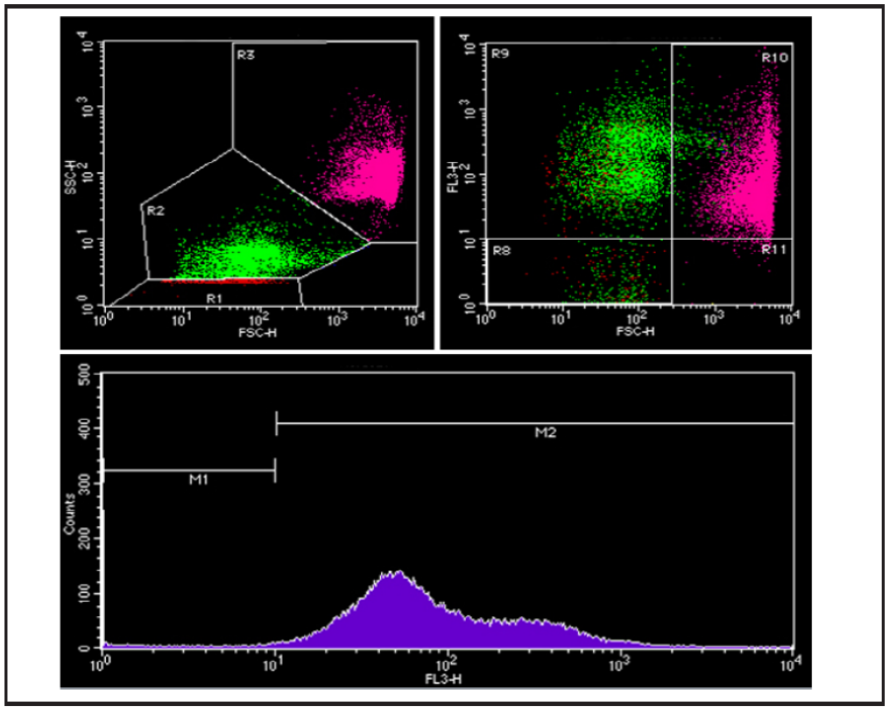

Fig. 5. Flow cytometry analysis of stimulated RBCs stained with the fluorescent dye Dil. The dot plots display the characteristics of the stimulated RBCs with LPA for 2 h. The SSC *vs.* FSC (upper left) and the FL3 *vs.* FSC (upper right); instrument noise (R1); MVs and exosomes (R2); intact RBCs (R3); population of MVs and exosomes showing negative signal and instrument noise (R8); population of MVs and exosomes showing positive signal (R9); population of stimulated RBCs showing positive signal (R10); population of RBCs showing negative signal (R11); In histogram (lower), population of MVs and exosomes showing negative signal and instrument noise (M1); population of simulated RBCs, MVs and exosomes showing positive signal with Dil (M2).

of MVs displayed no signal (gate R4). In all experiments, instrument noise was accounted for less than 1% of all detected events.

Particle size and zeta potential analysis

After removing intact cells, cell debris and apoptotic bodies, all MVs released from stimulated RBCs were collected by centrifugation at 200,000 g for 2 h at 4°C. DLS analysis showed that the size of released particles was very heterologous (PDI = 1.0). A symmetric multimodal distribution of particles in the range from 70 to 1000 nm with the mean value of about 200 nm was observed (Fig. 7A).

The population of larger particles (MVs) obtained by centrifugation at 25,000 g for 1 h (see Materials and methods) has sizes from 150 nm to 300 nm (Fig. 7B). The mean value of the size of MVs from 3 different measurements was 205.8 ± 51.4 nm. After collecting MVs, the population of MVs with smaller size was obtained by a further step of ultracentrifugation at 200,000 g for 2 h. DLS data showed that the size of these small MVs was 125.6 ± 31.4 nm (Fig. 7C). There was an overlapping in the size of two populations in the region from 150 to 200 nm (Fig. 7B and C) Under the experimental conditions, no significant difference was observed in the size distribution of MVs released from RBCs stimulated by LPA, PMA or A23187.

Under experimental conditions, MVs are negatively charged (Fig. 8). There was no significant difference in the charge between the populations of MVs. Data analysis showed

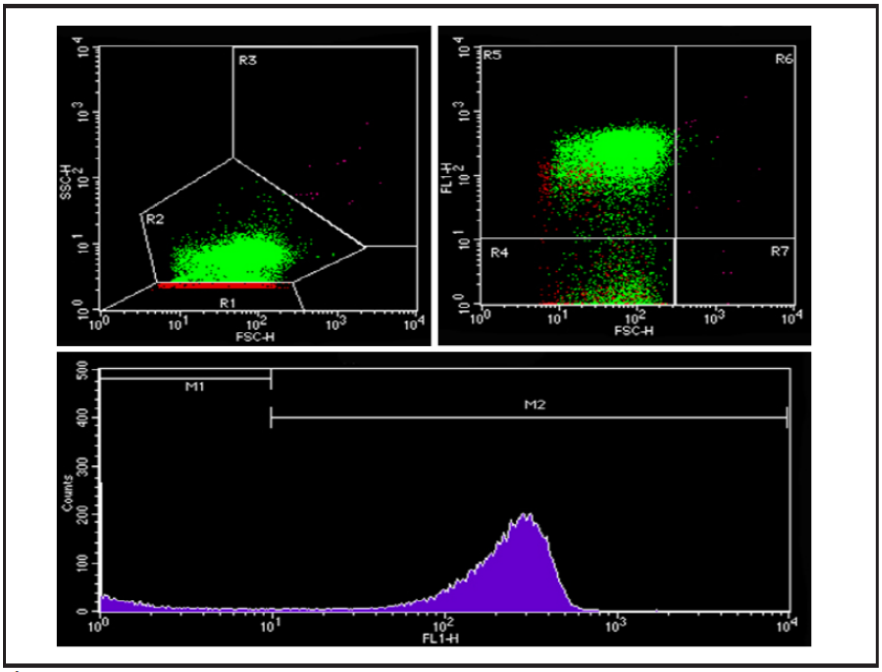

Fig. 6. Isolated MVs from RBCs stimulated by LPA for 2 h. The dot plots display the characteristics of the RBCs and MVs, the SSC *vs.* FSC (left) and the FL1 *vs.* FSC (right). Gates R1: instrument noise; R2: MVs and exosomes; R3: intact RBCs; R4: negative populations of small particles (MVs, exosomes, noise); R5: positive population of MVs and exosomes; R6: positive population of RBCs; R7: negative population of RBCs. Histogram shows the number of events with positive signal of annexin V-FITC (M2); events with negative signal and instrument noise (M1).

that the charge of MVs depend on the concentration of ions and the pH of solutions or buffers ($p < 0.01$). No significant difference in the charge of MVs released from RBCs stimulated by A23187 and LPA was observed (Fig. 8). However, there was a slight difference in the charge of MVs released from RBCs stimulated by PMA in comparison to those released after LPA or A23187 treatment ($p < 0.05$) when they were measured in Milli-Q water. Under all stimulating conditions, the lowest negative charge of MVs was determined of approximately -40 mV in Milli-Q water (Fig. 8). In case of phosphate saline buffer, the zeta potential values of MVs were recorded of about -10 mV, however, no distribution curve was observed (data not shown).

Particle morphological analysis

The morphology and size of stimulated RBCs, MVs were analyzed by SEM (Fig. 9). In comparison to control (RBCs in PBS), the morphology of stimulated RBCs was altered. The formation of MVs has been observed on the surface of stimulated RBCs. In addition, an adhesion of stimulated RBCs was clearly observed (Fig. 9 A1, A2, B1, B2 and C). Under all stimulating conditions, released MVs showed spherical shape and high polydispersity in their size. Statistical analysis showed that the size of MVs is in the range from 100 to 300 nm with the average value of about 200 nm (Fig. 9 E and F).

The size and morphology of MVs were also analyzed by AFM technique using tapping-mode. Data analysis from height, amplitude and phage modes showed that the size of these particles varied from about 70 to 200 nm (Fig. 10). There was no significant difference in size and morphology of MVs released from stimulated RBCs using PMA, LPA or A23187. In addition, the adhesion of MVs was observed in all samples.

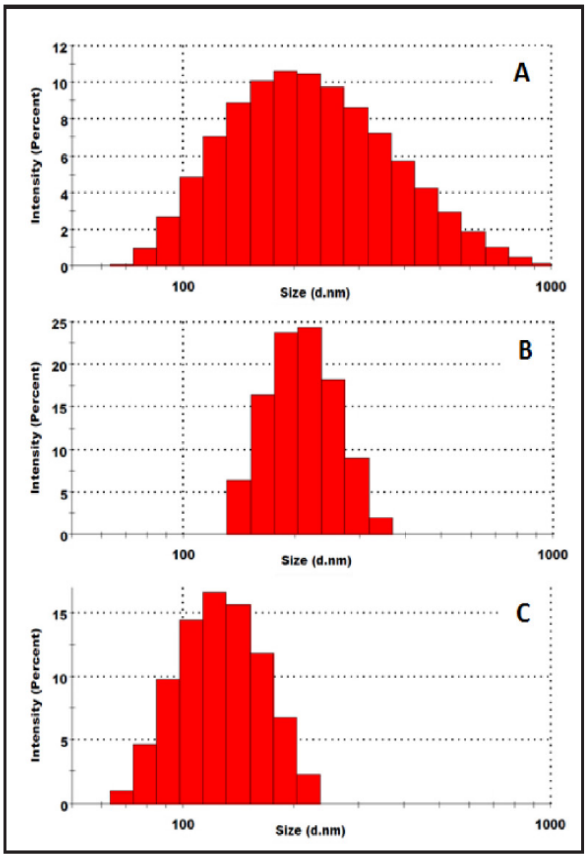

Fig. 7. Size distribution (d – diameter, in nm) of intensity of MVs and exosomes from RBCs stimulated with PMA. Symmetric multimodal distribution of all particles including MVs and exosomes (A), population of MVs (B) and population of exosomes (C).

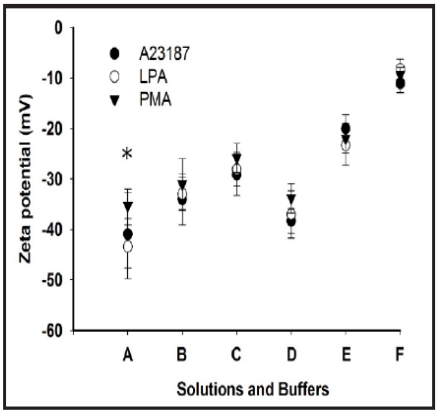

Fig. 8. Zeta potential distribution of MVs released from stimulated RBCs. Different solutions and buffers were used to measure zeta potential, Milli-Q water (A); NaCl 5 mM, pH 7.0 (B); NaCl 15 mM, pH 7.0 (C); Tris-HCl 5 mM, pH 7.0 (D); Tris-HCl 15 mM, pH 7.0 (E); Phosphate buffered saline, pH 7.4 (F). MVs released from RBCs stimulated with A23187 (●); MVs released from RBCs stimulated with LPA (○); MVs released from RBCs stimulated with PMA (▼). Error bars represent S.D. from 3 different experiments. In Mili-Q water, a significant difference in the charge of MVs released from RBCs stimulated by PMA was shown in comparison to LPA and A23187 (Student's t-test, $p < 0.05$(*)).

Discussion

Already 5 - 10 min after stimulation of RBCs with LPA, PMA or A23187 changes of cell volume and cell morphology were observed. In addition, exposure of PS on the outer cell membrane leaflet together with the formation and shedding of MVs were clearly seen on the surface of the cells by staining with annexin V-FITC. There was a relation between the exposure of PS and the formation of MVs. In the population of MVs released from RBCs stimulated by A23187 and LPA, the number of MVs showing positive signal for annexin

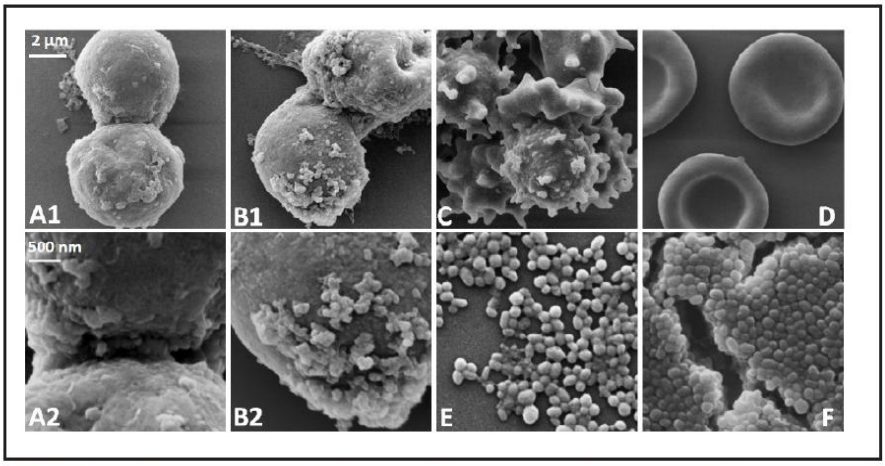

Fig. 9. SEM analysis of stimulated RBCs, released MVs and exosomes. Upper row: RBCs stimulated with PMA (A1); LPA (B1) or A23187 (C); RBCs in PBS/control (D). Lower row: Magnification of the binding area of two RBCs stimulated with PMA (A2); formation of MVs on the surface of RBCs stimulated with LPA (B2); MVs isolated from RBCs stimulated with PMA (E); large stack of MVs adhered together (F). The scale bars of 2 µm and 500 nm are applied for images in the upper row and lower row, respectively.

Fig. 10. Tapping-mode image of glutaraldehyde-fixed MVs and exosomes released from RBCs stimulated with LPA. Overview scan (1.5 × 1.5 µm) of a typical sample, height mode (upper), amplitude mode (lower left) and phase mode (lower right).

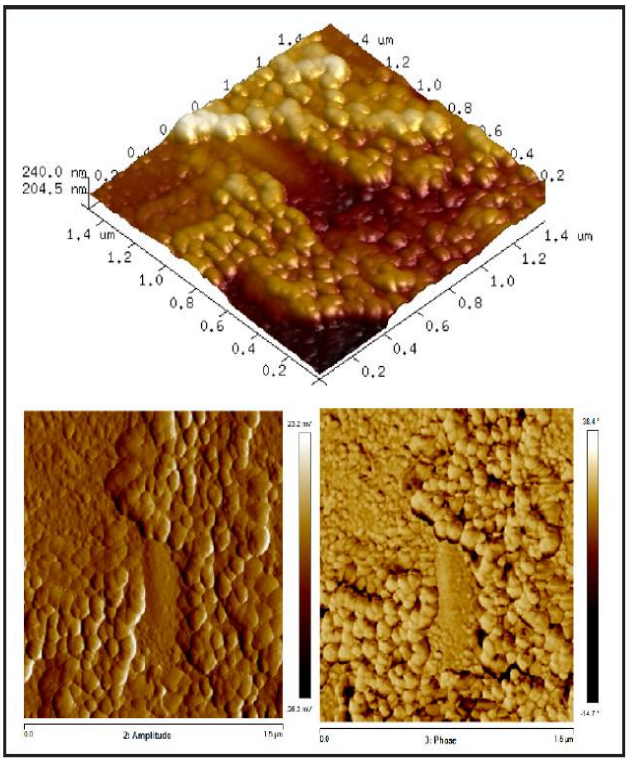

V-FITC was accounted for about 85%. In case of PMA, the number of MVs with positive signal was only about 60% (see gates R4 and R5 of Fig. 4). By comparison the obtained data from MVs stained with annexin V-FITC and Dil, a lipophilic tracer, it revealed that not all MVs showed PS in their outer surface (Fig. 5).

So far, the mechanism for the exposure of PS and shedding of MVs in human RBCs have been described by sustained elevation of intracellular calcium [30, 38-40] and other events associated with Ca^{2+} such as the opening of the Gardos channel leading to K^+ efflux, accompanied by an Cl^- efflux, and subsequently to a water efflux and reduction of cell volume [41]; activation of the scramblase [42, 43]; activation of calcium-dependent proteases, including calpain [17, 44, 45]; cytoskeletal alterations [46, 47] and change in erythrocyte morphology from the normal discoid shape to a spherical shape [48]. However, in case of PMA, the formation and shedding of MVs occurs in both Ca^{2+}-dependent and -independent ways (Figs. 2 and 3.1). The results suggest that this process is not only affected by Ca^{2+}-dependent parameters. Other pathways, e.g., the activation of protein kinase C, could also play a substantial role [30, 33]. However, a direct physical effect of PMA due to partitioning in the cell membrane on annexin V-FITC binding and releasing of MVs cannot be ruled out completely.

NAC has been reported as a thiol-oxidizing agent which is able to decrease the level of intracellular GSH in RBCs [49] and finally leading to the formation of MVs in G6PD deficient RBCs [50]. However, in the present study we show that treatment of RBCs from healthy people with NAC in the absence of PMA does not result in any changes of cell morphology and formation of MVs (Figs. 3.1 and 3.2). In the presence of PMA, the morphology of RBCs changed from echinocytes or discocytes to stomatocytes coupled with the release of MVs. However, there was no significant difference between RBCs treated with only PMA and both NAC and PMA (Figs. 3.1 and 3.2). It suggests that the effect of oxidative stress caused by the reduction of GSH level is not sufficient to stimulate the formation of MVs within the time-course of the experiment.

At the moment, it is unclear whether the MVs are formed and shed randomly or only in certain regions of the plasma membrane [3, 6]. If this process takes place randomly, in principle, the phospholipid components and membrane proteins in MVs will be comparable with the plasma membrane. Therefore, the regions of plasma membrane of RBCs showing PS on the outer leaflet may be a part of all MVs. However, as mentioned above, there was a subpopulation of MVs showing no PS on their outer layer. This suggests that in the whole population of MVs there exist different types of MVs carrying different components of phospholipids and probably membrane proteins on their surfaces. By differential centrifugation, the population of MVs at different size can be partly separated. However, these particles should be clearly separated based on other criteria rather than merely based on their size. However, so far efficient and specific markers to distinguish populations of MVs released from human RBCs have not been described [6, 51].

The negative charge of MVs can be explained based on the negative charged PS on the outer layer of MVs [17, 52]. Therefore, the negative charge of MVs depends on the number of PS on their outer layer. In addition, the adhesion of MVs themselves and RBCs carrying MVs should be clarified (Fig. 9). Since MVs have a negative surface charge they will repel each other and spread apart. However, Ca^{2+}could play an intermediate role forming molecular cross-bridges among MVs or stimulated RBCs showing PS on their surfaces. In this case it is not easy to explain the adhesion of stimulated RBC with PMA in the absence of Ca^{2+} [35]. In order to explain this adhesion, the involvement of receptors and adhesion proteins should be taken into account [4, 8, 17, 35]. Based on these findings, one could suggest that the exposure of PS in the outer cell membrane leaflet and the release of MVs may be directly involved in the aggregation of RBCs during thrombus formation as well as the RBC clearance by macrophages under normal physiological conditions or at certain diseases [37, 53, 54].

Conclusion

Treatment of RBCs with LPA, PMA or A23187 in the presence of Ca^{2+} led to the exposure of PS on the outer cell membrane leaflet and the release of MVs. A similar effect was seen in RBCs when protein kinase C was activated. The exposure of PS was observed in almost

all MVs. However, there was a subpopulation of these particles, which did not show PS on their outer layers. The size of released MVs varied from 70 to 1000 nm. By differential centrifugation, two populations of MVs were separated with size of 205.8 ± 51.4 nm and 125.6 ± 31.4 nm, respectively. All population of MVs revealed a negative charge of about - 40 mV in Milli-Q water. Adhesion among MVs and simulated RBCs was also observed. These findings suggest that the MVs may be involved in blood clot formation and the RBC clearance by macrophages.

Acknowledgements

This research is funded by Vietnam National Foundation for Science and Technology Development (NAFOSTED) under grant number 106-YS.06-2013.16 and Researcher Links Travel Grant from British Council. MCW is supported by a grant from CNPq (Brasil).

Disclosure Statement

The authors declare no conflict of interest.

References

1 Holme PA., Solum NO, Brosstad, F, Roger M, Abdelnoor M: Demonstration of platelet-derived microvesicles in blood from patients with activated coagulation and fibrinolysis using a filtration technique and western blotting. Thromb Haemost 1994;72:666-671.
2 Hess C, Sadallah S, Hefti A, Landmann R, Schifferli JA: Ectosomes released by human neutrophils are specialized functional units. J Immunol 1999;163:4564-4573.
3 Cocucci E, Racchetti G, Meldolesi J: Shedding microvesicles: artefacts no more. Trends Cell Biol 2009;19:43-51.
4 Gyorgy B, Szabo TG, Pasztoi M, Pal Z, Misjak P, Aradi B, Laszlo V, Pallinger E, Pap E, Kittel A, Nagy G, Falus A, BuzasEI: Membrane vesicles, current state-of-the-art: emerging role of extracellular vesicles. Cell Mol Life Sci 2011;68:2667-2688.
5 Trams, EG, Lauter C J, Salem N, Jr Heine U: Exfoliation of membrane ecto-enzymes in the form of micro-vesicles. Biochim Biophys Acta 1981;645, 63-70.
6 Akers J C, Gonda D, Kim R, Carter BS, Chen CC: Biogenesis of extracellular vesicles (EV): exosomes, microvesicles, retrovirus-like vesicles, and apoptotic bodies. J Neurooncol 2013;113:1-11.
7 Raposo G, Stoorvogel W: Extracellular vesicles: exosomes, microvesicles, and friends, J Cell Biol 2013;200:373-383.
8 Colombo M, Raposo G, Thery C: Biogenesis, secretion, and intercellular interactions of exosomes and other extracellular vesicles. Annu Rev Cell DevBiol 2014;30:255-289.
9 Comelli L, Rocchiccioli S, Smirni S, Salvetti A, Signore G, Citti L, Trivella, MG, Cecchettini A: Characterization of secreted vesicles from vascular smooth muscle cells. Mol Biosyst 2014;10:1146-1152.
10 Crescitelli R, Lasser C, Szabo TG, Kittel A, Eldh M, Dianzani I, BuzasEI, Lotvall J: Distinct RNA profiles in subpopulations of extracellular vesicles: apoptotic bodies, microvesicles and exosomes. J Extracell Vesicles 2013;2:20677- http://dx.doi.org/10.3402/jev.v2i0.20677.
11 Johnstone RM, Adam M, Hammond JR, Orr L, Turbide C: Vesicle formation during reticulocyte maturation. Association of plasma membrane activities with released vesicles (exosomes). J Biol Chem 1987;262:9412-9420.
12 Simons M, Raposo G: Exosomes-vesicular carriers for intercellular communication. Curr Opin Cell Biol 2009;21:575-581.
13 Thery C, Boussac M, Veron P, Ricciardi-Castagnoli P, Raposo G, Garin J, Amigorena S: Proteomic analysis of dendritic cell-derived exosomes: a secreted subcellular compartment distinct from apoptotic vesicles. J Immunol 2001;166:7309-7318.

14 Thery C, Ostrowski M, Segura E: Membrane vesicles as conveyors of immune responses. Nat Rev Immunol 2009;9:581-593.
15 Inal JM, Kosgodage U, Azam S, Stratton D, Antwi-Baffour S, Lange S: Blood/plasma secretome and microvesicles. Biochim Biophys Acta 2013;1834:2317-2325.
16 Muralidharan-Chari V, Clancy JW, Sedgwick A, D'Souza-Schorey C: Microvesicles: mediators of extracellular communication during cancer progression. J Cell Sci 2010;123:1603-1611.
17 Tissot J.-D, Canellini G, Rubin O, Angelillo-Scherrer A, Delobel J, Prudent M, Lion N: Blood microvesicles: From proteomics to physiology. Translat Proteom 2013;1:38-52.
18 Allan, D, Billah MM, Finean JB, Michell RH: Release of diacylglycerol-enriched vesicles from erythrocytes with increased intracellular (Ca2+). Nature 1976;261:58-60.
19 Allan D, Hagelberg C, Kallen KJ, Haest CW: Echinocytosis and microvesiculation of human erythrocytes induced by insertion of merocyanine 540 into the outer membrane leaflet. Biochim Biophys Acta 1989;986:115-122.
20 Allan D, Thomas P: Ca2+-induced biochemical changes in human erythrocytes and their relation to microvesiculation. J BioChem 1981;198:433-440.
21 Allan D, Thomas P, Limbrick AR: The isolation and characterization of 60 nm vesicles ('nanovesicles') produced during ionophore A23187-induced budding of human erythrocytes. J Bio Chem 1980;188:881-887.
22 Minetti G, Egee S, Morsdorf D, Steffen P, Makhro A, Achilli C, Ciana A, Wang J, Bouyer G, Bernhardt I, Wagner C, Thomas S, Bogdanova A, Kaestner L: Red cell investigations: art and artefacts. Blood Rev 213;27:91-101.
23 Lutz HU, Bogdanova A: Mechanisms tagging senescent red blood cells for clearance in healthy humans. Front Physiol 2013;4:387(doi: 10.3389/fphys.2013.00387).
24 Lutz HU, Liu SC, Palek J: Release of spectrin-free vesicles from human erythrocytes during ATP depletion. I. Characterization of spectrin-free vesicles. J Cell Biol 1977;73: 548-560.
25 Alaarg A, Schiffelers RM, van Solinge WW, van Wijk R: Red blood cell vesiculation in hereditary hemolytic anemia. Front Physiol 2013;4:365 (doi: 10.3389/fphys.2013.00365).
26 Camus SM, De Moraes JA, Bonnin P, Abbyad P, Le Jeune S, Lionnet F, Loufrani L, Grimaud L, Lambry JC, Charue D, Kiger L, Renard JM, Larroque C, Le Clésiau H, Tedgui A, Bruneval P, Barja-Fidalgo C, Alexandrou A, Tharaux PL, Boulanger CM, Blanc-Brude OP: Circulating cell membrane microparticles transfer heme to endothelial cells and trigger vasoocclusions in sickle cell disease. Blood 125;24:3805-3814.
27 Sheetz MP, Singer SJ: Biological membranes as bilayer couples. A molecular mechanism of drug-erythrocyte interactions. Proc Natl Acad Sci USA 1974;71:4457-4461.
28 Lang F, Gulbins E, Lerche H, Huber SM, Kempe DS, Foller M: Eryptosis, a window to systemic disease. Cell Physiol Biochem 2008;22:373-380.
29 Foller M, Huber SM, Lang F: Erythrocyte programmed cell death, IUBMB Life 2008;60:661-668.
30 Nguyen DB, Wagner-Britz L, Maia S, Steffen P, Wagner C, Kaestner L, Bernhardt I: Regulation of Phosphatidylserine Exposure in Red Blood Cells, Cell Physiol Biochem 2011;28:847-856.
31 Frasch SC, Henson PM, Kailey JM, Richter DA, Janes MS, Fadok VA, Bratton DL: Regulation of phospholipid scramblase activity during apoptosis and cell activation by protein kinase C delta. J BiolChem 2000;275:23065-23073.
32 Kaestner L, Steffen P, Nguyen DB, Wang J, Wagner-Britz L, Jung A, Wagner C. Bernhardt I: Lysophosphatidic acid induced red blood cell aggregation in vitro. Bioelectrochemistry 2012;87:89-95.
33 Wagner-Britz L, Wang J, Kaestner L, Bernhardt I: Protein kinase C alpha and P-type Ca channel CaV2.1 in red blood cell calcium signaling. Cell Physiol Biochem 2013;31:883-891.
34 Torr EE, Gardner DH, Thomas L, GoodallDM, Bielemeier A, Willetts R, Griffiths HR, Marshall LJ, Devitt A: Apoptotic cell-derived ICAM-3 promotes both macrophage chemoattraction to and tethering of apoptotic cells. Cell Death Differ 2012;19:671-679.
35 Steffen P, Jung A, Nguyen DB, Müller T, Bernhardt I, Kaestner L, Wagner C: Stimulation of human red blood cells leads to Ca2+-mediated intercellular adhesion. Cell Calcium 2011;50:54-61.
36 Pilpel Y, Segal M: The role of LPA1 in formation of synapses among cultured hippocampal neurons. J Neurochem 2006;97:1379-1392.
37 Chung SM, Bae ON, Lim KM, Noh JY, Lee MY, Jung YS, Chung JH: Lysophosphatidic acid induces thrombogenic activity through phosphatidylserine exposure and procoagulantmicrovesicle generation in human erythrocytes. Arterioscler Thromb Vasc Biol 2007;27:414-421.

38 Williamson P, Kulick A, Zachowski A, Schlegel RA, Devaux PF: Ca2+ induces transbilayer redistribution of all major phospholipids in human erythrocytes. Biochemistry 1992;31:6355-6360.
39 Bucki R, Bachelot-Loza C, Zachowski A, Giraud F, SulpiceJC: Calcium induces phospholipid redistribution and microvesicle release in human erythrocyte membranes by independent pathways. Biochemistry 1998;37:15383-15391.
40 KoshiarRL, Somajo S, Norstrom E, Dahlback B. Erythrocyte-derived microparticles supporting activated protein C-mediated regulation of blood coagulation. PLoS One 2014;9:e104200.
41 Lang PA, Kaiser S, Myssina S, Wieder T, Lang F, Huber SM: Role of Ca2+-activated K+ channels in human erythrocyte apoptosis. Am J Physiol Cell Physiol 2003;285:C1553-C1560.
42 Sahu SK, GummadiSN, Manoj N, AradhyamGK: Phospholipid scramblases: an overview. Arch Biochem Biophys 2007;462:103-114.
43 Basse F, Stout JG, Sims PJ, Wiedmer T: Isolation of an erythrocyte membrane protein that mediates Ca2+-dependent transbilayer movement of phospholipid. J Biol Chem 1996;271:17205-17210.
44 Berg CP, Engels IH, Rothbart A, Lauber K, Renz A, Schlosser SF, Schulze-Osthoff K, Wesselborg S: Human mature red blood cells express caspase-3 and caspase-8, but are devoid of mitochondrial regulators of apoptosis. Cell Death Differ 2001;8:1197-1206.
45 Tissot JD, Rubin O, Canellini G: Analysis and clinical relevance of microparticles from red blood cells. Curr Opin Hematol 2010;17:571-577.
46 Liu F, Mizukami H, Sarnaik S, Ostafin A: Calcium-dependent human erythrocyte cytoskeleton stability analysis through atomic force microscopy. J Struct Biol 2005;150:200-210.
47 Takakuwa Y: Protein 4.1, a multifunctional protein of the erythrocyte membrane skeleton: structure and functions in erythrocytes and nonerythroid cells. Int J Hematol 2000;72:298-309.
48 Gonzalez LJ, Gibbons E, Bailey RW, Fairbourn J, Nguyen T, Smith SK, Best KB, Nelson J, Judd AM, Bell JD: The influence of membrane physical properties on microvesicle release in human erythrocytes. PMC Biophys 2009;2:7 (doi:10.1186/1757-5036-2-7).
49 Kosower NS, Kosower EM, Wertheim B: Diamide, a new reagent for the intracellular oxidation of glutathione to the disulfide. Biochem Biophys Res Commun 1969;37:593-596.
50 Pantaleo A, Ferru E, Carta F, Mannu F, Simula LF, Khadjavi A, Pippia P, Turrini F: Irreversible AE1 tyrosine phosphorylation leads to membrane vesiculation in G6PD deficient red cells. PLoS One 2011;6:e15847.
51 Park JO, Choi DY, Choi DS, Kim HJ, Kang JW, Jung JH, Lee JH, Kim J, Freeman MR, Lee KY, GhoYS, KimKP: Identification and characterization of proteins isolated from microvesicles derived from human lung cancer pleural effusions. Proteomics 2013;13:2125-2134.
52 Rautou PE, Mackman N: Microvesicles as risk markers for venous thrombosis. Expert Rev Hematol 2013;6:91-101.
53 Andrews DA, Low PS: Role of red blood cells in thrombosis. Curr Opin Hematol 1999;6:76-82.
54 Bevers EM, WiedmerT, Comfurius P, Shattil SJ, Weiss HJ, Zwaal RF, Sims PJ: Defective Ca2+-induced microvesiculation and deficient expression of procoagulant activity in erythrocytes from a patient with a bleeding disorder: a study of the red blood cells of Scott syndrome. Blood 1992;79:380-388.

2.4 Robust automated image analysis of activated red blood cells

Jan Martens, Mauro Carlos Wesseling, Joachim Weickert, Ingolf Bernhardt

Submitted article to Open Biological Sciences Journal (2016).

Robust Automated Image Analysis of Activated Red Blood Cells

Jan Martens
Laboratory of Biophysics
Saarland University
jan.martens@uni.lu

Mauro C. Wesseling
Laboratory of Biophysics
Saarland University
m.wesseling@mx.uni-saarland.de

Joachim Weickert
Mathematical Image Analysis Group
Saarland University
weickert@mia.uni-saarland.de

Ingolf Bernhardt
Laboratory of Biophysics
Saarland University
i.bernhardt@mx.uni-saarland.de

June 9, 2016

Abstract

(Background:) The investigation of eryptosis, a process in red blood cells (RBCs) comparable to apoptosis, has medical importance due to a link to thrombosis. Eryptosis is indicated by an exposition of phosphatidylserine (PS) on the outer cellular membrane. Experimental data suggests a relation between an elevated intracellular Ca^{2+} content of RBCs and PS exposure.

Objective: To investigate this relation in wet-lab experiments, live cell imaging with fluorescence microscopy was carried out. RBCs from blood samples were labeled with fluorescence dyes to either mark exposed PS or intracellular Ca^{2+}. Manual analysis requires the experimenter to count all cells in the images and to classify them according to their activation states and shape changes.

Method: A combination of well-established image analysis techniques allows us to automate this task. A preprocessing step consisting of bandpass filtering and median filtering prepares the image such that a gradient operator and Otsu thresholding can extract cell boundaries. A Hough transform applied to the preprocessed image extracts the cells. We classify the activation state of the RBCs with a thresholding on the ratio between intracellular and outercellular brightness.

Measuring and thresholding intracellular fluctuations allows to classify cells into discocytes and echinocytes. With these techniques we yield robust results, while saving valuable time.

Results and Conclusion: Our results show that the automated system detects cells with high reliability and classifications are comparable to manual classifications.

1 Introduction

Even though eryptosis of RBCs is similar to apoptosis in nucleated cells, we still lack specific knowledge about the full process. It is known that PS exposition on the outer leaflet is an indicator for this process and serves as a signal for macrophages to remove the affected cells [9]. On a pathological level, PS exposing cells have shown a tendency to form blood clots which can cause thrombosis [12].

The process of PS exposition and the impact of involved factors are still being investigated. However, based upon current knowledge, the intracellular Ca^{2+} content plays a central role. An elevated intracellular Ca^{2+} concentration has an effect on proteins responsible for maintaining the distribution of lipids in the membrane leaflets. Such proteins include flippase and scram-

blase. When the scramblase (see e.g. Kaestner et al.[9]) is activated it leads to PS exposition on the outer membrane leaflet (PS is normally located in the inner membrane leaflet only [14]). As a side-effect, the Gardos channel is activated by the intracellular Ca^{2+}. This leads to an efflux of potassium, accompanied by Ca^{2+}, resulting in water loss and shrinkage of the cells. Normal cells are discocytes, whereas shrunken cells are transformed to echinocytes (for shapes of RBCs, see e.g. Lim et al.[8]). In addition to the effect on the Gardos channel, intracellular Ca^{2+} activates protein kinase C (PKC), which directly stimulates PS exposition in the outer membrane leaflet [9]. Considering these processes, it is obvious that Ca^{2+} plays a key role in the exposition of PS. The increase of the intracellular Ca^{2+} concentration can be induced by different activators.

With this goal, RBCs are isolated and incubated with either one of the activators: (i) lysophosphatidic acid (LPA) (ii) phorbol-12 myristate-13 acetate (PMA), or (iii) 4-bromo-A23187 (A23187). Each activator has a different on the cellular membrane or ion channels, such that influence and interactions of different factors on eryptosis can be investigated.

During the fluorescence imaging experiments, two types of images are obtained for analysis: (i) Brightfield images are regular grayscale images with

mild noise and strong illumination gradients. In most images, the RBC density is relatively low, such that cells rarely overlap, but this is not always the case. Dealing with overlapping cells is important to obtain reliable results.

(ii) Fluorescence images were obtained by using fluo-4 for Ca^{2+} imaging (fluo-4 binds intracellular Ca^{2+} and thus stains the cell from inside) or annexin-FITC for PS imaging (annexin binds to PS on the outer membrane leaflet and leads to signals on the cellular membrane). The strength of the fluorescence signals depending on the used activators have to be detected.

A dominant degradation in these images is strong noise, which at times, resembles impulse noise. The signals of activated cells are often well-distinguishable from the background due to their brightness. Some images also display weak fluorescence signals that are easily overlooked. The light of strongly fluorescent cells is often scattered around them, leading to subtle illumination gradients in areas with many activated cells.

Contributions. Our goal is to present a robust, efficient and user-friendly automated image analysis tool that offers two main advantages: Firstly, it requires only very simple image processing methods, such as bandpass filtering, median filtering and thresholding. Reducing the number of parameters to a minimum and keeping run times low is crucial to deliver a reliable yet

simple-to-use tool. Secondly, it is not necessary to train our system. In comparison, few attempts for automated blood cell counting and classification have been described in recent years. These publications focused on different goals and used different sorts of images. Noteworthy examples are the works of Hamouda et al. [3] (automated RBC counting for hemacytometers), Won et al. [15], Hiremath et al. [4](identification and differentiation of white blood cells) and Tomari et al. [13]. In contrast to our system, machine learning techniques such as neuronal networks and supervised clustering are required within these approaches. Most images used by the other works are blood smear images with only minor perturbations.

2 Materials Methods

2.1 Blood Sample Preparation

Human blood samples from healthy donors were obtained from the Institute of Clinical Hematology and Transfusion Medicine of Saarland University Hospital. These samples were treated with the anticoagulant EDTA and stored at 4 °C in physiological solution (145 mM NaCl, 7.5 mM KCl, 10 mM glucose,

10 mM HEPES Tris, pH 7.4). They were used within one day.

The separation of RBCs was performed in three washing and centrifugation steps at 2000 g for 5 min at room temperature, such that the buffy coat and the blood plasma were removed.

The remaining sample was diluted with physiological solution and subsequently incubated with one of the activators (2.5 μM LPA, 6 μM PMA, 2 μM A23187). Each activator leads to a specific cellular reaction. LPA is released by blood platelets after their activation. It is known to activate a non-selective voltage-dependent cation channel in RBCs [6]. PMA activates PKC_α which leads to PS exposition on the outer membrane leaflet [9]. As a positive control for an increased intracellular Ca^{2+} content, A23187 is used in some experiments. It is an ionophore that directly leads to Ca^{2+} uptake. Fluorescence microscopy was performed in time steps ranging from 0 min to 30 min after activation, with pictures taken in 20 second intervals. For staining, either fluo-4 (concentration 1 μM; for Ca^{2+} imaging) or annexin-FITC (concentration 4.5 μM; for PS imaging) were used. Both dyes can be excited at a wavelength 488 nm, but have different binding regions. Fluo-4 binds directly to intracellular Ca^{2+}, leading to signals inside the cell. FITC binds on the outer cellular leaflet, leading signals on the cellular borders. For

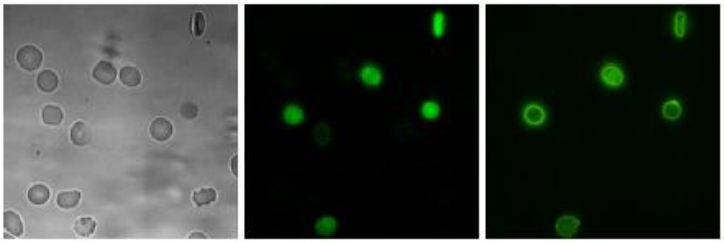

Figure 1: Images of RBCs from a typical experiment. Here, doublestaining with to dyes was performed and the signals of the dyes was separated into two different images.
Left: Brightfield image. **Middle:** Corresponding fluorescence image with fluorescence dye fluo-4. **Right:** Corresponding fluorescence image with the fluorescence dye annexin-FITC. Note the fluorescence signal on the outer cell membrane.

image acquisition, cells were kept in a petri dish.

The used fluorescence microscope is an Eclipse TE 2000-E from Nikon Corporation, using a CCD77 Visitron System GmbH camera. Pictures were taken and saved with the software Metavue Visitron System. Typical RBC images are shown in Fig. 1.

2.2 Image Analysis Techniques

Depending on the image type, different tasks are to be solved and thus different processing steps need to be applied. Brightfield images require the detection of RBCs and the classification of their shapes as either discocytes

or echinocytes (stomatocytes are rarely present in described experiments). Cell detection gives information on the location of each individual cell such that assigning the fluorescence signals in the corresponding fluorescence images becomes possible.

In case of brightfield images, the interest lies in the detection of the RBCs. We typically use grayscale images, which offer a decent resolution, but suffer from image degradations. Such degradations involve slowly varying illumination gradients and minor noise. These gradients result from either uneven illumination or shades of cells outside the focal plane. For brightfield image processing, a preprocessing step (subdivided into four single steps) and a cell recognition step are performed (as illustrated in Fig. 2).

Noise and illumination gradients are addressed by using difference of Gaussians and median filtering. Difference of Gaussians is used as a band-pass filter, which only preserves elements of a specified frequency. This is done by subtracting two Gaussian-blurred images with different standard deviations from one another. In the underlying case, preserving high-frequent features such as the ones of RBCs is desirable, which is why a Gaussian-blurred image is subtracted from the original image (we are using the standard deviations $\sigma_1 = 0$ and $\sigma_2 = 10$). Illumination gradients and shades are effectively re-

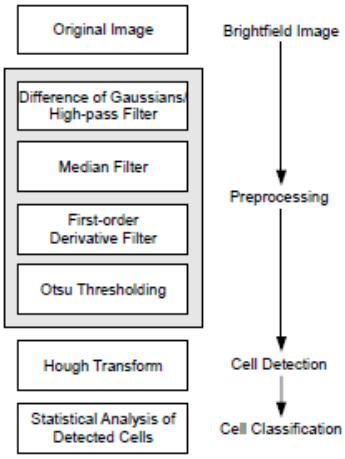

Figure 2: Sequence of image processing steps for RBC detection.

moved with this technique.

Afterwards, we remove noise using a median filter with a disc-shaped neighborhood of radius 2 pixels. As a side-effect, the median filter is smoothing the image and preparing it for upcoming steps.

The next two preprocessing steps are used for extraction of the cell boundaries. This is done by calculating the gradient magnitude of the image. The gradient is approximated by means of central differences. Under normal conditions, it is favorable to apply some presmoothing beforehand or to apply Sobel operators. Due to the median filtering, the image is already presmoothed and no additional smoothing is necessary.

The resulting image contains information on the cell boundaries. Thresholding segments this image and allows the identification of important structures. For fast, automated threshold selection, Otsu's method [10] is used (the threshold is chosen such that it maximizes the between-class variance given in Eq. (1)):

$$\sigma_B^2(T) = \omega(T)(\mu_0 - \mu_{total})^2 + (1 - \omega(T))(\mu_1 - \mu_{total})^2, \qquad (1)$$

where μ_0 and μ_1 are the mean gray values of the resulting segments, μ_{total} the

mean gray value of the image, and $\omega(T)$ the percentage of all pixels below the threshold T.

With the preprocessed image containing the relevant edge information, the Hough Transform [5] is used to find circular objects within the image and is the only step requiring user parameters; note that the preprocessing steps consisting of difference of Gaussians and median filtering work sufficiently well with fixed, predetermined parameters. The result is a dataset describing the properties of located circles, with data including circle position, area, radius, location, and score. The detected circles correspond to the RBCs found in the image.

After the detection of the RBCs has been performed, the task of classifying them according to their shape remains. This is done by measuring the variance inside the respective cell of the fully preprocessed image. The preprocessed image contains only information about the most relevant edges in the images and benefits from robustness with respect to illumination gradients. Following the observation that the texture of echinocytes is more complex than the flat one of discocytes, this technique allows for a robust and simple classification of these two cell shapes based on a threshold value, which can be adapted by the user. In order to exclude the edge of the cell

borders, pixels at the cell boundaries are neglected.

RBCs with an increased fluorescence intensity are considered *activated* by the experimenters. The classification of the program is based on the gray values inside the respective region in the fluorescence image. If the ratio of the mean value inside the region of the cell and the background region around it exceed a user-defined threshold, we consider this cell as activated. A value based on expert experience is used for this purpose.

Since the ratio of gray values in the fluorescence images might be altered by contrast and brightness changes, an optional affine rescaling is offered as a means of normalization before measuring the fluorescence intensity.

3 Results

The developed software was tested in a variety of experiments. In each case, the program's default parameters (difference of Gaussians with standard deviations $\sigma_1 = 0$ and $\sigma_2 = 10$; median filter with circular structuring element of radius 2; Hough transform with expected circle radius in range $[15, 30]$ and a circle threshold of 130). The first results were generated by running the program on six different image sets and evaluating the program's results

Table 1: Wet lab conditions of the analyzed image sets. Each image set was obtained in a different experiment and contains a varying number of fluorescence and brightfield images.

Image set	Activator	Time after incubation	Fluorescence dye
1	*None*	0 min	*None*
2	*None*	0 min	fluo-4
3	LPA	1 min	fluo-4
4	PMA	15 min	fluo-4
5	A23187	15 min	fluo-4
6	A23187	30 min	FITC

afterwards. The image sets resulted from experiments under various conditions (an overview is listed in Table 1). The program was executed on a system with an *Intel Core i3-2330M CPU* with 2.20 GHz, 4 GB RAM and a 64 bit version of the operating system Windows 7. Execution times are given in Table 2.

The first set serves as a negative control for fluorescence measurements since cells in the image were neither stained with a fluorescence dye nor treated with an activator. Cells are rather densely packed in some areas and require to cope with overlaps. In the second set cells were only treated with the dye fluo-4, resulting in weak fluorescence signals. Around two thirds of all cells are echinocytes and very few cells are activated. In the third image set, the activator LPA was used, leading to rather weak signals for Ca^{2+} and a

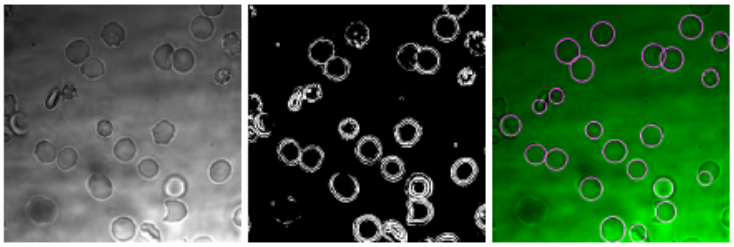

Figure 3: Typical sequence of one single processed image from an experiment without activator.
Left: Original brightfield image. **Middle:** Fully preprocessed image. Note how sharp edges such as cell boundaries are extracted. **Right:** Original image with drawn in circles.

balanced amount of echinocytes and discocytes. Cells have plenty of room and did not overlap. Image set four used the activator PMA, resulting in some very strong cellular responses for Ca^{2+}. In this case echinocytes were not observed. The conditions are similar in the fifth image set, but cells were incubated for an extended period with A23187 (positive control), resulting in strong signals for Ca^{2+}. The last image set provides similar conditions, but the fluorescence dye FITC was used, leading to bright signals of PS at the outer cellular membrane.

As a statistical performance measure, sensitivity, specificity, positive predictive value and accuracy were calculated. These values are based on the numbers of the true positive (TP), true negative (TN), false positive (FP)

Table 2: Program execution times for the image sets in seconds. The set numbers correspond to the set numbers in Table 1. Each image set contains a varying number of brightfield images, with each one having an associated fluorescence image (we refer to them as *image pairs*).

Image set	**Number of image pairs**	**Execution time (sec)**
1	10	17
2	10	17
3	5	9
4	6	10
5	10	18
6	5	8

and false negative (FN) classification of the program in comparison to human experimenter annotations. If at least one of these values is 0, the calculation of the statistical values is not possible, resulting in an indeterminable value (labeled as NaN). For their defintion, refer to the appendix.

One should note that the specificity and accuracy were not calculated for cell detection due to the difficulty of defining TN hits for this task.

As shown in Fig. 4, cell detection is generally very reliable, showing perfect or almost perfect positive predictive value. The very few detected false positive RBC detections result from overlapping cell borders in areas where RBCs are densely packed. The sensitivity proves that at worst, around 80% of the cells are detected, but in sets with better image conditions higher values are easily achieved, such that all RBCs can potentially be recognized. Fig. 3

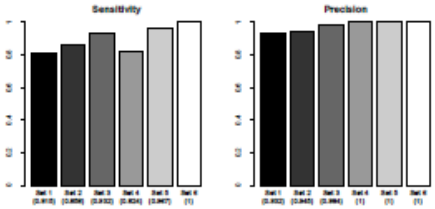

Figure 4: Sensitivity and positive predictive value for cell detection. The set numbers correspond to the set numbers in Table 1. The labels refer to the respective image sets, the numbers in parenthesis are the calculated statistical values.

illustrates the typical result of this cell recognition process.

Activation classification proves to be similarly robust. As shown in the plots in Fig. 5, only image set 5 contains false negative hits, but otherwise the methods and default values of the algorithm work well and offer solid results. Sensitivity and positive predictive value are indeterminable in image set 1 since cells were not stained and thus no fluorescence signal could be measured. We are thus unable to calculate this value (labeled as NaN).

The plots in Fig. 6, which relate to cell differentiation were generated with respect to the recognition of discocytes. As the plots indicate, these results are weaker than the previous ones. Even though the percentage of detected discocytes only drops below 70% in the image sets 1 and 4, the simple classification method based on the variance of an RBCs texture works. The lack of

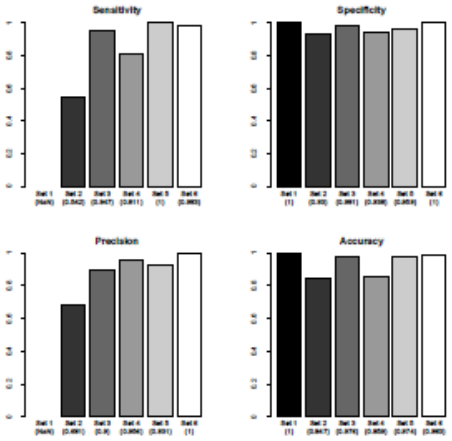

Figure 5: Sensitivity, specificity, positive predictive value and accuracy for cell activation classification. The set numbers correspond to the set numbers in Table 1. The labels refer to the respective image sets, the numbers in parenthesis are the calculated statistical values.

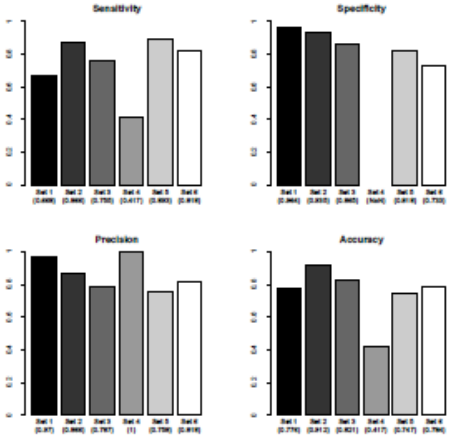

Figure 6: Sensitivity, specificity, positive predictive value and accuracy for cell classifcation. The values relate to discocyte recognition. The set numbers correspond to the set numbers in Table 1. The labels refer to the respective image sets, the numbers in parenthesis are the calculated statistical values.

echinocytes in set 4 does however falsify the results, leading to an unreliable values for positive predictive value. The specificity can not be calculated. One could argue that there is still room for improvement, but considering the complexity of other potential classifiers, the results are still acceptable. Additionally, the program's results were compared with the results of two different human experimenters. For this purpose, two experiments were conducted and the two human experimenters were asked to manually annotate

the images. These annotated images were subsequently compared with the results generated by the program. For these experiments, cells were incubated with the dye fluo-4 in a 2 mM Ca^{2+} solution. One experiments served as a control (see Fig. 7(a)), in the second one the activator PMA was used (Fig. 7(b)).

Cell activation state classification of the developed program in comparison to the results of the experimenters, shows in both experiments reliable results. The difference for the control experiment in terms of sensitivity and positive predictive value results from the fact that one experimenters annotated some RBCs as strongly responding, while the other experimenter annotated no cells in the set as strongly responding. The fact that some decisions for classification are subjective shows its consequences in the plots.

Cell shape classification shows more stable and also generally better results. Notable differences between expert annotation and program annotation are seen in the experiment were the activator PMA was used. In this case it is very important to note that these images contained stomatocytes which were classified as echinocytes. Up to this point, the program has been designed to differentiate between echinocytes and discocytes only, since stomatocytes are very rare under normal conditions. These wrong classifications have a no-

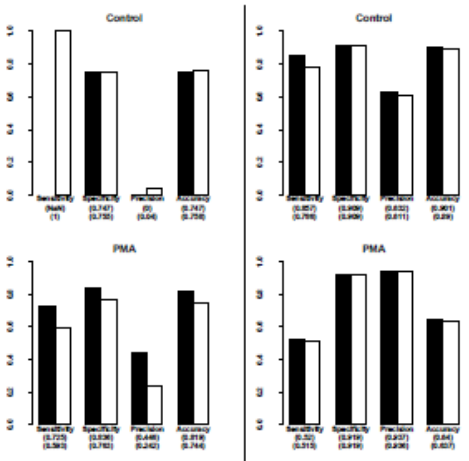

(a) *Activation classification* **(b)** *Shape classification*

Figure 7: Comparison of experimenter annotations with the program results. Plots indicate the results two experiments. In the first one, the activator PMA was deployed and a set of 8 brightfield images with their fluorescence counterparts were taken. The second experiment serves as a control experiment without activator with overal 9 brightfield images and corresponding fluorescence images. IN both cases, the dye fluo-4 was used. The two experimenter annotations were considered as two different gold standards and used for calculating sensitivity, specificity, positive predictive value and accuracy. Subfigure **(a)** depicts two plots for activation classifcation, Subfigure **(b)** shows two plots for shape classification for discocytes. Control describes the experiment without an activator, PMA denotes the experiment where the activator PMA was used. Results for the first experimenter are marked in black, while the values for the second experimenter are marked in white.

tably negative impact on the results and are the reason why sensitivity and accuracy are lower than in earlier plots. This incident shows that a more robust model would be favorable to deal with such rare, unexpected issues.

The plots presented in Fig. 7 (a) make it clear that the performance of the image analysis tool depends from the subjective decision of each expert. Especially activation state classification shows strong differences and revealed a weakness in terms of classification. However, the experimenters showed tolerance for the program's decision in corner cases, where differentiating between activation states for Ca^{2+} was difficult. In these cases, the experimenters were willing to agree with the program, even when their own annotations were initially different. The true performance of the classifier can thus be considered to be better than Fig. 7 (a) indicates.

4 Discussion and Conclusion

The methods for detecting and classifying RBCs are relatively fast and the generated results are reliable.

Cell detection works very well and recognizes most cells on the images. Images with ideal conditions lead to almost perfect or even perfect results,

proving that the method for automated cell detection is a valid alternative to manual cell counting. Classification of fluorescence activation states and cell shapes also work surprisingly well, even if images suffer from minor perturbations. Yet again, it is obvious that images with conditions close to the underlying assumptions about noise and illumination yield the best results. The possibilities that a combination of more advanced methods such as texture descriptors and other active contour models offer, suggest that cell detection and differentiation can be improved further, making the overall model more robust. As an alternative to the proposed methods, we also attempted to use more sophisticated methods. Applying active contour models such as geodesic active contours [1, 7], the Chan-Vese model [2], or statistical models like the one proposed by Zhang et al. [16] gave unsatisfactory results. This problem is largely caused by inconsistent illumination. Even subtle illumination inconsistencies are enough to influence segmentation with active contours negatively. A preprocessing with an edge-enhancing diffusion filter[11] did not yield notable improvements.

Machine learning approaches such as clustering and principal component analysis could offer alternative and possibly more reliable ways for cell state and cell shape classification.

Putting the possibilities of image analysis into perspective, it appears promising to view it as the foundation of upcoming findings. In comparison to other techniques, it is possible to identify more features that might be linked to biophysical processes. Flow cytometry for example, might have a higher throughput, but does not allow the classification of cell shapes and imposes cellular stress onto the RBCs. Extracting and interpreting visual features and their correlations will be the key for future projects and scientists might be able to use 2D information provided by the images for the approximation of 3D information, e.g. to calculate cellular volume based on theoretical models such as presented by Lim et al. [8]. Thus, in conjunction with innovative ideas and interdisciplinary knowledge, image analysis has the potential to become a powerful tool.

However, it is unlikely that high-throughput analysis methods such as flow cytometry will be substituted by image analysis methods in the near future. On the other hand, manual analysis of microscope images can be sped up considerably. Optimizing algorithms and using parallel computing methods are most promising and future projects will surely result in tools allowing for computer-aided data analysis in real time.

5 Conflict of Interest

The authors declare no conflict of interest.

6 Acknowledgements

Mauro C. Wesseling has been supported by the *CNPq* (Brazil).

References

[1] V. Caselles, R. Kimmel, and G. Sapiro. Geodesic active contours. *International Journal of Computer Vision*, 22:61–79, 1997. [doi:10.1109/iccv.1995.466871].

[2] T.F. Chan and L.A. Vese. Active contours without edges. *IEEE Transactions on Image Processing*, 10:266–277, 2001. [doi:10.1109/83.902291].

[3] A. Hamouda, A.Y. Khedr, and R.A. Ramadan. Automated red blood cell counting. *International Journal of Computing Science*, 1(2):13–16, 2012.

[4] P.S. Hiremath, P. Bannigidad, and S. Geeta. Automated identification and classification of white blood cells (leukocytes) in digital microscopic

images. *International Journal of Computer Applications, Special Issue on Recent Trends in Image Processing and Pattern Recognition*, 2:59–63, 2010.

[5] P.V.C. Hough. Method and means for recognizing complex patterns, December 18 1962. US Patent 3,069,654.

[6] L. Kaestner, P. Steffen, D.B. Nguyen, J. Wang, L. Wagner-Britz, A. Jung, C. Wagner, and I. Bernhardt. Lysophosphatidic acid induced red blood cell aggregation in vitro. *Bioelectrochemistry*, 87:89–95, 2012. [doi:10.1016/j.bioelechem.2011.08.004].

[7] S. Kichenassamy, A. Kumar, P. Olver, A. Tannenbaum, and A. Yezzi. Conformal curvature flows: from phase transitions to active vision. *Archive for Rational Mechanics and Analysis*, 134:275–301, 1996. [doi:10.1007/bf00379537].

[8] H.W.G. Lim, M. Wortis, and R. Mukhopadhyay. Stomatocyte-discocyte-echinocyte sequence of the human red blood cell: evidence for the bilayer- couple hypothesis from membrane mechanics. *Proceedings of the National Academy of Sciences of the U.S.A.*, 99(26):16766–16769, 2002. [doi:10.1073/pnas.202617299].

[9] D.B. Nguyen, L. Wagner-Britz, S. Maia, P. Steffen, C. Wagner, L. Kaestner, and I. Bernhardt. Regulation of phosphatidylserine exposure in red blood cells. *Cellular Physiology and Biochemistry*, 28:847–856, 2011.

[10] N. Otsu. A threshold selection method from gray-level histograms. *IEEE Transactions on Systems, Man and Cybernetics*, 9(1):62–66, 1979. 10.1109/TSMC.1979.4310076.

[11] P. Perona and J. Malik. Scale-space and edge detection using anisotropic diffusion. *IEEE Transactions on Pattern Analysis and Machine Intelligence*, 12:629–639, 1990. [doi:10.1109/34.56205].

[12] P. Steffen, A. Jung, D.B. Nguyen, T. Mueller, I. Bernhardt, L. Kaestner, and C. Wagner. Stimulation of human red blood cells leads to Ca^{2+}-mediated intercellular adhesion. *Cell Calcium*, 50(1):54–61, 2011. [doi:10.1016/j.ceca.2011.05.002].

[13] R. Tomari, W.N.W. Zakaria, M.M.A. Jamil, F.M. Nor, and N.F.N. Fuad. Computer aided system for red blood cell classification in blood smear images. *Procedia Computer Science*, 42(0):206–213, 2014. [doi:10.1016/j.procs.2014.11.053].

[14] A.J. Verkleij, R.F.A. Zwaal, B. Roelofsen, P. Comfurius, D. Kastelijn, and L.L.M. van Deenen. The asymmetric distribution of phospholipids in the human red cell membrane. A combined study using phospholipases and freeze-etch electron microscopy. *Biochimica et Biophysica Acta - Biomembranes*, 323(2):178–193, 1973. [doi:10.1016/0005-273690143-0].

[15] C.S. Won, J.Y. Nam, and Y. Choe. Extraction of leukocytes in a cell image with touching red blood cells, 2005. [doi:10.1117/12.593335].

[16] K. Zhang, L. Zhang, H. Song, and W. Zhou. Active contours with selective local or global segmentation: a new formulation and level set method. *Image and Vision Computing*, 28(4):668–676, 2010. [doi:10.1016/j.imavis.2009.10.009].

A Appendix

Table 3: Raw data for cell counting. Values for can not be determined to to the difficulty of defining them on images.

Image set	TP	TN	FP	FN
1	244	NaN	13	51
2	223	NaN	13	37
3	123	NaN	2	9
4	84	NaN	0	18
5	60	NaN	0	2
6	74	NaN	0	0

Table 4: Raw data for cell activation classification. Cells displaying a strong fluorescence signal a considered as activated.

Image set	TP	TN	FP	FN
1	0	244	0	0
2	32	200	15	27
3	18	103	2	1
4	43	30	2	10
5	27	47	2	0
6	58	1	0	1

Table 5: Raw data for Cell shape classification. This data relates to the detection of discocytes and their classification as such.

Image set	TP	TN	FP	FN
1	129	106	4	64
2	71	157	11	11
3	37	64	10	12
4	35	0	0	49
5	25	36	8	3
6	36	22	8	8

Table 6: Raw data for cell activation annotations by two separate experimenters. The numbers are related to two different experiments, one control experiment without activator and one with PMA. Cells with a sufficiently strong fluorescence signal are considered as activated. Experimenter annotations are considered as gold standard.

Experimenter	Activator	TP	TN	FP	FN
None (Control)	1	0	74	25	0
None (Control)	2	1	74	24	0
PMA	1	29	184	36	11
PMA	2	16	161	50	11

Table 7: Raw data for cell shape annotations by two separate experimenters. The numbers are related to two different experiments, one control experiment without activator and one with PMA. The values are derived with respect to discocyte classification. Discocytes classified as TP agree with experimenter annotations. Experimenter annotations are considered as gold standard.

Experimenter	**Activator**	**TP**	**TN**	**FP**	**FN**
None (Control)	1	12	70	2	7
None (Control)	2	11	70	3	7
PMA	1	89	68	82	6
PMA	2	88	68	83	6

2.5 Phosphatidylserine exposure in human red blood cells: Role of scramblase, protein kinase C, Gardos channel, and cell volume

Mauro C. Wesseling, Lisa Wagner-Britz, Nguyen Duc Bach, Salome Asanidze, Judy Mutua, Nagla Mohamed, Mira Türknetz, Benjamin Hanf, Mehrdad Ghashghaeinia, Lars Kaestner, Ingolf Bernhardt

Submitting form. Article will be submitted to Cellular Physiology and Biochemistry (2016)

Phosphatidylserine exposure in human red blood cells: Role of scramblase, protein kinase C, Gardos channel, and cell volume

Mauro C. Wesseling[1], Lisa Wagner-Britz[1], Nguyen Duc Bach[2], Salome Asanidze[1], Judy Mutua[1], Nagla Mohamed[1], Mira Türknetz[1], Benjamin Hanf[1], Mehrdad Ghashghaeinia[3], Lars Kaestner[4,5,*], Ingolf Bernhardt[1,*]

[1]Laboratory of Biophysics, Faculty of Natural and Technical Sciences III, Saarland University, Campus, 66123 Saarbrücken, Germany
[2]Department of Molecular Biology, Faculty of Biotechnology, Vietnam National University of Agriculture, Ngo Xuan Quang, Gia Lam, Hanoi, Vietnam
[3]Departament of Cardiology, Vascular Medicine and Physiology, University of Tübingen 72076 Tübingen, Germany
[4]Institute for Molecular Cell Biology and Rearch Centre for Molecular Imaging and Screening, School of Medicine, Saarland University, Building 61, 66421 Homburg, Germany
[5]Experimental Physics, Saarland University, 66123 Saarbrücken, Germany

*Corresponding authors: Tel: +49 681 3026689 (IB); Fax: +49 681 3026690 (IB);
E-mail address: i.bernhardt@mx.uni-saarland.de
Tel: +49 6841 1626129 (LK); Fax: +49 6841 1626293 (LK);
E-mail address: anlkae@uks.eu

Short title:
Phosphatidylserine exposure in red cells

Abstract

Background/Aims: In previous publications we were able to demonstrate that there is no correlation between the intracellular Ca^{2+} content and the exposure of phosphatidylserine (PS) in the outer membrane leaflet after activation of red blood cells (RBCs) by lysophosphatidic acid (LPA), phorbol-12 myristate-13acetate (PMA), or 4-bromo-A23187 (A23187). It has been concluded that three different mechanisms are responsible for the PS exposure in human RBCs: (i) Ca^{2+}-stimulated scramblase activation (and flippase inhibition) by A23187, LPA, and PMA; (ii) PKC activation by LPA and PMA; and (iii) enhanced lipid flip flop caused by LPA. The aim of our further studies was to find out the relation between the increased Ca^{2+} content, scramblase- and PKC-activation, and PS exposure of RBCs. Another question was to investigate the role of the Ca^{2+}-activated K^+ channel activity in the process of PS exposure. In addition, cell volume changes have to be taken into consideration.

Methods: The intracellular Ca^{2+} content and the PS exposure of RBCs have been investigated after treatment with LPA (2.5 µM), PMA (6 µM), or A23187 (2 µM). Fluo-4 and annexin V-FITC has been used to detect intracellular Ca^{2+} content and PS exposure, respectively. Both parameters (Ca^{2+} content, PS exposure) were studied using flow cytometry. Conditions to inhibit the scramblase, the PKCα, and the Ca^{2+}-activated K^+ channel have been applied.

Results: The percentage of RBCs showing PS exposure after activation with LPA, PMA, or A23187 is significantly reduced after inhibition of the scramblase using the specific inhibitor R5421 as well as after the inhibition of the PKCα using chelerythrine chloride or calphostin C. The inhibitory effect is more pronounced when the scramblase and the PKCα are inhibited simultaneously or when both PKCα inhibitors are used simultaneously. In addition, the inhibition of the Ca^{2+}-activated K^+ channel using charybdotoxin resulted in a significant reduction of the perentage oof RBCs showing PS exposure. A simple change of the cell volume was without effect.

Conclusion: It can be concluded that not only Ca^{2+} activating the scramblase but also the PKCα activated by LPA and PMA in a Ca^{2+}-dependent and a Ca^{2+}-independent manner play a substantial role in affecting the PS exposure. Furthermore, the activity of the Ca^{2+}-activated K^+ channel seems to be of importance for the PS exposure.

Keywords

Red blood cells, Ca^{2+} content, phosphatidylserine exposure, protein kinase C, flow cytometry, fluorescence imaging

Introduction

When the endothelium of blood vessels is damaged, platelets become activated and transport phosphatidylserine (PS) to their external membrane surface [1]. The exposed PS provides a catalytic surface for the formation of active enzyme-substrate complexes of the coagulation cascade, especially for the tenase and prothrombinase complexes [2]. Under these circumstances exposed PS provides a pro-coagulant surface and is, in general, needed as a response to injury. So it is logical that the mechanism of PS exposure has to occur with a relative high transport rate of the lipids. Platelets treated with a Ca^{2+} ionophore show a scrambling rate of 87×10^{-3} per second [2]. Human red blood cells (RBCs) also show the mechanism of PS exposure after increased intracellular Ca^{2+} content [3-5] and are able to adhere to endothelial cells under pathophysiological conditions [6-9]. In addition, exposure of PS at the external membrane of RBCs is a typical sign of eryptosis (a term introduced by Lang et al. [10]), defining the suicidal death of RBCs. Exposed PS is sought to serve as a signaling component for macrophages to eliminate old or damaged RBCs from the circulation [11-14]. Since eryptotic RBCs can adhere to the vascular wall, which may lead to disturbance of the microcirculation [15], the elimination of these cells is a very important mechanism. Beyond that, it was also shown that RBCs with an increased Ca^{2+} content adhere towards each other under *in vitro* conditions [16]. However, compared to platelets, RBCs have a lower scrambling rate (0.45×10^{-3} per second) [2].

The outward-directed transport of PS is realized by a protein stimulated by an increased intracellular Ca^{2+} content termed ‘scramblase’ [17-19]. The identity of this protein has been identified only recently as a member of the TMEM16 or anoctamin family of proteins and the crystal structure was published [20].

Ca^{2+} uptake of RBCs through Ca^{2+}-permeable channels [21-24] does not only activate the scramblase, it also leads to an activation of the Ca^{2+}-activated K^+ channel (Gardos channel) [24, 26]. The result is an efflux of KCl and osmotically obliged H_2O, which causes shrinkage of the cells [26, 27].

Another consequence of increased intracellular Ca^{2+} content is the activation of the protein kinase Cα (PKCα) [28]. Since mature RBCs lack nuclei and organelles,

cellular responses have to be modulated by post-translational modifications. Therefore, phosphorylation mediated by the PKCα is of great importance for intracellular signal transduction pathways [29]. In addition, it has been discussed that an activation of the PKCα results in an enhanced uptake of Ca^{2+} into the cells, i.e. acting as a positive feedback [30]. It has also been speculated that an activation of the PKC induces PS exposure via a Ca^{2+}-independent mechanism [30].

In recently published papers of our research group we investigated the PS exposure of RBCs after stimulating the cells with different substances. Phorbol 12-myristate 13-acetate (PMA) has been used to activate the PKCα. For comparison, lysophosphatidic acid (LPA) and the Ca^{2+} ionophore A23187 (as positive control) was used to stimulate the increase of the intracellular Ca^{2+} content of the RBCs [3, 21, 31, 32].

From the results obtained it has been concluded that three different mechanisms are responsible for the PS exposure in human RBCs: (i) Ca^{2+}-stimulated scramblase activation (and flippase inhibition) by A23187, LPA, and PMA; (ii) PKCα activation by LPA and PMA; and (iii) enhanced lipid flip flop caused by LPA [3].

Therefore, the aim of our further studies was to find out the relation between the increased Ca^{2+} content, PKCα activation, and PS exposure of RBCs. Another question was to investigate the role of the Ca^{2+}-activated K^+ channel activity in the process of PS exposure. In addition, cell volume changes and/or changes of the K^+ concentration have to be taken into consideration. To solve the raised questions, conditions to inhibit the PKCα, the Ca^{2+}-activated K^+ channel, and the scramblase have been applied.

Material and Methods

Blood and solution

Human venous blood from healthy human volunteers was obtained from the Institute of Clinical Haematology and Transfusion Medicine, Saarland University Hospital, Homburg, or from the Institute of Sports and Preventive Medicine, Saarland University, Saarbruecken. EDTA or heparin was used as anticoagulants. Freshly drawn blood samples were stored at 4°C and used within one day. Blood was centrifuged (2,000 g, 5 min) at room temperature and the plasma and buffy coat was removed by aspiration. Subsequently, RBCs were washed 3 times in HEPES-buffered physiological solution (HPS) containing (mM): 145 NaCl, 7.5 KCl, 10 glucose, 10 HEPES, pH 7.4 under the

same conditions. Finally, RBCs were re-suspended in HPS and stored at 4°C until the beginning of the experiment. The experiment was started immediately after resuspension of the cells.

RBC labelling

The procedure to prepare RBCs for measurements of intracellular Ca^{2+} content as well as PS exposure is based on the protocols of Nguyen et al. [3] and Wesseling et al. [31, 32].

Measurement of intracellular Ca^{2+} content: RBCs were loaded with 1 µM fluo-4 AM from a 1 mM stock solution in dimethyl sulfoxide (DMSO) in 2 ml HPS as described before [xx]. The extracellular Ca^{2+} concentration was 2 mM, i.e. $CaCl_2$ was added to the HPS. Cells were incubated at a haematocrit of about 0.1 % in the dark for 30 min at 37°C with continuous shaking. Then the cells were washed again (16,000 g, 10 s) with an ice-cold HPS, re-suspended and used for measurements, i.e used for control measurements or for activation by different substances (A23187, LPA, PMA).

Measurement of PS exposure: PS exposure was detected using annexin V-FITC at a concentration of 4.5 µM. The cells were prepared as for measurement of the Ca^{2+} content. The RBCs were incubated with different substances (A23187, LPA, PMA) between 1 min and 30 min at 37°C. Then the cells were washed again (16,000 g, 10 s) with an ice-cold HPS and re-suspended. Finally annexin V-FITC was added and the cells were incubated in HPS with the addition of 2 mM Ca^{2+} at a haematocrit of 0.1 % and room temperature for 10 min in the dark. The measurements were performed at room temperature.

Treatment of RBCs with different substances / under different experimental conditions

Cells in HPS containing additionally 2 mM $CaCl_2$ (haematocrit 0.1 %) were activated with A23187 or PMA for 30 min and with LPA for 1 min in Eppendorf tubes under continuous shaking at 37°C. When chelerythrine chloride was used, the cells were pre-incubated for 20 min under the same conditions [xx]. In case of pre-incubation with calphostin C, charybdotoxin, or R5421 the incubation time was 30 min [xx]. Before substances to activate the RBCs were added (A23187, LPA, PMA), the cells were washed once in HPS containing additionally 2 mM $CaCl_2$.

To avoid KCl efflux and cell shrinkage, i.e. to block the Ca^{2+}-dependent K^+ channel, RBCs were transferred into a high K^+ HEPES-buffered solution containing (mM): 150 KCl, 2.5 NaCl, 10 glucose, 10 HEPES, pH 7.4. Again 2 mM $CaCl_2$ was added

to the solutions before activating the RBCs with different substances. To change the volume of the RBCs, they were transferred into a sucrose-containing HPS containing (mM): 145 NaCl, 7.5 KCl, 2 $CaCl_2$, 10 glucose, 30 sucrose, 10 HEPES, pH 7.4 (for shrinkage) or into HPS with reduced NaCl concentration containing (mM): 130 NaCl, 7.5 KCl, 2 $CaCl_2$, 10 glucose, 10 HEPES, pH 7.4 (for swelling).

Flow cytometry and fluorescence microscopy

To analyse the RBCs we used the flow cytometer 'FACSCalibur' and the software Cell Quest Pro (Becton Dickinson Biosciences, Franklin Lakes, USA) as described before [3, 31, 32]. The fluo-4 and annexin V-FITC fluorescence signals were measured in the FL-1 channel, with an excitation wavelength of 488 nm and an emission wavelength of 520/15 nm. Forward scatter (FSC) was analysed to determine cell volume changes. For each experiment 30,000 cells were collected.

Fluorescence microscopy was carried out with the inverted fluorescence microscope Eclipse TE2000-E (Nikon, Tokyo, Japan) and the imaging software VisiView (Visitron Systems, Puchheim, Germany) as described before [3, 31, 32].. Images were taken with the camera CCD97 (Photometrics, Tucson, USA) using a 100×1.4 (NA) oil immersion lens with infinity corrected optics. Diluted RBC samples (haematocrit 0.1 %) were placed on a cover slip in the dark at room temperature. From each RBC sample 5 images from different positions of the cover slip randomly chosen were taken.

Reagents

Ca^{2+} ionophore A23187, lysophosphatidic acid (LPA), phorbol 12-myristate 13-acetate (PMA), chelerythrine chloride, calphostin C, and charybdotoxin were purchased from Sigma-Aldrich (Munich, Germany). All substances (except charybdotoxin, which was dissolved at 20 µM in HPS) were dissolved at 1 mM in DMSO and stored at -20°C. For each experiment a new aliquot was used. R5421 was obtained from the company Endotherm (Saarbruecken, Germany) where it has been synthesized according to the structure published by Dekkers et al. [19] (see Fig. 3 therein), dissolved at 100 mM in DMSO, and stored at room temperature. The substance has not been patented. Fluo-4 AM and annexin V-FITC was obtained from Molecular Probes (Eugene, USA).

Statistics

Data are presented as mean values +/- S.D. of at least 3 independent experiments. The significance of differences was tested by ANOVA. Statistical significance of the data was defined as follows: (**): $p \leq 0.01$, (*): $p \leq 0.05$, not significant: $p > 0.05$.

Results

It has been shown before that there is no correlation of the percentage of RBCs with increased Ca^{2+} content and the percentage of PS exposing cells after stimulating the cells with different substances [3, 32]. The highest amount of RBCs showing PS exposure was obtained after stimulating the cells with PMA (in comparison to LPA or A23187 (positive control)), although in this case the percentage of cells with increased intracellular Ca^{2+} content was lowest. This effect is due to a PMA-induced PS exposure in the absence of extracellular Ca^{2+}, which was not seen in case of treatment with LPA or A23187 [3].

To investigate the involvement of the scramblase, the PKCα and the Ca^{2+}-activated K^+ channel in changes of the intracellular Ca^{2+} content and PS exposure in more detail, inhibitors for each pathway have been used.

Inhibition of the scramblase

A pre-incubation with 100 µM of the scramblase inhibitor R5421 ([19], for details see Reagents) leads to different results when the RBCs are activated with A23187, LPA, or PMA (Fig. 1A). For A23187, a pre-incubation with R5421 does not affect the percentage of cells with elevated intracellular Ca^{2+} content. In case of LPA, the number of cells with elevated intracellular Ca^{2+} is slightly increased after incubation with R5421 compared to control. For PMA the opposite effect can be seen, i.e. the percentage of RBCs with increased intracellular Ca^{2+} content is significantly reduced after incubation with R5421. The control value for RBCs with elevated Ca^{2+} content in the absence of any activating substance was 0.80 ± 0.09 % in the absence of R5421 and 1.12 ± 0.20 %, in presence of R5421. For A23187 and LPA, the fluo-4 intensity was not influenced by a pre-incubation with R5421 (data not shown). However, for PMA the fluo-4 intensity was significantly reduced from 567.85 a.u. to 302.54 a.u. after treatment with R5421.

The situation for PS exposure is different. As shown in Fig. 1B, pre-incubation with R5421 leads to a significant reduction of the percentage of RBCs showing PS exposure in all three cases of activation (A23187, LPA, PMA). The strongest effect of inhibition using R5421 can be seen for A23187 activation. Inhibition of LPA- and PMA-activated PS exposure is less pronounced. The control value for RBC showing PS exposure in the absence of any activating substance was 0.98 ± 0.15 % in the absence of R5421 and 1.99 ± 0.80 % in the presence of R5421. Higher concentrations of R5421 (up to 1 mM) did not lead to significant higher reductions but caused strong haemolysis (data

not shown). As can be seen from the images presented in Fig. 2, the inhibitor R5421 causes also shape changes of the RBCs.

Inhibition of the PKCα

Chelerythrine chloride and calphostin C have been used to inhibit the PKCα. Chelerythrine chloride is an inhibitor of the active site of PKCα, whereas calphostin C blocks the PMA- and diacylglycerol-binding site of the PKCα [33, 34].

The percentage of RBCs that show an increase in the intracellular Ca^{2+} content is not affected by an inhibition of the PKCα using chelerythrine chloride in case of A23187- and LPA-activation. In contrast, a significant reduction can be seen after PMA activation (Fig. 3A). The control value for RBCs with elevated Ca^{2+} content in the absence of any activating substance was 1.15 ± 0.30 % in the absence and 1.50 ± 0.72 %, in presence of chelerythrine chloride, respectively.

The situation for PS exposure is slightly different. Although there is no significant change of the PS exposing RBCs after A23187 activation, a significant reduction of the cells showing PS exposure can be seen after activation with LPA or PMA (Fig. 3B). The control value for RBC showing PS exposure in the absence of any activating substance was 1.13 ± 0.13 % in the absence and 1.24 ± 0.40 % in the presence of chelerythrine chloride, respectively.

Using the PKCα inhibitor calphostin C, the following results have been obtained: The percentage of cells showing an increased Ca^{2+} content does not change significantly after A23187 activation but is slightly (but not significantly) decreased after LPA activation. The decrease after PMA activation is much more pronounced and significant (Fig. 3A). The control value for RBCs with elevated Ca^{2+} content in the absence of any activating substance was 1.16 ± 0.16 % in the absence and 1.39 ± 0.68 %, in presence of calphostin C, respectively. The data for the PS exposure are comparable with the results obtained for the inhibition with chelerythrine chloride. No significant change of the PS exposing RBCs after A23187 activation has been observed but a significant reduction of the cells showing PS exposure can be seen after activation with LPA or PMA (Fig. 3B). The control value for RBC showing PS exposure in the absence of any activating substance was 1.08 ± 0.03 % in the absence and 1.02 ± 0.32 % in the presence of calphostin C, respectively.

Inhibition of the scramblase and the PKCα using 2 inhibitors simultaneously

We carried out experiments where RBCs have been activated with LPA and the PKCα has been inhibited by using chelerythrine chloride and calphostin C simultaneously. In this case, the percentage of cells showing an increased Ca^{2+} content was significantly reduced (Fig. 4A, cp. with Fig. 3A). The reduction of the PS exposing cells was even more pronounced compared with the situation of the inhibition using one of the two PKCα inhibitors alone (Fig. 4B, cp. with Fig. 3B). In addition, RBCs have been activated with PMA. The obtained data show that in this case a double inhibition using chelerythrine chloride and calphostin C does not lead to a larger inhibition of the percentage of RBCs with an elevated Ca^{2+} content compared with an inhibition using one of the substances alone (Fig. 4A, cp. with Fig. 3A). However the percentage of cells with PS exposure is much more pronounced compared with the data measured with one inhibitor only (Fig. 4B, cp. with Fig. 3B).

In another set of experiments we inhibited the PKC and the scramblase simultaneously using one PKC inhibitor and the scramblase inhibitor R5421. In case of RBC activation with LPA, the simultaneous inhibition of the PKC using chelerythrine chloride and the scramblase using R5421 did not result in a decrease of the percentage of the cells with a higher Ca^{2+} content but resulted in a dramatic decrease of the cells showing PS exposure (Fig. 4A and B). When the PKC and the scramblase were inhibited simultaneously with calphostin C and R5421, respectively, a significant reduction of the percentage of cells with an enhanced intracellular Ca^{2+} content has been observed (Fig. 4A). For the PS exposure again a dramatic (significant) decrease can be seen like in cases of chelerythrine chloride and calphostin C or chelerythrine chloride and R5421 (Fig. 4B). The control values in the absence of the activating substances for all combinations of inhibition presented in Fig. 4A and B are not significantly different from the values obtained for inhibition with one of the substances.

Inhibition of the K^+ efflux via the Ca^{2+}-activated K^+ channel and change of cell volume

To inhibit the Ca^{2+}-activated K^+ channel, the classical inhibitor charybdotoxin has been applied [26, 35]. The inhibitor did not affect the percentage of cells showing an increased intracellular Ca^{2+} content after stimulation with A23187, i.e. nearly all RBCs showed an evaluated Ca^{2+} level in the absence or presence of charybdotoxin (Fig. 5A). The PS exposure, however, was reduced to a very low level, i.e. close to values of the PS exposure obtained in the absence of any activating substance (Fig. 5B). Interestingly, in case of LPA activation, the percentage of cells with increased intracellular Ca^{2+} content

was significantly decreased and again PS exposure decreased to a very low level (Fig. 5A and B). This effect has been observed over a time period of 60 min (not shown). In case of PMA activation, again the percentage of cells with increased Ca^{2+} content was not affected by charybdotoxin (Fig. 5A). However, the PS exposure was significantly decreased in the presence of the inhibitor (Fig. 5B).

In another set of experiments, we increased the extracellular K^+ concentration of the HPS, compensating the osmolarity by reducing the Na^+ concentration. Elevation of the extracellular K^+ concentration reduces the efflux of K^+ through the Ca^{2+}-activated K^+ channel, resulting in a decreased loss of KCl and osmotically obliged H_2O. This in turn leads to a diminished shrinkage of the cells. One can assume that an elevation of the extracellular KCl concentration to 150 mM (instead of 145 mM NaCl plus 7.5 mM KCl of the normal HPS the high K^+ HPS contains 150 mM KCl plus 2.5 mM NaCl) completely blocks the K^+ efflux via the Ca^{2+}-activated K^+ channel, i.e. the cell volume remains constant. The cell volume has been taken as the forward scatter (FSC) measured with flow cytometer (data obtained with A23187 activation are presented in Fig. 6, a similar change of the FSC was obtained for LPA- and PMA-activation (data not shown)). The percentage of RBCs showing an increased intracellular Ca^{2+} content does not change in solution of high extracellular K^+ content (high K^+ HPS) in all 3 cases of activation (LPA, PMA, A23187) compared to the normal HPS (data not shown). However, as shown in Fig. 7, an inhibition of the K^+ efflux in high K^+ HPS is able to significantly reduce the A23187- as well as the LPA-induced PS exposure. In contrast, the PMA-induced PS exposure is not affected by high K^+ HPS (Fig. 7). The addition of charybdotoxin to the normal and high K^+ HPS resulted in a significant reduction of the percentage of RBCs showing PS exposure after PMA activation from 63.79 ± 5.31 % to 33.18 ± 8.87 % (n = 3) and from 57.55 ± 4.95 % to 32.27 ± 7.88 % (n = 3), respectively. The corresponding values in the absence and presence of charybdotoxin are not significantly different.

To investigate a possible effect of the cell volume on the intracellular Ca^{2+} content as well as PS exposure of RBCs, the cells were shrunken by adding 30 mM sucrose to the HPS and swollen by using the HPS with reduced NaCl concentration (130 mM NaCl instead of 145 mM). Surprisingly, there is neither a significant change in the percentage of cells with elevated intracellular Ca^{2+} content nor of the PS exposure compared to control (data not shown). Therefore, one can conclude that a simple change of the RBC

volume does not have a significant influence on the Ca^{2+} content as well as the PS exposure.

Discussion

From our findings one can conclude that the mechanism of PS exposure cannot be explained by a simple increase of the intracellular Ca^{2+} content alone. Treatment of RBCs with the ionophore A23187 leads to an artificial increase in the intracellular Ca^{2+} content of all cells. This in turn induces a number of mechanisms: (i) activation of the scramblase (and inhibition of the flippase), which results in an exposure of PS to the outer membrane leaflet [36], (ii) activation of the Ca^{2+}-activated K^+ channel resulting in an efflux of KCl and osmotically obliged H_2O [25, 27, 37], (iii) activation of the PKCα [30] leading to an activation of calpain, which results in cytoskeleton destruction, microvesicle generation and membrane blebbing [10, 38, 39]. Our results also show that RBC activation with A23187 leads only in one third of the cells to PS exposure, although the intracellular Ca^{2+} is increased in nearly all cells. Similar results can be seen also for the RBC activation with LPA. However, interestingly the situation is opposite for PMA activation. In this case a much higher fraction of cells showing PS exposure can be observed although only a small fraction of cells react with an elevated intracellular Ca^{2+} content. Therefore, one can conclude that the increase in the intracellular Ca^{2+} is not solely responsible for PS exposure. To gain further insight into the correlation of increased intracellular Ca^{2+} content and PS exposure, we used the specific scramblase inhibitor R5421 [19, 40, 41]. Its mechanism of action is still unknown, but it seems to act as an irreversible inhibitor, since its inhibitory effect could not be reversed by washing the cells [40]. Inhibition of the scramblase leads to a significant reduction of PS exposure in all 3 cases of RBC activation, most pronounced with about 80% inhibition for A23187 activation (Fig. 1). It might be that a higher concentration of R5421 would reduce the amount of RBCs with PS exposure to lower values. However, higher concentrations led to haemolysis of the cells. It cannot be excluded that in case of LPA activation, based on an insertion of the molecule into the membrane, the flip-flop process is enhance leading to a higher amount of cells with PS exposure. In case of PMA activation it seems obvious that there is a Ca^{2+}-independent pathway resulting in an enhanced PS exposure. Such a mechanism has already been discussed by Nguyen et al. [3] and Wagner-Britz el al. [21].

We also used 2 conventional inhibitors of the PKC, chelerythrine chloride [33, 42, 43] and calphostin C [30, 34], to gain further insight. Both inhibitors leading to the same result, reducing the amount of cells with evaluated Ca^{2+} content in case of PMA activated. Such an effect can be explained taking into consideration that PKCα phosphorylates the ω-agatoxin-TK-sensitive, $Ca_v2.1$-like (P/Q-type) Ca^{2+} channel [43]. This phosphorylation is reduced when the PKCα is inhibited. This is not the case when the RBCs are activated with LPA. In this case the NSVDC channel is activated, which is not affected by the PKCα. That the number of cells with PS exposure is significantly decreased using the PKCα inhibitors in both cases of activation (LPA, PMA) can be explained assuming that LPA and PMA activate the PKCα, which in turn activates the scramblase [30]. By comparing RBCs to other hematopoietic cells another possibility cannot be excluded. It seems likely that LPA acts over a G protein-coupled receptor. For other cell types it is known that this receptor activates a C-type phospholipase, producing diacylglycerol (DAG) and inostitol-3-phosphate (I_3P). These second messengers activate the PKCα and trigger the Ca^{2+} influx into the cells [23].

A double inhibition of the PKCα using chelerythrine chloride and calphostin C has a significant effect on the PS exposure (Fig. 4B). The values obtained are smaller compared to the results for PKCα inhibition using one inhibitor alone. Therefore, one can assume that both sides of inhibitor – PKCα interaction are of importance. That there is also a clear reduction of the percentage of RBCs showing PS exposure in case one inhibitor of the PKCα and the scramblase inhibitor R5421 is applied together (compared to the results where they have been used separately) shows that at least two different pathways exist, which are involved in the process of PS exposure.

We carried out 2 different sets of experiments to block the Ca^{2+}-activated K^+ channel. In one series of experiment we used the inhibitor charybdotoxin [35], in another series we enhanced the extracellular KCl concentration up to 150 mM. Charybdotoxin does not affect the amount of cells with elevated Ca^{2+} content in case of RBC activation with A23187 or PMA (Fig. 5A). That there is a significant reduction in case of LPA activation can be explained assuming that charybdotoxin inhibits not only the Ca^{2+}-activated K^+ channel but also channels permeable for cations like the NSVDC channel. This channel is opened by LPA and responsible for the Ca^{2+} uptake as has been described before [5, 44]. It cannot be excluded that charybdotoxin blocks the ω-agatoxin-TK-sensitive, $Ca_v2.1$-like (P/Q-type) Ca^{2+} channel. Interestingly, the PS exposure was

significantly reduced by charybdotoxin in all 3 cases of RBC activation (A23187, LPA, PMA). Although the effect observed after LPA activation seems due to the fact that the percentage of cells with increased intracellular Ca^{2+} content is reduced, the data for A23187- and PMA-activation clearly show that the Ca^{2+}-activated K^+ channel is involved in the process of PS exposure. Such an assumption is supported by the findings that an enhancement of the extracellular KCl leads also to a reduction of the PS exposure, at least in case of RBC activation with A23187 or LPA. The only discrepancy we found for PMA activation where an increase of the KCl concentration was without significant effect. Interestingly, charybdotoxin reduced the percentage of RBCs showing PS exposure in normal HPS as well as in solution containing 150 mM KCl. Therefore, it might be that charybotoxin in addition to the inhibition of the Ca^{2+}-activated K^+ channel and Ca^{2+}-permeable channels affects also the Ca^{2+}-independent pathway relevant for PS exposure. The percentage of RBCs with PS exposure is smaller in case of PMA activation compared to A23187- or LPA-activation. One could speculate that in case of PMA activation the effect on the Ca^{2+}-activated K^+ channel is less pronounced compared to the activation with A23187 or LPA when the KCl concentration of the extracellular solution is changed.

For A23187 one can see from the forward scatter measurements (Fig. 6) that the RBCs do not change the cell volume when there is no K^+ efflux via the Ca^{2+}-activated K^+ channel, i.e. in high K^+ HPS. A simple effect of the cell volume on PS exposure can be ruled out since shrinkage or swelling of the RBCs by using solutions with a lower NaCl concentration compared to the normal HPS (for shrinkage) or with the addition of sucrose to the normal HPS (for swelling) was without effect.

Acknowledgements

This research is funded by a grant from CNPq program “science without borders” to M. C. Wesseling, process number: 202426/2012-2 (Brasil), a grant from Vietnam National Foundation for Science and Technology Development (NAFOSTED) under grant number 106-YS.06-2013.16 to D. B. Nguyen, and grants from the European Union’s Seventh Framework Programme for research, technological development and demonstration under grant agreement No 602121 (CoMMiTMenT) and the EU Framework Programme for Research and Innovation Horizon 2020, Maria Curie Innovative Training Network

project under grant agreement No 675115 (RELEVANCE) to L. Kaestner. The authors thank Jörg Riedel for technical support.

Disclosure Statement

The authors declare no conflict of interest.

References

1. Heemskerk JW, Bevers EM, Lindhout T: Platelet activation and blood coagulation. Thromb Haemost 2002;88:186-193.

2. Williamson P, Christie A, Kohlin T, Schlegel RA, Comfurius P, Harmsma M, Zwaal RF, Bevers EM: Phsopholipid scramblase activation pathways in lymphocytes. Biochemistry 2001;40:8065-8072.

3. Nguyen DB, Wagner-Britz L, Maia S, Steffen P, Wagner C, Kaestner L, Bernhardt I: Regulation of Phosphatidylserine exposure in red blood cells. Cell Physiol Biochem 2011;28:847-856.

4. Bevers EM and Williamson PL: Phospholipid scramblase: An update. FEBS letters 2010;584:2724-2730.

5. Kaestner L, Steffen P, Nguyen DB, Wang J, Wagner-Britz L, Jung A, Wagner C, Bernhardt I: Lysophosphatidic acid induced red blood cell aggregation in vitro. Bioelechtrochemistry 2012;87:89-95.

6. Betal SG and Setty YB: Phosphatidylserine-positive erythrocytes bind to immobilized and soluble thrombospndin-1 via its heparin binding domain. Transl Res 2008;152:165-177.

7. Closse C, Dachary-Progent J, Boisseau MR: Phosphatidylserine-related adhesion of human erythrocytes to vascular endothelium. BJH 1999;107:300-302.

8. Gallagher PG, Chang SH, Rettig MP, Neely JE, Hillery CA, Smith BD, Low PS: Altered erythrocyte endothelial adherence and membrane phospholipid asymmetry in hereditary hydrocytosis. Blood 2003;101:4625-4627.

9. Chung SM, Bae ON, Lim KM, Noh JY, Lee MY, Jung YS, Chung JH: Lysophosphatidic acid induces thrombogenic activity through phosphatidylserine exposure and procoagulant microvesicle generation in human erythrocytes. Arterioscler Thromb Vasc Biol 2007;27:414-421.

10. Lang KS, Lang PA, Bauer C, Duranton C, Wieder T, Huber SM, Lang F: Mechanisms of suicidal erythrocyte death. Cell Physiol Biochem 2005;15:195-202.
11. Boas FE, Forman L, Beutler E: Phosphatidylserine exposure and red cell viability in red cell aging and in hemolytic anemia. Proc Natl Acad Sci USA 1998;95:3077-3081.
12. Fadok VA, Bratton DL, Rose DM, Pearson A, Ezekewitz RA, Henson PM: A receptor for phosphatidylserine-specific clearance of apoptotic cells. Nature 2000;405:85-90.
13. McEvoy L, Williamson P, Schlegel RA: Membrane phospholipid asymmetry as a determinant of erythrocyte recognition by macrophages. Proc Natl Acad Sci 1986;83:3311-3315.
14. Schroit AJ, Madsen JW, Tanaka Y: *In vivo* recognition and clearance of red blood cells containing phosphatidylserine in their plasma membranes. JBC 1985;260:5131-5138.
15. Lang F and Qadri SM: Mechanisms and significance of eryptosis, the suicidal death of erythrocytes. Blood Purif 2012;33:125-130.
16. Steffen P, Jung A, Nguyen DB, Mueller T, Bernhardt I, Kaestner L, Wagner C: Stimulation of human red blood cells leads to Ca^{2+}-mediated intercellular adhesion. Cell Calcium 2011;50:54-61.
17. Zhou Q, Zhao J, Wiedmer T, Sims PJ: Normal hemostasis but defective hematopoietic response to growth factors in mice deficient in phospholipid scramblase 1. Blood 2002;99:4030-4038.
18. Woon LA, Holland JW, Kable EP, Roufogalis BD: Ca^{2+} sensitivity of phospholipid scrambling in human red cell ghosts. Cell Calcium 1999;25:313-320.
19. Dekkers DW, Comfurius P, Bevers EM, Zwaal RF: Comparison between Ca^{2+}-induced scrambling of various fluorescently labeled lipid analogues in red blood cells. Biochem J 2002;362:741-747.
20. Brunner JD, Lim NK, Schenck S, Duerst A, Dutzler R: X-ray structure of a calcium-activated TMEM16 lipid scramblase. Nature 2014;516:207-212.
21. Wagner-Britz L, Wang J, Kaestner L, Bernhardt I: Protein kinase Cα and P-type Ca^{2+} channel $Ca_v2.1$ in red blood cell calcium signalling. Cell Physiol Biochem 2013;32:883-891.
22. Kaestner L: Channelizing the red blood cell: molecular biology competes with patch-clamp. Front Mol Biosci 2015;2:article 46.

23. Yang L, Andrews DA, Low PS: Lysophosphatidic acid opens a Ca^{2+} channel in human erythrocytes. Blood 2000;95:2420-2425.
24. Makhro A, Wang J, Vogel J, Boldyrev AA, Gassmann M, Kaestner L, Bogdanova A: Functional NMDA receptors in rat erythrocytes. Am J Physiol Cell Physiol 2010;299:1571-1573.
25. Gardos G: The permeability of human erythrocytes to potassium. Acta Physiol Hung 1956;10:185-189.
26. Maher AD, Kuchel PW: The Gardos channel: A review of the Ca^{2+}-activated K^+ channel in human erythrocytes. Int J Biochem Cell Biol 2003;35:1182-1197.
27. Lang PA, Kaiser SJ, Myssina S, Wieder T, Lang F, Huber SM: Role of Ca^{2+}-activated K^+ channels in human erythrocyte apoptosis. Am J Physiol – Cell Physiol 2003;285:C1553-C1560.
28. Raval PJ and Allan D: The effects of phorbol ester, diacylglycerol, phospholipase C and Ca^{2+} ionophore on protein phosphorylation in human and sheep erythrocytes. Biochem J 1985;232:43-47.
29. Govekar RB and Zingde SM: Protein kinase C isoforms in human erythrocytes. Ann Hematol 2001;80:531-534.
30. DeJong K, Rettig MP, Low PS, Kuypers FA: Protein kinase C activation induces phosphatidylserine exposure on red blood cells. Biochemistry 2002; 41:12562-12567.
31. Wesseling MC, Wagner-Britz L, Huppert H, Hanf B, Hertz L, Nguyen DB, Bernhardt I: Phosphatidylserine exposure in human red blood cells depending on cell age. Cell Physiol Biochem 2016;38:1376-1390.
32. Wesseling MC, Wagner-Britz L, Boukhdoud F, Asanidze S, Nguyen DB, Kaestner L, Bernhardt I: Measurements of intracellular Ca^{2+} content and phosphatidylserine exposure in human red blood cells: methodological issues. Cell Physiol Biochem 2016;38:2414-2425.
33. Herbert JM, Augereau JM, Gleye J, Maffrand JP: chelerythrine is a potent and specific inhibitor of protein kinase C. Biochim Biophys Res Commun 1990;172:939-999.
34. Kobayashi E, Nakano H, Morimoto M, Tamaoki T: Calphostin C (UCN-1028C), a novel microbial compound, is a highly potent and specific inhibitor of protein kinase C. Biochem Biophys Res Commun 1989;159:548-553.

35. Wolff D, Cecchi X, Spalvins A, Canessa M: Charybdotoxin blocks with high with high affinity the Ca-activated K^+ channel of Hb A and Hb S red cells: individual differences in the number of channels. J Membr Biol 1988;106:243-252.
36. Daleke DL: Regulation of phospholipid asymmetry in the erythrocyte membrane. Curr Opin Hematol 2008;15:191-195.
37. Hoffman JF, Joiner W, Nehrke K, Potapova O, Foye K, Wickrema a: The hSK4 (KCNN4) isoform is the Ca^{2+}-activated K^+ channel (Gardos channel) in human red blood cells. PNAS 2003;100:7366-7371.
38. Foeller M, Huber SM, Lang F: Erythrocyte programmed cell death. IUBMB Kife 2008;60:661-668.
39. Nguyen DB, Thuy Ly TB, Wesseling MC, Hittinger M, Torge A, Devitt A, Perrie Y, Bernhardt I: Characterization of microvesicles released from human red blood cells. Cell Physiol Biochem 2016;38:1085-1099.
40. Dekkers DW, Comfurius P, Vuist WM, Billheimer JT, Dicker I, Weiss HJ, Zwaal RF, Bevers EM: Impaired Ca^{2+}-induced tyrosine phosphorylation and defective lipid scrambling in erythrocytes from a patient with Scott syndrome: A study using an inhibitor for Scramblase that mimics the defect in Scott Syndrome. Blood 1998;91:2133-2138.
41. Smith SK, Farnbach AR, Harris FM, Hawes AC, Jackson LR, Judd AM, Vest RS, Sanchez S, Bell JD: Mechanisms by which intracellular calcium induces susceptibility to secretory phospholipase A_2 in human erythrocytes.
42. Chao MD, Chen IS, Cheng JT: Inhibition of protein kinase C translocation from cytosol to membrane by chelerythrine. Planta Med 1998;64:662-663.
43. Andrews DA, Yang L, Low PS: Phorbol ester stimulates a protein kinase C-mediated agatoxin-TK-sensitive calcium permeability pathway in human red blood cells. Blood 2002;100:3392-3399.
44. Kaestner L, Tabellion W, Lipp P, Bernhardt I: Prostaglandin E2 activates channel-mediated calcium entry in human erythrocytes: an indicator for a blood clot formation supporting process. Thromb Haemost 2004;92:1269-1272.

Figure legends

Figure 1

Percentage of RBCs (A) responding with increased intracellular Ca^{2+} content (elevated fluo-4 intensity) and (B) responding with increased PS exposure (annexin V-positive cells) after activation with A23187 (2 µM) for 30 min, LPA (2.5 µM) for 1 min, or PMA (6 µM) for 30 min in the absence or presence of the scramblase inhibitor R5421 (100 µM) using flow cytometry. Mean values of at least 5 different blood samples (150.000 cells), error bars = S.D. (only have error bars are shown for convenience). Significant differences, ANOVA ($0.01 < p \leq 0.05$ (*); $0.001 < p \leq 0.01$ (**)) are shown in the figure.

Figure 2

Fluorescence microscopy images of RBCs after activation with A23187 (2 µM) for 30 min, LPA (2.5 µM) for 1 min, and PMA (6 µM) for 30 min as well as control (absence of any activating substance) in the absence or presence of the scramblase inhibitor R5421 (100 µM). Upper rows – transmitted light, lower rows – fluorescence images to detect PS exposure using annexin V-FITC. RBCs in HPS with additional $CaCl_2$ (2 mM). Representative images out of 4 independent experiments.

Figure 3

Percentage of RBCs (A) responding with increased intracellular Ca^{2+} content (elevated fluo-4 intensity) and (B) responding with increased PS exposure (annexin V-positive cells) after activation with A23187 (2 µM) for 30 min, LPA (2.5 µM) for 1 min, or PMA (6 µM) for 30 min in the presence of the PKCα inhibitors chelerythrine chloride (Chel., 10 µM) or calphostin C (Cal. C, 1 µM) compared to control (absence of PKCα inhibitors) using flow cytometry. Mean values of at least 3 different blood samples (90.000 cells), error bars = S.D. (only have error bars are shown for convenience). Significant differences, ANOVA ($0.01 < p \leq 0.05$ (*); $0.001 < p \leq 0.01$ (**); $p \leq 0.001$ (***)) are shown in the figure.

Figure 4

Percentage of RBCs (A) responding with increased intracellular Ca^{2+} content (elevated fluo-4 intensity) and (B) responding with increased PS exposure (annexin V-positive

cells) after activation with A23187 (2 µM) for 30 min, LPA (2.5 µM) for 1 min, or PMA (6 µM) for 30 min in the presence of the PKCα inhibitors chelerythrine chloride (Chel., 10 µM) plus calphostin C (Cal. C, 1 µM), the PKCα inhibitor chelerythrine chloride (Chel., 10 µM) plus the scrambles inhibitor R5421 (100 µM), or the PKCα inhibitor calphostin C (Cal. C, 1 µM) plus the scrambles inhibitor R5421 (100 µM), compared to control (absence of inhibitors) using flow cytometry. Mean values of at least 3 different blood samples (90.000 cells), error bars = S.D. (only have error bars are shown for convenience). Significant differences, ANOVA ($0.01 < p \leq 0.05$ (*); $0.001 < p \leq 0.01$ (**); $p \leq 0.001$ (***)) are shown in the figure.

Figure 5

Percentage of RBCs (A) responding with increased intracellular Ca^{2+} content (elevated fluo-4 intensity) and (B) responding with increased PS exposure (annexin V-positive cells) after activation with A23187 (2 µM) for 30 min, LPA (2.5 µM) for 1 min, or PMA (6 µM) for 30 min in the absence or presence of Ca^{2+}-activated K^+ channel inhibitor charybdotoxin (CTX, 20 nM) using flow cytometry. Mean values of at least 3 different blood samples (90.000 cells), error bars = S.D. (only have error bars are shown for convenience). Significant differences, ANOVA ($0.001 < p \leq 0.01$ (**); $p \leq 0.001$ (***)) are shown in the figure.

Figure 6

Flow cytometry analysis (forward scatter, FSC) of RBCs after activation with A23187 (2 µM) for 30 min in normal physiological solution (HPS) containing 7.5 mM KCl, and solutions with higher KCl concentrations (compensated by a reduction of the NaCl concentration to keep the osmolarity constant) in comparison to control (absence of A23187). To all solutions 2 mM $CaCl_2$ were added. Mean values of at least 4 different blood samples (120.000 cells), error bars = S.D. (only have error bars are shown for convenience). Significant differences, ANOVA ($0.01 < p \leq 0.05$ (*); $0.001 < p \leq 0.01$ (**)) are shown in the figure.

Figure 7

Percentage of RBCs (A) responding with increased PS exposure (annexin V-positive cells) after activation with A23187 (2 µM) for 30 min, LPA (2.5 µM) for 1 min, or PMA

(6 µM) for 30 min in normal physiological solution (HPS) containing 7.5 mM KCl and a solution containing 150 mM KCl (compensated by a reduction of the NaCl concentration to keep the osmolarity constant, for detailed composition see Material and Methods) using flow cytometry. Mean values of at least 6 different blood samples (180.000 cells), error bars = S.D. (only have error bars are shown for convenience). Significant differences, ANOVA ($0.001 < p \leq 0.01$ (**)) are shown in the figure.

Figures

Figure 1

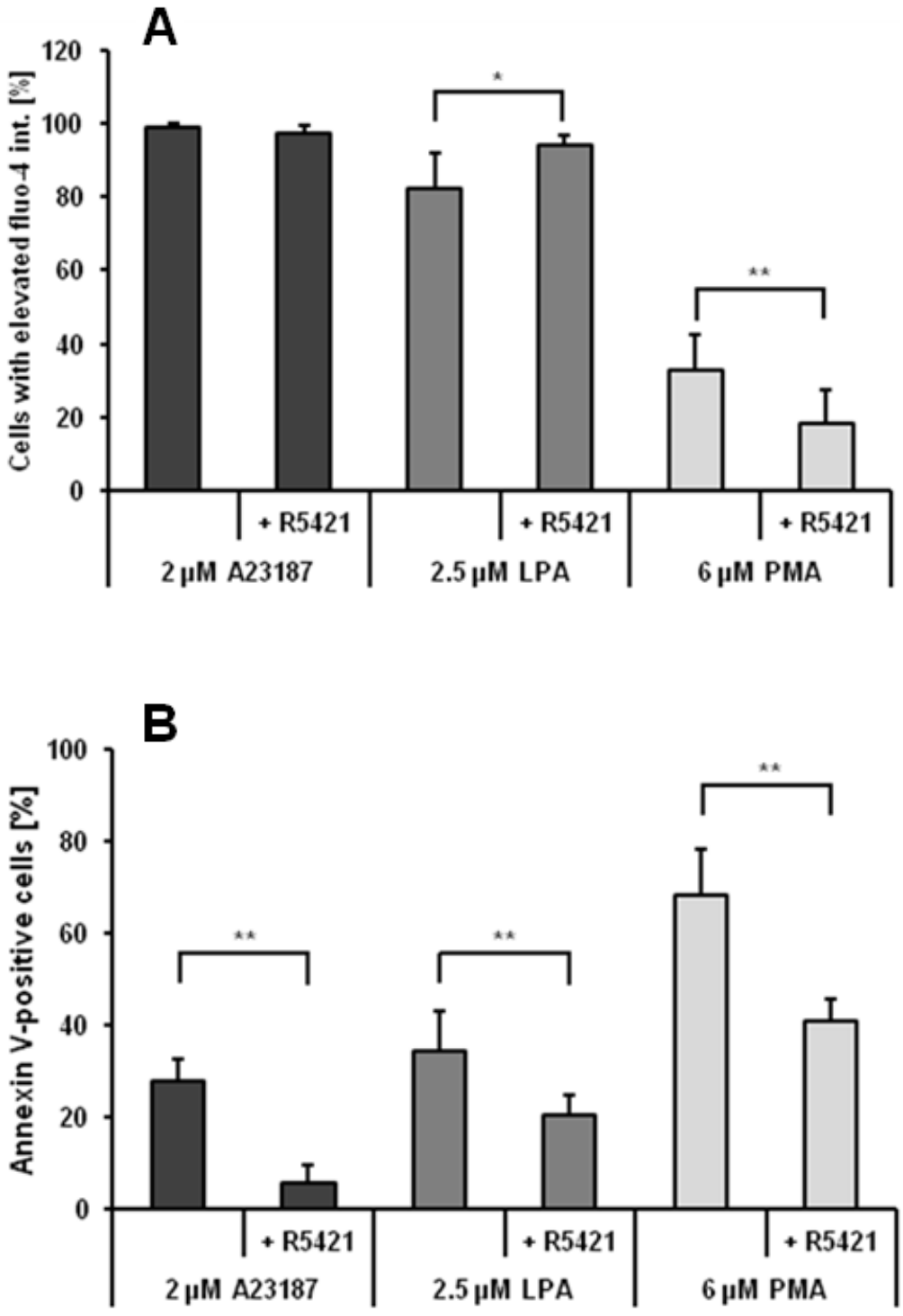

Figure 2

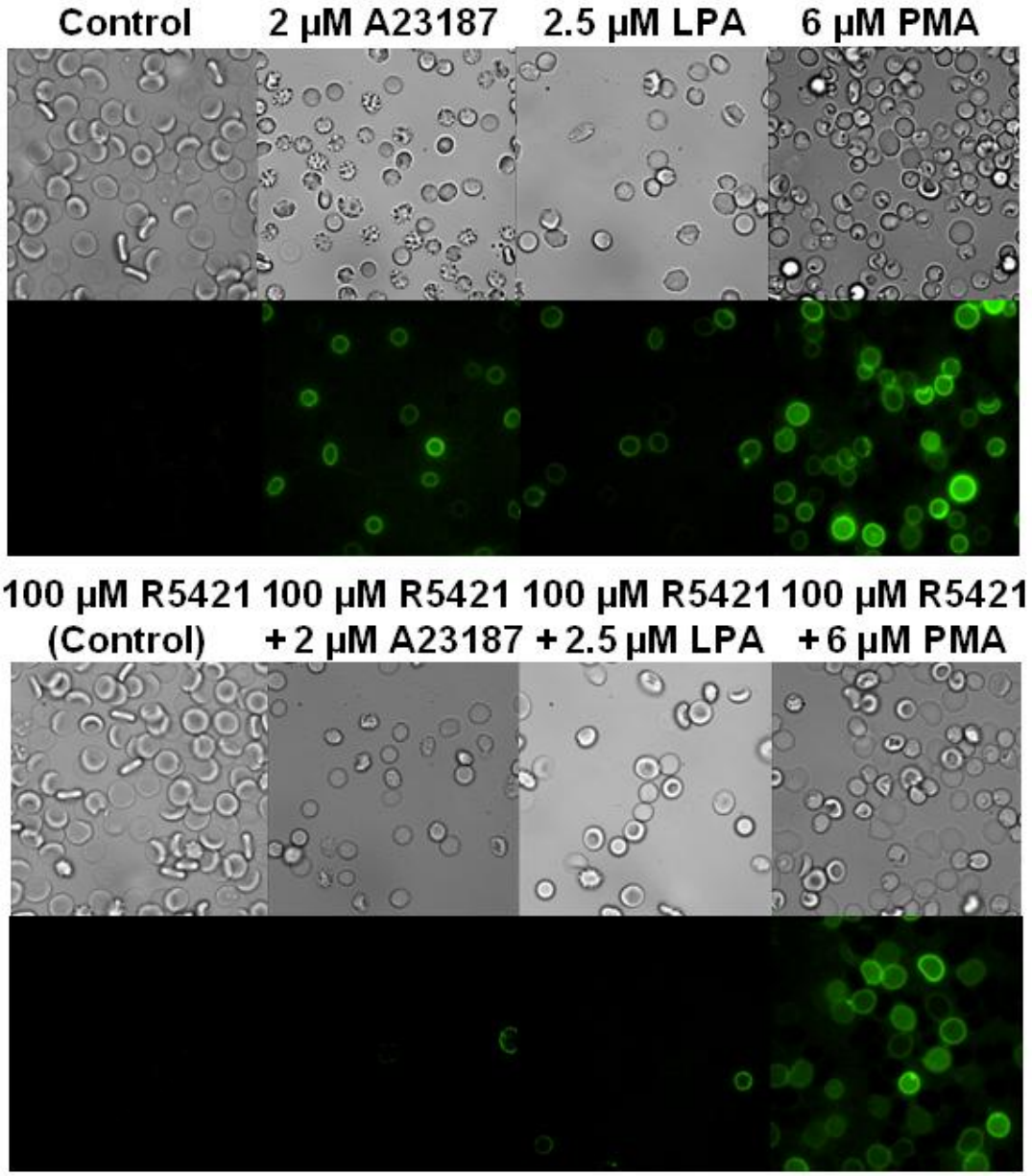
Control
2 µM A23187
2.5 µM LPA
6 µM PMA
100 µM R5421 (Control)
100 µM R5421 + 2 µM A23187
100 µM R5421 + 2.5 µM LPA
100 µM R5421 + 6 µM PMA

Figure 3

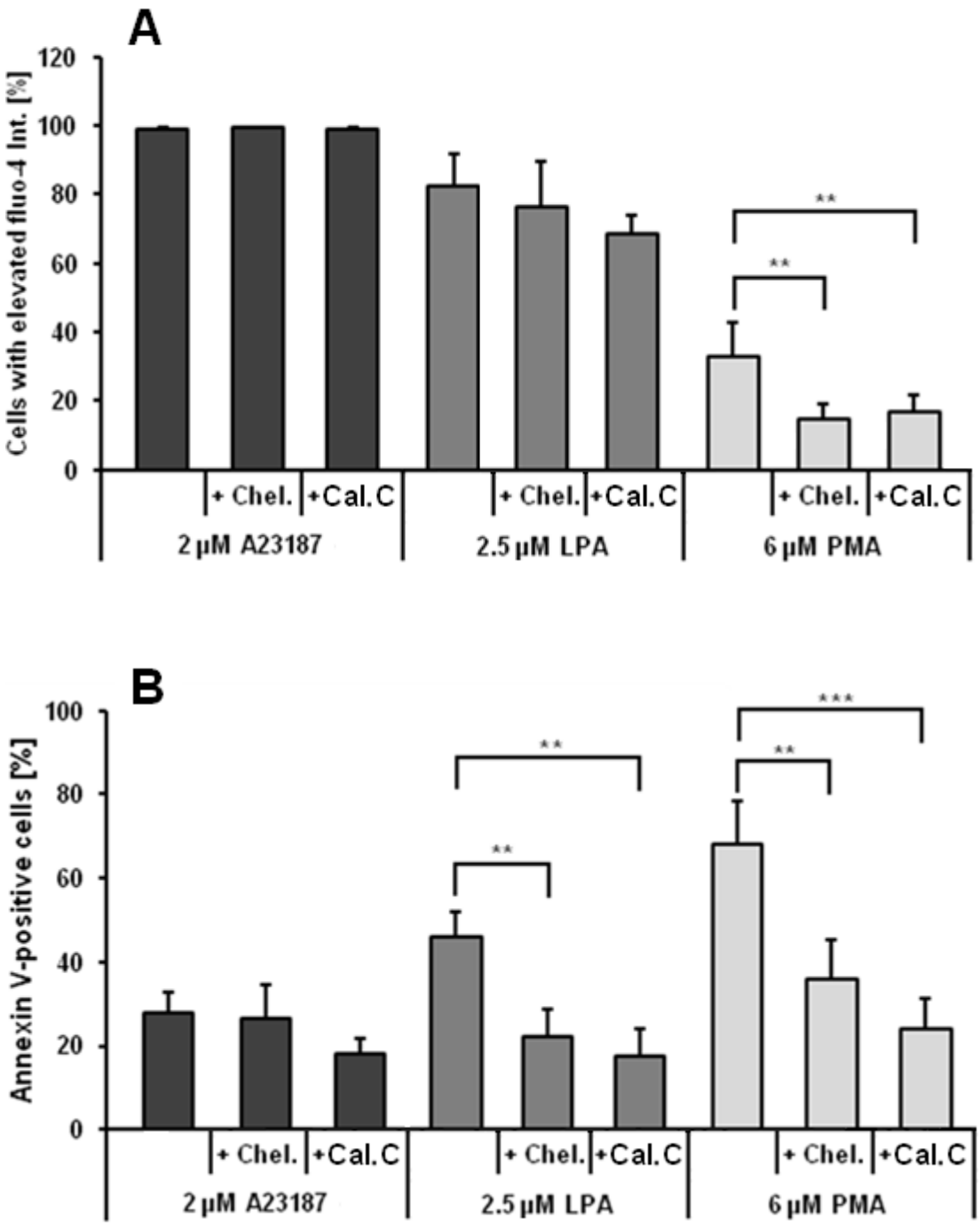
A
Cells with elevated fluo-4 Int. [%]
120
100
80
60
40
20
0
**
**
+ Chel.
+Cal.C
+ Chel.
+Cal.C
+ Chel.
+Cal.C
2 µM A23187
2.5 µM LPA
6 µM PMA
B
Annexin V-positive cells [%]
100
80
60
40
20
0
***
**
**
+ Chel.
+Cal.C
+ Chel.
+Cal.C
+ Chel.
+Cal.C
2 µM A23187
2.5 µM LPA
6 µM PMA

Figure 4

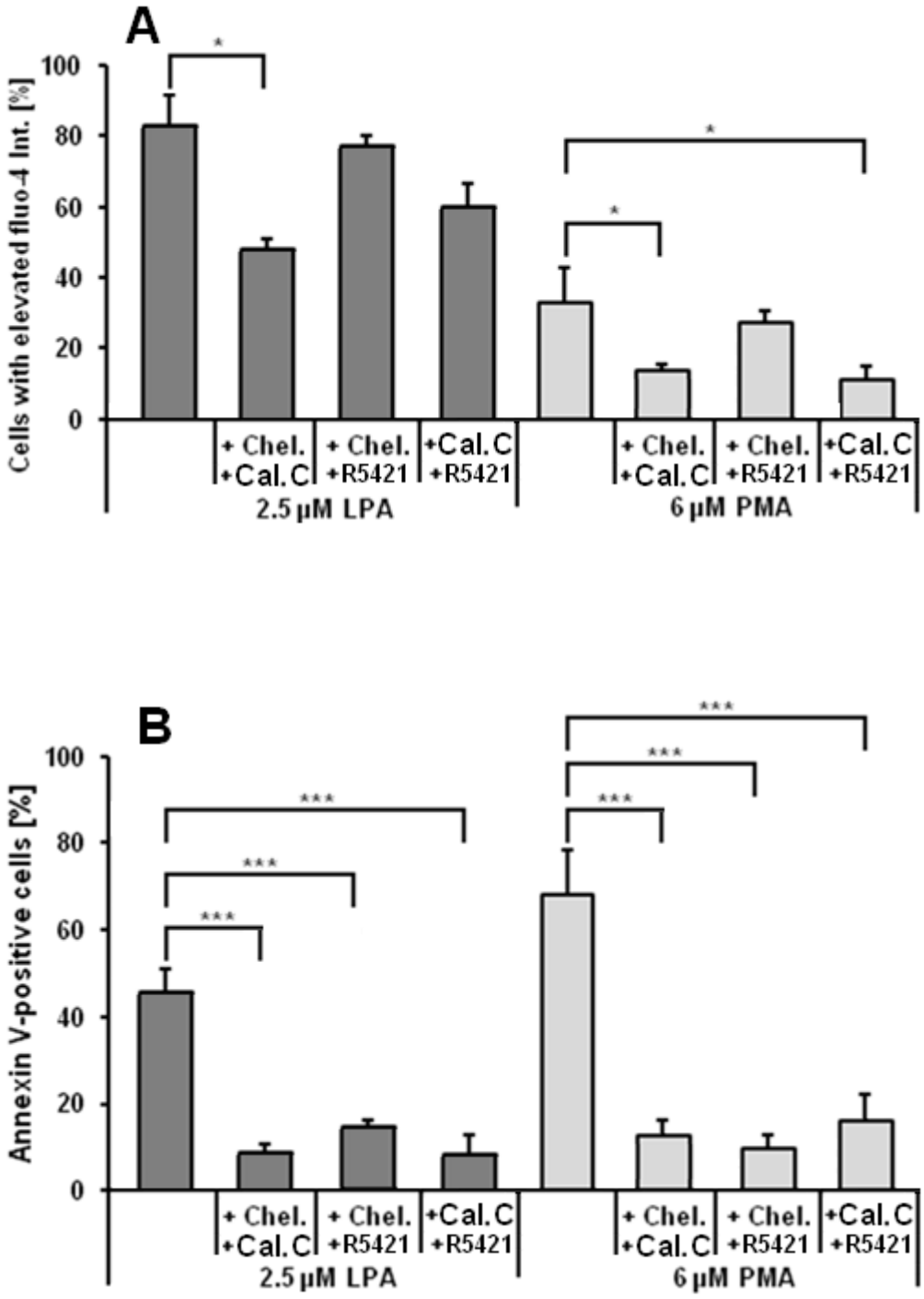
A
Cells with elevated fluo-4 Int. [%]
100
80
60
40
20
0
*
*
*
+ Chel. +Cal.C
+ Chel. +R5421
+Cal.C +R5421
2.5 µM LPA
+ Chel. +Cal.C
+ Chel. +R5421
+Cal.C +R5421
6 µM PMA
B
Annexin V-positive cells [%]
100
80
60
40
20
0
***
***
***
***
***
***
+ Chel. +Cal.C
+ Chel. +R5421
+Cal.C +R5421
2.5 µM LPA
+ Chel. +Cal.C
+ Chel. +R5421
+Cal.C +R5421
6 µM PMA

Figure 5

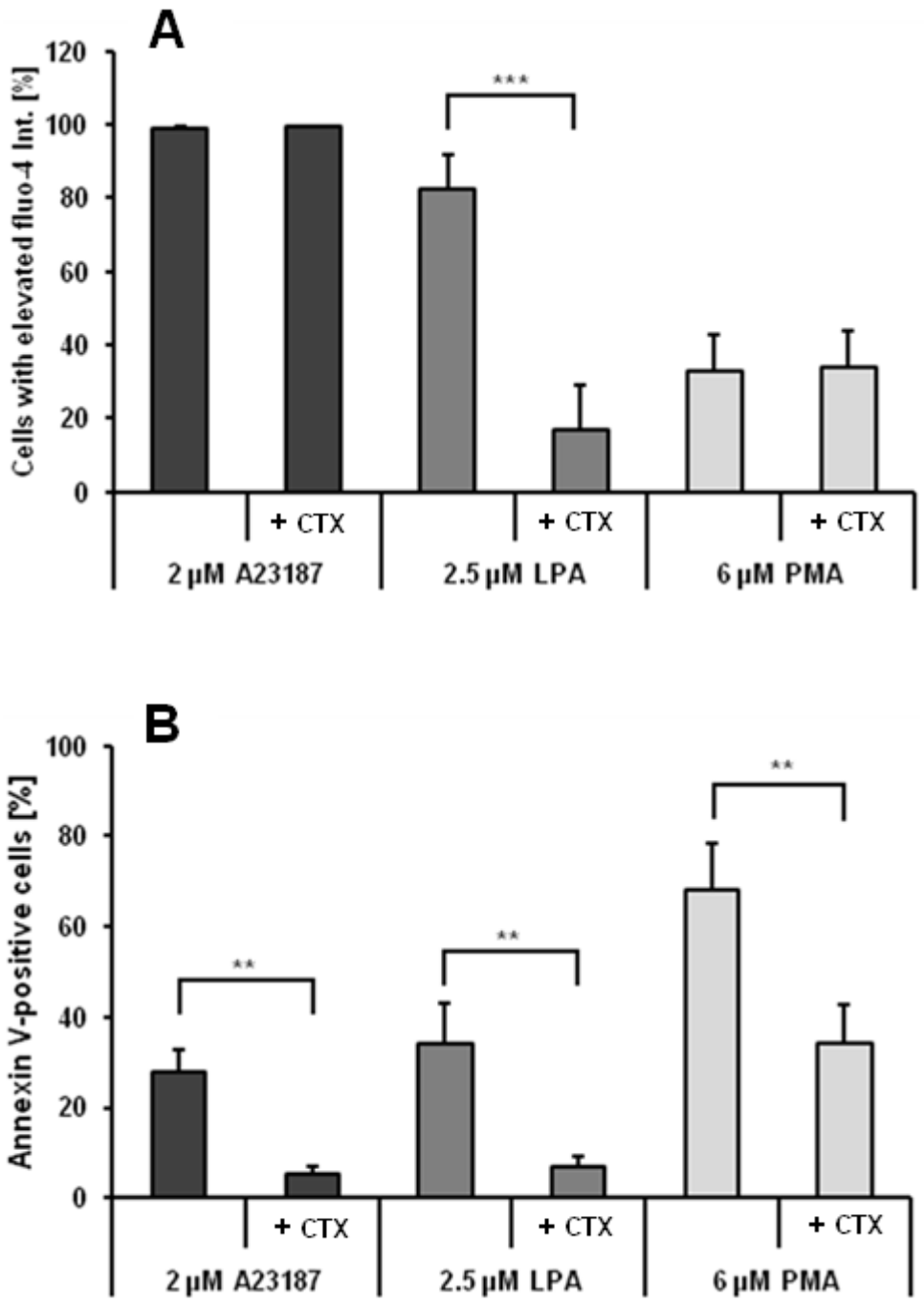
A
Cells with elevated fluo-4 Int. [%]
120
100
80
60
40
20
0
***
+ CTX
+ CTX
+ CTX
2 µM A23187
2.5 µM LPA
6 µM PMA
B
Annexin V-positive cells [%]
100
80
60
40
20
0
**
**
**
+ CTX
+ CTX
+ CTX
2 µM A23187
2.5 µM LPA
6 µM PMA

Figure 6

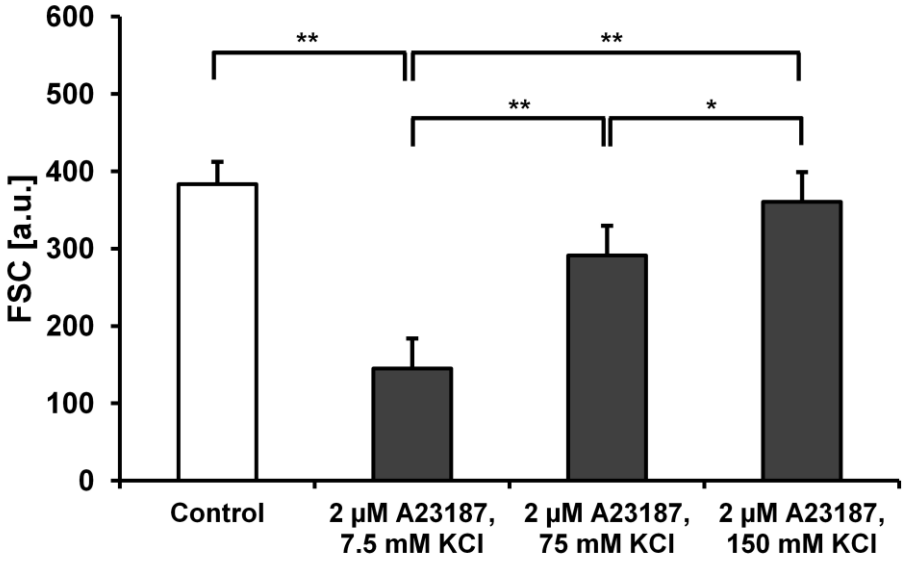

Figure 7

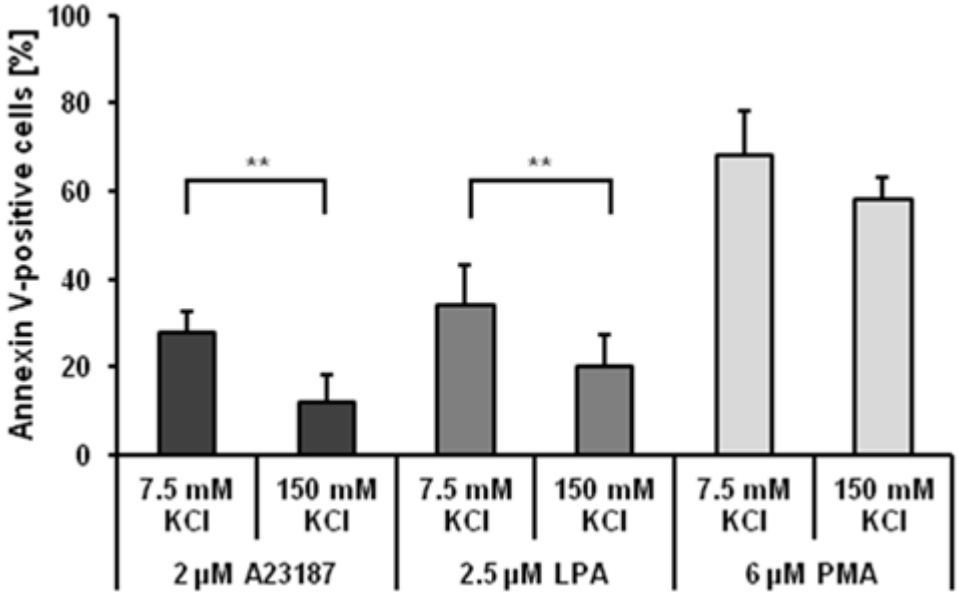

3. Discussion and conclusions

The aim of this work was to investigate the relationship between increased intracellular Ca^{2+} content and PS exposure in human RBCs. Hence, two substances, LPA and PMA, have been used to induce Ca^{2+} uptake of RBCs. Another substance, A23187, served as positive control. First of all, some methodological issues have been taken into consideration. In our experiments we realised that RBC stimulation with LPA from different batches led to significant different results of the intracellular Ca^{2+} content as well as the PS exposure. The investigator and the experimental conditions as well as successive re-frozen/thawing processes of the substance batches (in our publication only LPA has been tested, however, the other substances could also have a similar behaviour) can also have an influence on the obtained results (see below). In addition, we realized differences comparing the results of single and double labelling experiments (for Ca^{2+} and PS). For this reason, single and double labelling experiments using a verity of fluorescent dyes were carried out to understand the challenge and to be able to compare results obtained by different research groups. It was also necessary to investigate the participation of the Ca^{2+}-activated K^{+} channel in the process of PS exposure. Furthermore, it has to be clarified why do exist some RBCs with increased intracellular Ca^{2+} content but no PS exposure and *vice versa* some RBCs showing PS exposure but no increased intracellular Ca^{2+} content. To investigate this effect, RBCs separated by age were analyzed. In addition, the shape of the RBCs was taken into consideration.

3.1 Methodological issues by measurements of intracellular Ca^{2+} content and phosphatidylserine exposure in human red blood cells

To investigate in more detail why different LPA batches lead to different response in the increasing intracellular Ca^{2+} content as well as PS exposure of RBCs, we performed experiments with LPA from 4 different batches, obtained from three different companies. All 4 LPA probes were freshly used, re-frozen only once and were applied to the same blood on the same day and using the same physiological solution. In addition, all experiments were carried out by the same investigator under identical experimental conditions. The obtained results are published in the paper of Wesseling et al. [101]. In

all cases of LPA activation there is a significant increase in the percentage of RBCs showing increased intracellular Ca^{2+} content and PS exposure compared to control. Interestingly, there are significant differences in the percentages of RBCs responding with increased intracellular Ca^{2+} content as well as PS exposure depending on the LPA batch used. In addition, we found that the LPA activation efficiency within a single batch decreased with the number of times the LPA stock solution was frozen and thawed.

To study a possible effect of the experimenter on the results obtained, we performed experiments with two different ways of mixing the RBC suspensions after LPA activation. Double labelling experiments for Ca^{2+} content (using x-rhod-1) and PS exposure (using annexin V-FITC) after activation of RBCs with LPA were compared following simple shaking by hand and with vortexing the RBC suspensions (both in Eppendorf tubes, 5 s each). One can observe a significant higher percentage of RBCs responding with increased intracellular Ca^{2+} content as well as PS exposure when the suspension has been vortexed after addition of LPA compared with simple shaking by hand. These results suggest that a mechanosensitve channel, like the recently reported Piezo1, may contribute to the LPA-induced Ca^{2+} entry ([102] and references therein).

The intracellular Ca^{2+} content and the PS exposure of RBCs can be measured on the basis of single as well as double labelling experiments. Furthermore, different fluorescent dyes are available for the detection of both parameters. For intracellular Ca^{2+} content there is no significant difference between single and double labelling experiments. In addition, the results do not depend on the fluorescent dye (or the combination of the fluorescent dyes) used. However, the values for PS exposure of double labelling experiments are significantly lower for both fluorescent dyes (annexin V-FITC and annexin V alexa fluor® 647 (for PS), in combination with x-rhod-1 and fluo-4 (for Ca^{2+}), respectively) compared to single labelling experiments (annexin V-FITC or annexin V alexa fluor® 647 alone (for PS)). In addition, the amount of RBCs showing PS exposure is also significantly different in single labelling experiments when the cells were stained with annexin V-FITC in comparison to annexin V alexa fluor® 647 as well as compared to the corresponding double labelling experiments.

The reasons for the differences in single labelling *versus* double labelling experiments are multifactorial and can be explained by three major effects: (i) the Ca^{2+} buffering capacities of the Ca^{2+} fluorophores, (ii) the properties of the fluorescent dyes, and (iii) the temporal development of the Ca^{2+} signals (as discussed in [101]).

(i) Fluo-4 and x-rhod-1 have *in vitro* dissociation constants K_d for Ca^{2+} of 345 nM and 700 nM, respectively [103]. In living cells these K_d's are, dependent on their cellular localisation, and are usually increased [104]. Especially when taking the low resting Ca^{2+} concentration in RBCs of around 60 nM [60] into account, the buffering capacity of the Ca^{2+} fluorophors loaded into the cells is high. The variety of the cellular responses [105] may add to the observed effects. Although the EC_{50} of the scramblase (30-70 µM) compared to the *in vivo* K_d of Fluo-4 (1 µM) [107] is several fold higher, there are observations suggesting that scrambling may actually require much less Ca^{2+} [107], and therefore the buffering of the Ca^{2+} is the most likely explanation for a lower PS exposure in the double labelled cells as depicted in Figs. 3B and 4B. The relative decrease in PS exposure of the double labelling compared the single labelling is much higher for fluo-4 compared to x-rhod-1 (Fig. 3B). This observation is also in agreement with the K_d´s of the two fluorophors (see above) and hence their buffering properties.

(ii) Other aspects that may contribute to the differences between FITC and alexa fluor® 647 results are the photophysical properties of the dyes. Assuming that the fluorescence quantum yield of a cyanine dye (alexa fluor® 647) may change when the surrounding conditions are changed, e.g. in RBC haemoglobin close to the plasma membrane could be a factor influencing alexa fluor® 647. Isomerisation of double bonds of cyanine dyes is well known [108, 109]. Such changes in combination with wavelength dependencies of the detectors may account, at least partly, for the differences observed for PS detection based on FITC and alexa fluor® 647. Differences in incubation times for single and double labelling experiments as well as the solvent DMSO can be ruled out as sources for different results (we tested this by incubating the RBCs for 30 min in DMSO but without fluo-4, data not shown).

(iii) Apart from the different LPA batches, measurements between Fig. 3 and Fig. 4 differ in their measurement time after LPA stimulation (1 min *versus* 30 min, respectively). After 30 min LPA stimulation, the PS exposure, which is a cumulative process, reaches in the presence of x-rhod-1 the same value as that in the absence of x-rhod-1. As mentioned before, due to its K_d, x-rhod-1 buffers the Ca^{2+} at a higher level compared to fluo-4. This Ca^{2+} level allows a basal scramblase activity, which in combination with the temporal aspects explains the differences observed between Fig. 3B and Fig. 4B.

Furthermore it is worthwhile to mention that de-esterification of the Ca^{2+} fluorophores may generate formaldehyde and thus affect RBC behaviour, namely by ATP-depletion [111], which can be prevented by the addition of pyruvate [111].

3.2 Automated image analysis of red blood cells

To analyse fluorescent images taken from RBCs in fluorescence microscope we developed an automated image analysis system. Manual analysis of fluorescence images of RBCs requires the experimenter to count all cells in the images and to classify them according to their activation state. To classify the cells strongly depends on the experience of the investigator. A combination of well established image analysis techniques allows us to automate this task. With this technique we yield robust results, while saving valuable time. The automated system detects cells with high reliability and classifications are comparable to manual classifications. The manuscript containing the data of this paragraph has been submitted for publication [112].

3.3 Influence of cell age on the intracellular Ca^{2+} content and phosphatidylserine exposure

In a population of human RBCs one can find cells with different age. They have a life span of about 120 days [5]. Depending on age, their density is different. Young cells have a lower density in comparison to old cells [113]. This makes it possible to separate them into fractions with different ages by density gradient centrifugation using Percoll [114]. Which factors are crucial for the aging process and the mechanisms for the removal of damaged or old RBCs from the blood stream is not yet fully understood. Assuming a higher intracellular Ca^{2+} concentration in old RBCs one could assume a higher amount of PS in the outer membrane leaflet of old RBCs compared to young once. On this basis it has been speculated that macrophages recognise old and senescent RBCs with a certain amount of PS in the outer membrane leaflet and remove them from the blood stream [54-56]. It has been described that older RBCs have a higher intracellular Ca^{2+} content [115, 116]. However, Makhro et al. [38] and de Haro et al. [117] reported that rat and human reticulocytes, respectively, have a higher Ca^{2+} content than the mature RBCs.

Furthermore, other authors have shown recently that PS exposure of human RBCs is independent of cell age [118]. Only after long-time incubation for 48 h in Ringer solution a significant increase in the intracellular Ca^{2+} content as well as PS exposure with cell age could be detected [119]. To solve the mentioned discrepancies as well as to understand why not all RBCs after stimulation do not react equally with an increased intracellular Ca^{2+} content as wells as PS exposure, we performed short-time incubation experiments. The RBCs were separated in 5 fractions with different cell age. The results can be seen in Wesseling et al. [120].

Our data at time zero, i.e. before the stimulation show also a slightly higher percentage of older RBCs showing increased intracellular Ca^{2+} content and PS exposure compared to young ones. However, this effect is not significant and probably also not pronounced enough to explain the clearance of old RBCs from the blood stream on the basis of such mechanism. We could demonstrate that there are no significant differences in the intracellular Ca^{2+} content as well as PS exposure of RBCs of different age after stimulation of Ca^{2+} uptake and after short-time incubation. In addition, the findings of Nguyen et al. [89], showing that some RBCs have an increased intracellular Ca^{2+} content but no enhanced PS exposure and that some other cells have an elevated PS exposure but no significant increase of the intracellular Ca^{2+} content cannot be explained assuming that this effect is depending on the age of the RBCs. Our results also clearly show that only a relative small amount of the cells show PS exposure, although the intracellular Ca^{2+} is increased in all cells by activation with the Ca^{2+} ionophore A23187. There is also no clear correlation between Ca^{2+} increase and PS exposure in case of LPA or PMA activation. Therefore one can conclude that the increase in the intracellular Ca^{2+} is not solely responsible for PS exposure in human RBCs.

3.4 Participation of the scramblase, protein kinase C and Ca^{2+}-activated K^+ channel in the phosphatidylserine exposure in human RBCs

To gain further insight into the correlation of increased intracellular Ca^{2+} content and PS exposure, we used specific inhibitors for some pathways that are correlated with PS exposure in human RBCs. Inhibition of the scramblase (using the scramblase inhibitor R5421) leads to a reduction of PS exposure of the cells. It seems obvious that the small

remaining population, reacting with PS exposure, does so upon the increase in the intracellular Ca^{2+} content, which is a trigger for the scramblase. The inhibition of the PKC with either, chelerythrine chloride (that inhibits the active site of the PKC [121]), or calphostin C (a blocker of the DAG and PMA binding site of the PKC [122]) also reduces the number of cells with PS exposure after stimulation with LPA or PMA. It was reported that it has no effect on Ca^{2+} uptake [17].

An elevated extracellular K^+ concentration up to 150 mM (NaCl was replaced by KCl to have a constant osmolarity) leads to an inhibition of the Ca^{2+}-induced K^+ efflux through the Ca^{2+}-activated K^+ channel. Since activation of the Ca^{2+}-activated K^+ channel leads to a hyperpolarisation of the membrane, accompanied by a shrinkage of the cells due to a loss of KCl and osmotically obliged H_2O [57], the cell shrinkage can be prevented by inhibition of the K^+ efflux. If the K^+ efflux blocked, PS exposure is reduced. So, the activity of the Ca^{2+}-activated K^+ channel seems to be of importance for the PS exposure. Since we found out that the shrinkage of the cells alone has no influence on intracellular Ca^{2+} content or PS exposure, the K^+ efflux via the Ca^{2+}-activated K^+ channel could somehow be a trigger for PS exposure or possibly for the scramblase itself. The data presented in this section are parts of a manuscript to be submitted (see publication of the results, section 2.5).

3.5 Role of cell shape in the intracellular Ca^{2+} content and phosphatidylserine exposure

Starting from the classical biconcave discocyte shape, the RBCs are able to transform to either, echinocyte or stomatocyte shapes [95]. Furthermore, another large variety of abnormal cell shapes can be observed in human RBCs [123]. Cell shape transformations have been investigated for many years and there are hundreds of publications about this topic [95-100]. The crucial point for the explanation of cell shape transformations is the bilayer-couple hypothesis developed by Sheetz and Singer [86]. Changes of the membrane curvature are based on an expansion of the inner or outer membrane leaflet relative to the other one, since the two leaflets cannot separate from each other due to their coupling by hydrophobic interactions [86]. The change of the membrane curvature leads to a shape change of the cells. An expansion of the outer membrane leaflet leads to

a formation of echinocytes, whereas an expansion of the inner membrane leaflet leads to a formation of stomatocytes [97-100].

The expansion of the membrane depends on a large variety of membrane and cytoplasmatic parameters [95-97]. An expansion of one of the leaflets can occur after transversal redistribution of the membrane phospholipids or an insertion of amphiphilic compounds intro the membrane (some amphiphils are staying in the outer membrane leaflet, some other compounds are moving to the inner membrane leaflet). Both processes need at least several minutes. On the other hand, a quickly transformation can occur due to conformational changes of integral membrane proteins. Such a process happens in a few seconds [97]. Since RBCs contain a protein, existing in 1,000,000 copies per cell (and occupying about 50 % of the cell surface), a conformational change of this protein can lead to a sudden shape change, which has been demonstrated by Betz et al. [124].

Using the protocol of Betz et al., [124] to induce RBC shape changes by applying different solutions we were able to transform RBCs predominantly into stomatocytes or echinocytes. Control experiments with discocytes in physiological solution have been carried out. After stimulating the Ca^{2+} influx in RBCs (with substances previously mentioned like A23187, LPA or PMA) of different cell shapes no significant differences has been observed in the percentage of RBCs with increased intracellular Ca^{2+} content. Interestingly, for the PS exposure the situation was different: echinocytes showed significantly less PS exposure while discocytes or stomatocytes showed higher values of the percentage of RBCs with PS exposure. The results of the experiments investigating the role of cell shape transformation for Ca^{2+} uptake and PS exposure can be seen in the appendix.

Since the observed effect of existing some RBCs with PS exposure but no elevated Ca^{2+} content is not depending on the age of the cells [120], we propose that the reason is due to the beginning of cell damage. This is probably accompanied by a loss of the Ca^{2+}-sensitive fluorescent dye (see Figure 5 in the appendix). On the other side, cells which have an increased intracellular Ca^{2+} content but no PS exposure are due to the fact that PS exposure depends on the cell shape (echinocytes do show PS exposure to a much lower extent compared to dicocytes or stomatocytes, see above and Figures 6 and 7 in the appendix). However, it cannot be excluded completely that in some of these cells PS exposure occurs at a time later than the measuring time and therefore these cells show only elevated intracellular Ca^{2+} content.

3.6 Conclusions

The most raised questions (see aims and scope, 1.8) have been answered. Not completely answered is the question of existing RBCs with an increased Ca^{2+} content but no PS exposure. Although there is some evidence that this effect is due to different shapes of the RBCs, more effort is needed to be completely convinced. It would be interesting to see a change of the PS exposure in a single RBC during the process of the shape change. Such study could be possible to see under a fluorescence microscope applying amphiphilic substances.

3.7 Outlook

It has been demonstrated that Ca^{2+} uptake of RBCs activates the Ca^{2+}-activated K^{+} channel. In the present work it has been shown that the Ca^{2+}-activated K^{+} channel participate in the PS exposure of RBCs. However, further experiments under activating/inhibiting conditions should be performed to investigate the correlation between the Ca^{2+}-activated K^{+} channel, cell size and fluorescence intensity of RBCs using fluorescence microscopy.

The existence of a Ca^{2+}-independent pathway of PS exposure has not been investigated in this work in detail. Further experiments using Lactadherin (a Ca^{2+}-free PS binding fluorescent dye) could help to get more insight.

Furthermore, experiments using amphiphilic substances to induce cell shape transformations, could solve the remaining open questions about the effect of RBC shape for PS exposure.

4. Appendix

The results of the experiments investigating the reason of existing some RBCs with increased intracellular Ca^{2+} content but no PS exposure and *vice versa* some RBCs showing PS exposure but no increased intracellular Ca^{2+} content as well as the role of cell shape transformation for Ca^{2+} uptake and PS exposure are presented here, since the manuscript has not been submitted for publication yet.

4.1 Why some RBCs show only PS exposure without an elevated Ca^{2+} content?

To investigate the kinetics of Ca^{2+} uptake and PS exposure (and how both parameters affect each other), RBCs have been stimulated with LPA. Images were taken under a fluorescence microscope. A randomly position has been chosen and several images of the same position on the cover slip (to study the same RBCs) were taken over a certain time period. In Figure 5 one can see at the left images that all five RBCs show an increased intracellular Ca^{2+} content (detected using x-rhod-1, in orange). Four of them also show PS exposure (detected using annexin V-FITC, in green). Surprisingly, a RBC (indicated with the white arrow) shows increased intracellular Ca^{2+} content but the cell suddenly disappeared from the transmitted light image (upper right picture).

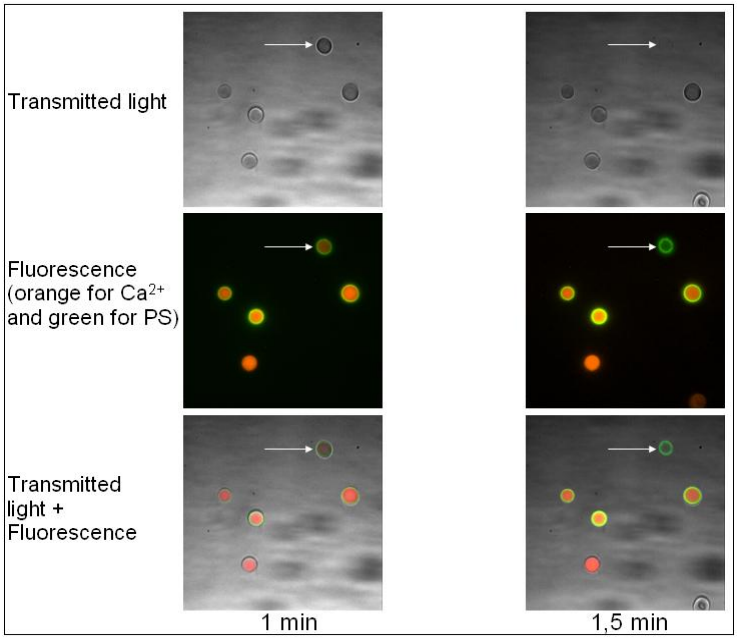

Figure 5: Fluorescence microscope images of RBCs with measurements of Ca^{2+} uptake (x-rhod-1, orange) and PS exposure (annexin V-FITC, green), after LPA stimulation.

However, PS exposure of this cell still can be seen (right middle picture). Therefore, it can be assumed that this cell undergoes eryptosis. This means that the cell is already damaged (although existing as a structure with holes) and Ca^{2+} and/or Ca^{2+} with the Ca^{2+}-sensitive fluorescent dye leave the cell.

4.2 Why some RBCs show only an elevated Ca^{2+} content without PS exposure?

Taken the RBC shape into consideration in the measurement of intracellular Ca^{2+} content and PS exposure an interesting observation was made in experiments using a fluorescence microscope. After stimulating the Ca^{2+} influx in RBCs (with substances previously mentioned like LPA, PMA, or A23187), single labelling experiments using fluo-4 (to detect Ca^{2+}) and annexin V-FITC (to detect PS) have been performed. Several pictures of RBCs in randomly chosen positions on the cover slip have been taken under fluorescence microscope. The obtained results are depicted in Figure 6. Figure 6 A shows transmitted light and fluorescence images of RBCs for detection of the intracellular Ca^{2+} content. Different cell shapes can be observed in the transmitted light pictures in case of all three activators. However, the fluorescence images reveal no differences or preferences of the cell shape for the increase of the Ca^{2+} content. However, the situation changes when analysing the PS exposure of the cells with different shape (Figure 6 B). In this Figure the transmitted light and fluorescence images of RBCs for the detection of the PS exposure is shown. Again different cell shapes can be observed, but in case of PS exposure the cell shape seems to play a decisive role. Indicated with white arrows some echinocytes can be seen in the transmitted light images. Almost all of them do not show PS exposure (see the corresponding fluorescence image). Only one echinocyte (indicated with the black arrow) can be observed showing PS exposure.

To investigate this phenomenon in more detail shape changes of RBCs by applying different solutions/substances have been carried out according to the protocol of Betz et al. [124]. The following solutions have been used: Normal HEPES-buffered physiological solution (HPS) containing, in mM: 145 NaCl, 7.5 KCl, 10 glucose, 10 HEPES, pH 7.4 (mostly discocytes); Low ionic strength solution (containing, in mM: sucrose 250, KCl 7.5, glucose 10, HEPES 10, pH 7.4) + 10 µM DIDS (predominantly

echinocytes); HPS + 10 µM DIDS; predominantly stomatocytes or discocytes: Low ionic strength solution (blue); HPS pH 5.6 (violett).

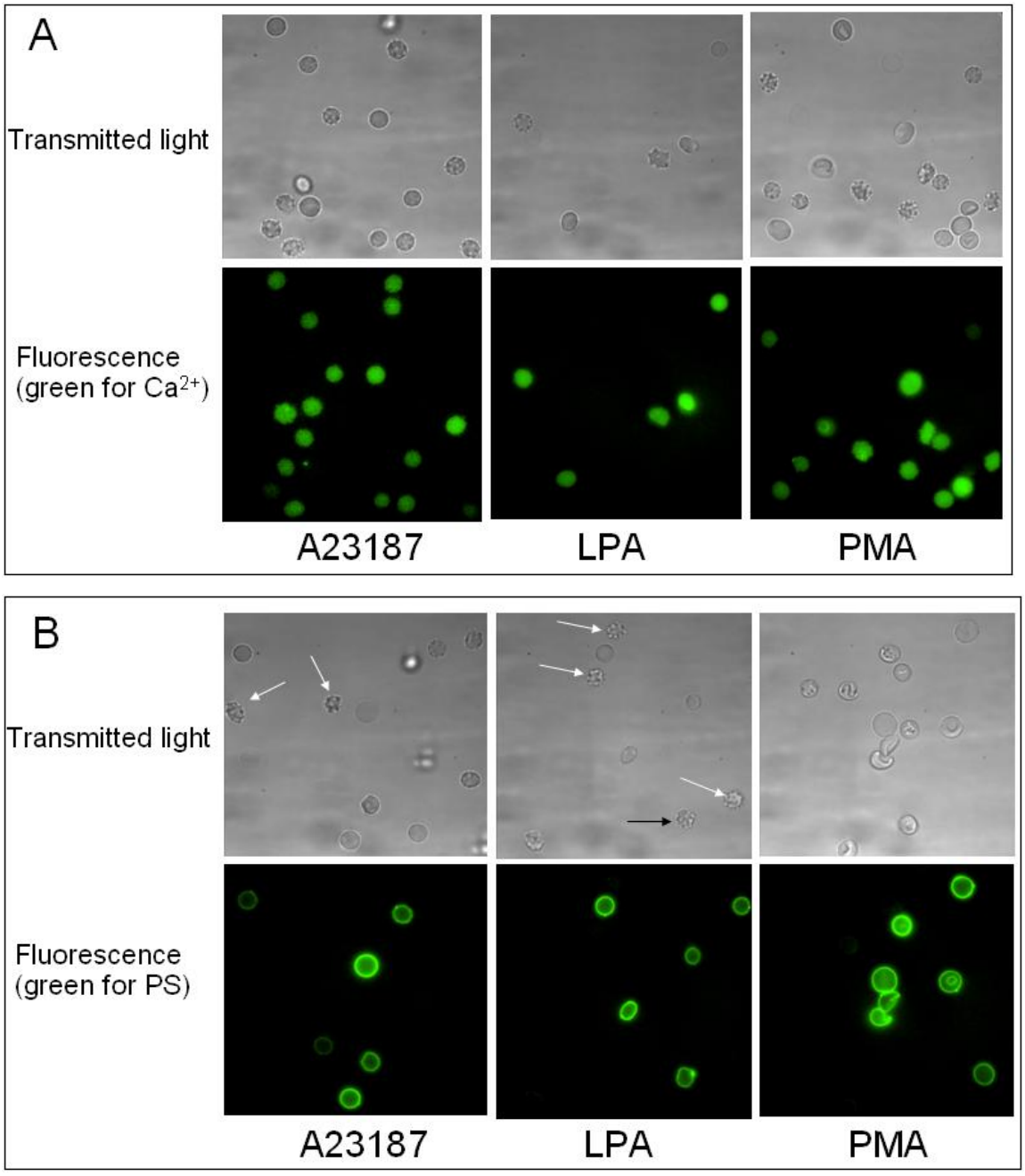

Figure 6: Transmitted light (up) and the corresponding fluorescence (down) images of RBCs showing intracellular Ca^{2+} content (detected using fluo-4) (A) and PS exposure (detected using annexin V-FITC) (B). In A can be observed that the shape of the RBCs seems not to play a role in the Ca^{2+} uptake of the RBCs. Contrarily, in B can be observed that the shape of the RBCs are important for the PS exposure. Most of the cells showing PS exposure are discocytes or stomatocytes. Most echynocytes (indicated with arrows) are not showing PS exposure.

Using these solutions we were able to transform RBCs predominantly into stomatocytes or echinocytes. Transmitted light images of these RBCs on the microscope confirmed the RBC shape transformation (data not shown). Control experiments have been carried out to show that mostly discocytes exist in HPS solution. The Ca^{2+} uptake and the PS exposure of the RBCs were then stimulated with LPA and detected with double labelling (x-rhod-1 was used for Ca^{2+} and annexin V-FITC was used for PS). Kinetic measurements have been performed using flow cytometry. The obtained results are shown in Figure 7.

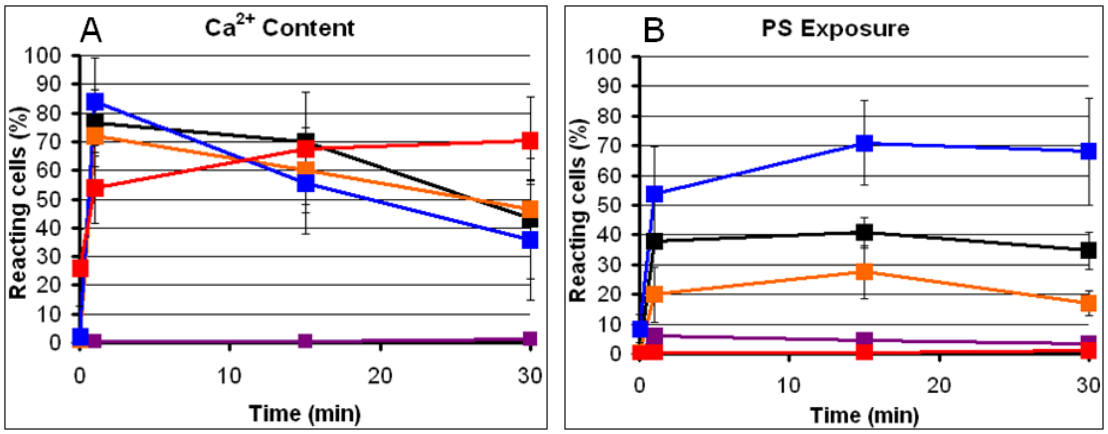

Figure 7: Double labelling measurements of intracellular Ca^{2+} content (A) and PS exposure (B) detected with x-rhod-1 and annexin V-FITC, respectively, of human RBCs using flow cytometry. Different solutions to induce cell shape transformation have been used. Normal HPS solution with predominantly discocytes (black); predominantly echinocytes: Low ionic strength solution + 10 µM DIDS, (red); HPS + 10 µM DIDS (orange); predominantly stomatocytes or discocytes: Low ionic strength solution (blue); HPS pH 5.6 (violett). Composition of the solutions: see text.

It can be seen in Figure 7 A that there is no clear correlation between cells shape and increased intracellular Ca^{2+} content. There is a slight, but not significant difference in the percentage of RBCs with increased intracellular Ca^{2+} content after 30 min activation with LPA in the solution with predominantly echinocytes (red curve). Interestingly, for the PS exposure the situation is different (Figure 7 B): echinocytes show significantly less PS exposure while discocytes or stomatocytes show higher values of the percentage of RBCs with PS exposure. This result suggests that the shape of the RBCs plays a substantial role in the PS exposure and maybe even of importance for the clearance of the RBCs from the blood stream. This is in accordance with results discussed by Sosale et al. [125].

5. References

1. Moyes CD, Schulte PM.: Tierphysiologie. (Original titel: Principles of Animal Physiology, translated by Niehaus M and Vogel S), ed 1, Munich, Pearson, 2008.

2. Campbell N, Reece JB, Urry LA, Cain ML, Wassermann SA, Minorsky PV, Jackson RB: Biology, ed 9, Boston, Pearson, 2011.

3. Gray, H: Anatomy of the human body. Philadelphia, Lea & Febiger, 1918.

4. Richter S, Hamann J, Kummerow D, Bernhardt I: The monovalent cation „leak“ transport in human erythrocytes: an electroneutral exchange process. Biophys J 1997;73:733-745.

5. Lang F, Qadri SM: Mechanisms and significance of eryptosis, the suicidal death of erythrocytes. Blood Purif. 2012;33:125-130.

6. Silbernagel S, Despopoulus A: Taschenatlas der Physiologie. Stuttgart, Thieme. 2007;7:89.

7. Dzierzak E, Philipsen S: Erythropoiesis: Development and Differentiation. Cold Spring Harb Perspect Med 2013;3:a011601.

8. Fried W: Erythropoietin and erythropoiesis. Experim Hematol 2009;37:1007-1015.

9. Haest, CWM: Distribution and movement of membrane lipids. In: Red cell membrane transport in health and disease (eds. Bernhardt I, Elorry JC), ed 1, Berlin, Springer-Verlag, 2003, pp. 1-25.

10. Verkleij AJ, Zwaal RF, Roelofsen B, Comfurius P, Kastelijn D, van Deenen LL: The asymmetric distribution of phospholipids in the human red cell membrane. A combined study using phospholipases and freeze-etch electron microscopy. Biochim Biophys Acta 1973;323:178-193.

11. Devaux PF, Herrmann A, Ohlwein N, Kozlov MM: How lipid flippases can modulate membrane structure. Biochim Biophys Acta 2006;1778:1591-1600.

12. Bevers EM, Comfurius P, Dekkers DW, Zwaal RF: Lipid translocation across the plasma membrane of mammalian cells. Biochim Biophys Acta 1999;1439:317-330.

13. Zwaal RF, Comfurius P, Bevers EM: Surface exposure of phosphatidylserine in pathological cells. Cel Mol Life Sci 2005;6:971-988.

14. Perez C, Gerber S, Boilevin J, Bucher M, Darbre T, Aebi M, Reymond JL, Locher KP: Structure and mechanism of an active lipid-linked oligosaccharide flippase. Nature 2015;524:433-438.

15. Dekkers DW, Comfurios P, van Gool RG, Bevers EM, Zwaal RF: Multidrug resistance protein 1 regulates lipid asymmetry in erythrocyte membranes. Biochem J 2000;350:531-535.

16. Lang KS, Lang PA, Bauer C, Duranton C, Wieder T, Huber SM, Lang F: Mechanisms of suicidal erythrocyte death. Cell Physiol Biochem 2005;15:195-202.

17. De Jong K, Rettig MP, Low PS, Kuypers FA: Protein kinase C activation induces Phosphatidylserine exposure on red blood cells. Biochemistry 2002;41:12562-12567.

18. Woon LA, Holland JW, Kable EP, Roufogalis BD: Ca^{2+} sensitivity of phospholipid scrambling in human red cell ghosts. Cell Calcium 1999;25:313-320.

19. Dekkers DW, Comfurius P, Bevers EM, Zwaal RF: Comparison between Ca^{2+}-induced scrambling of various fluorescently labelled lipid analogues in red blood cells. Biochem J 2002;362:741-747.

20. Herrmann A, Devaux PF: Alteration of the aminophospholipid translocase activity during in vivo and artificial aging of human erythrocytes. Biochim Biophys Acta 1990;1027:41-6.

21. Cribier S, Sainte-Marie J, Devaux PF: Quantitative comparison between aminophospholipid translocase activity in human erythrocytes and in K562 cells. Biochim Biophys Acta 1993;1148:85-90.

22. Bevers EM, Comfurius P, Zwaal, RF: Changes in membrane phospholipid distribution during platelet activation. Biochim Biophys Acta 1983;736:57-66.

23. Luxembourg B, Krause M, Lindhoff-Last E: Basiswissen Gerinnungslabor – Disorders of Blood Clotting. Dtsch Arztbl 2007;104:A-1489/B-1320/C-1260.

24. Brunner JD, Lim NK, Schenck S, Duerst A, Dutzler R: X-ray structure of a calcium-activated TMEM16 lipid scramblase. Nature 2014;516:207-212.

25. Barber LA, Palascak MB, Joiner CH, Franco RS: Aminophospholipd translocase and phospholipid scramblase activities in sickle erythrocyte subpopulations. Br J Haematol 2009;146:447-55.

26. Bernhardt I: Biomembranen – Wächter des zellulären Grenzverkehrs. Von Pumpen, Carriern und Kanälen. Biol in unserer Zeit, 2007;37:310-319.

27. Gardos G: The function of calcium in the potassium permeability of human erythrocytes. Biochim Biophys Acta 1958; 30: 653–654.

28. Christophersen P, Bennekou P: Evidence for a voltage-gated, non-selective cation channel in the human red cell membrane. Biochim Biophys Acta 1991;1065:103-106.

29. Bennekou P. The voltage-gated non-selective cation channel from human red cells is sensitive to acetylcholine. Biochim Biophys Acta 1993;1147:165-167.

30. Kaestner L, Bollensdorff C, Bernhardt I: Non-selective voltage-activated cation channel in the human red blood cell membrane. Biochim Biophys Acta 1999;1417:9-15.

31. Kaestner L, Christophersen P, Bernhardt I, Bennekou P: The non-selective voltage-activated cation channel in the human red blood cell membrane: Reconciliation between two conflicting reports and further characterization. Bioelectrochemistry 2000;52:117-125.

32. Grygorczyk R, Scwarz W: Properties of the Ca^{2+}-activated K^{+} conductance of human red cells as revealed by the patch-clamp technique. Cell Calcium 1983;4:499-510.

33. Kaestner L: Cation channels in erythrocytes – Historical and future perspective. Open Biol J 2011;4:27-34.

34. Li Q, Jungmann V, Kiyatkin A, Low PS: Prostaglandin E2 stimulates a Ca^{2+}-dependent K^{+} channel in human erythrocytes and alters cell volume and filterability. J Biol Chem 1996;271:18651-18656.

35. Kaestner L, Tabellion W, Lipp P, Bernhardt I: Prostaglandin E2 activates channel-mediated calcium entry in human erythrocytes: an indicator for a blood clot formation supporting process. Thromb Haemost 2004;92:1269-1272.

36. Föller M, Kasinathan RS, Koka S, Lang C, Shumilina E, Birnbaumer L, Lang F, Huber SM: TRPC6 contributes to the Ca(2+) leak of human erythrocytes. Cell Physiol Biochem 2008;21:183-192.

37. Bogdanova A, Makhro A, Goede J, Wang J, Boldyrev A, Gassmann M, Kaestner L: NMDA receptors in mammalian erythrocytes. Clin Biochem 2009;42:1858-1859.

38. Makhro A, Wang J, Vogel J, Boldyrev AA, Gassmann M, Kaestner L, Bogdanova A: Functional NMDA receptors in rat erythrocytes. Am J Physiol Cell Physiol 2010;299:1571-1573.

39. Andrews DA, Yang L, Low PS: Phorbol ester stimulates a protein kinase C-mediated agatoxin-TK-sensitive calcium permeability pathway in human red blood cells. Blood 2002;100:3392-3399.

40. Wagner-Britz L, Wang J, Kaestner L, Bernhardt I: Protein kinase Cα and P-type Ca^{2+} channel $Ca_V2.1$ in red blood cell calcium signalling. Cell Physiol Biochem 2013;31:883-891.

41. Thomas SL, Bouyer G, Cueff A, Egée S, Glogowska E, Ollivaux C: Ion channels in human red blood cell membrane: actors or relics? Blood Cells Mol Dis 2011;46:261-265.

42. Horne MK 3rd, Cullinane AM, Merryman PK, Hoddeson EK: The effect of red blood cells on thrombin generation. Br J Haematol 2006;133:403-8.

43. Wautier JL, Wautier MP: Molecular basis of erythrocyte adhesion to endothelial cells in diseases. Clin Hemorheol Microcirc 2013;53:11-21.

44. Wautier JL, Wautier MP, Schmidt AM, Anderson GM, Hori O, Zoukorian C, Capron L, Chappey O, Yan SD, Brett J: Advanced glycation end products (AGEs) on the surface of diabetic erythrocytes bind to the vessel wall via a specific receptor inducing oxidant stress in the vasculature: a link between surface-associated AGEs and diabetic complications. Proc Natl Acad Sci USA 1994;91:7742-6.

45. Stewart GW, Amess JA, Eber SW, Kingswood C, Lane PA, Smith BD, Mentzer WC: Thrombo-embolic disease after splenectomy for hereditary stomatocytosis. Br J Haematol 1996;93:303-10.

46. Wick TM, Eckman JR: Molecular basis of sickle cell-endothelial cell interactions. Curr Opin Hematol 1996;3:118-24.

47. Cines DB, Pollak ES, Buck CA, Loscalzo J, Zimmerman GA, McEver RP, Pober JS, Wick TM, Konkle BA, Schwartz BS, Barnathan ES, McCrae KR, Hug BA, Schmidt AM,

Stern DM: Endothelial cells in physiology and in the pathophysiology of vascular disorders. Blood 1998;91:35527-35561.

48. Hellem, AJ: The Adhesiveness of Human Blood Platelets in Vitro. Scand J Clin Lab Invest 1960;12:1–117.

49. Andrews D, Low PS: Role of red blood cells in thrombosis. Curr Opin Hematol 1999;6:76-82.

50. Whelihan, MF, Zachary V, Orfeo T, Mann KG: Prothrombin activation in blood coagulation: the erythrocyte contribution to thrombin generation. Blood 2013;120:3837-3845.

51. Chung, SM, Bae ON, Lim KM, Noh JY, Lee MY, Jung YS, Chung JH: Lysophosphatidic acid induces thrombogenic activity through phosphatidylserine exposure and procoagulant microvisicle generation in human erythrocytes. Arterioscler Thromb Vasc Biol 2007;27:414-21.

52. Kaestner L, Steffen P, Nguyen DB, Wang J, Wagner-Britz L, Jung A, Wagner C, Bernhardt I: Lysophosphatidic acid induced red blood cell aggregation in vitro. Bioelectrochemistry 2012;87:89-95.

53. Heemskerk JW, Bevers EM, Lindhout T: Platelet activation and blood coagulation. Thromb Haemost 2002;88:186-93.

54. Boas FE, Forman L, Beutler E: Phosphatidylserine exposure and red cell viability in red cell aging and in hemolytic anemia. Proc Natl Acad Sci USA 1998;95:3077-81.

55. Fadok VA, Bratton DL, Rose DM, Pearson A, Ezekewitz RA, Henson PM: A receptor for phosphatidylserine-specific clearance of apoptotic cells. Nature 2000;405: 85-90.

56. McEvoy L, Williamson P, Schlegel RA: Membrane phospholipid asymmetry as a determinant of erythrocyte recognition by macrophages. Proc Natl Acad Sci 1986;83: 3311-3315.

57. Maher AD, Kuchel PW. The Gardos channel: A review of the Ca^{2+}-activated K^{+} channel in human erythrocytes. Int. J. Biochem. Cell. Biol. 2003; 35: 1182-97.

58. Steffen P, Jung A, Nguyen DB, Müller T, Bernhardt I, Kaestner L, Wagner C: Stimulation of human red blood cells leads to Ca^{2+}-mediated intercellular adhesion. Cell Calcium 2011;50:54-61.

59. Closse C, Dachary-Progent J, Boisseau MR: Phosphatidylserine-related adhesion of human erythrocytes to vascular endothelium. Br J Haematol 1999;107:300-02.

60. Tiffert T., Bookchin RM, Lew VL: Calcium homeostasis in normal and abnormal human red cells. In: Red cell membrane transport in health and disease; Bernhardt I, Ellory JC. Eds. Springer Verlag: Heidelberg, Germany, 2003; pp.373-405.

61. de Jong K, Larkin SK, Styles LA, Bookchin RM, Kuypers FA: Characterization of the phosphatidylserine-exposing subpopulation of sickle cells. Blood 2001;98:860-7.

62. Sherman IW, Prudhomme J, Tait JF: Altered membrane phospholipid asymmetry in plasmodium falciparum-infected erythrocytes. Parasitol. Today 1997;13:242-3.

63. Wali RK, Jaffe S, Kumar D, Kalra VK: Alterations in organization of phospholipids in erythrocytes as factor in adherence to endothelial cells in diabetes mellitus. Diabetes 1988;37:104-111.

64. Bridge KR, Pearson HA: Anemias and other red cell disorders. Mc Graw Hill, 2008.

65. Setty BN, Kulkarni S, Stuart MJ: Role of erythrocyte phosphatidylserine in sickle red cell-endothelial adhesion. Blood 2002;99:1564-1571.

66. Nguyen DB, Thuy Ly TB, Wesseling MC, Hittinger M, Torge A, Devitt A, Perrie Y, Bernhardt I: Characterization of microvesicles released from human red blood cells. Cell Physiol Biochem 2016;38:1085-1099.

67. Akers JC, Gonda D, Kim R, Carter BS, Chen CC: Biogenesis of extracellular vesicles (EV): exosomes, microvesicles, retrovirus-like vesicles, and apoptotic bodies. J Neuro Oncol 2013;113:1-11.

68. Freikman I, Fibach E: Distribution and shedding of the membrane phosphatidylserine during maturation and aging of erythroid cells. Biochim Biophys Acta 2011;1808:2773-2780.

69. Johnstone RM, Adam M, Hammond JR, Orr L, Turbide C: Vesicle formation during reticulocyte maturation. Association of plasma membrane activities with released vesicles (exosomes). J Biol Chem 1987;262:9412- 9420.

70. Simons M, Raposo G: Exosomes-vesicular carriers for intercellular communication. Curr Opin Cell Biol 2009;21:575-581.

71. Thery C, Boussac M, Veron P, Ricciardi-Castagnoli P, Raposo G, Garin J, Amigorena S: Proteomic analysis of dendritic cell-derived exosomes: a secreted subcellular compartment distinct from apoptotic vesicles. J Immunol 2001;166:7309-7318.

72. Raposo G, Stoorvogel W: Extracellular vesicles: exosomes, microvesicles, and friends, J Cell Biol 2013;200:373-383.

73. Thery C, Ostrowski M, Segura E: Membrane vesicles as conveyors of immune responses. Nat Rev Immunol 2009;9:581-593.

74. Inal JM, Kosgodage U, Azam S, Stratton D, Antwi-Baffour S, Lange S: Blood/plasma secretome and microvesicles. Biochim Biophys Acta 2013;1834:2317-2325.

75. Muralidharan-Chari V, Clancy JW, Sedgwick A, D'Souza-Schorey C: Microvesicles: mediators of extracellular communication during cancer progression. J Cell Sci 2010;123:1603-1611.

76. Tissot J.-D, Canellini G, Rubin O, Angelillo-Scherrer A, Delobel J, Prudent M, Lion N: Blood microvesicles: From proteomics to physiology. Translat Proteom 2013;1:38-52.

77. Allan D, Billah MM, Finean JB, Michell RH: Release of diacylglycerol-enriched vesicles from erythrocytes with increased intracellular (Ca^{2+}). Nature 1976;261:58-60.

78. Allan D, Hagelberg C, Kallen KJ, Haest CW: Echinocytosis and microvesiculation of human erythrocytes induced by insertion of merocyanine 540 into the outer membrane leaflet. Biochim Biophys Acta 1989;986:115-122.

79. Allan D, Thomas P: Ca^{2+}-induced biochemical changes in human erythrocytes and their relation to microvesiculation. J BioChem 1981;198:433-440.

80. Allan D, Thomas P, Limbrick AR: The isolation and characterization of 60 nm vesicles ('nanovesicles') produced during ionophore A23187-induced budding of human erythrocytes. J Bio Chem 1980;188:881- 887.

81. Minetti G, Egee S, Morsdorf D, Steffen P, Makhro A, Achilli C, Ciana A, Wang J, Bouyer G, Bernhardt I, Wagner C, Thomas S, Bogdanova A, Kaestner L: Red cell investigations: art and artefacts. Blood Rev 2013;27:91-101.

82. Lutz HU, Bogdanova A: Mechanisms tagging senescent red blood cells for clearance in healthy humans. Front Physiol 2013;4:article 387.

83. Lutz HU, Liu SC, Palek J: Release of spectrin-free vesicles from human erythrocytes during ATP depletion. I. Characterization of spectrin-free vesicles. J Cell Biol 1977;73: 548-560.

84. Alaarg A, Schiffelers RM, van Solinge WW, van Wijk R: Red blood cell vesiculation in hereditary hemolytic anemia. Front Physiol 2013;4:article 365.

85. Camus SM, De Moraes JA, Bonnin P, Abbyad P, Le Jeune S, Lionnet F, Loufrani L, Grimaud L, Lambry JC, Charue D, Kiger L, Renard JM, Larroque C, Le Clésiau H, Tedgui A, Bruneval P, Barja-Fidalgo C, Alexandrou A, Tharaux PL, Boulanger CM, Blanc-Brude OP: Circulating cell membrane microparticles transfer heme to endothelial cells and trigger vasoocclusions in sickle cell disease. Blood 2015;125:3805-3814.

86. Sheetz MP, Singer SJ: Biological membranes as bilayer couples. A molecular mechanism of drug-erythrocyte interactions. Proc Natl Acad Sci USA 1974;71:4457-4461.

87. Lang F, Gulbins E, Lerche H, Huber SM, Kempe DS, Foller M: Eryptosis, a window to systemic disease. Cell Physiol Biochem 2008;22:373-380.

88. Foller M, Huber SM, Lang F: Erythrocyte programmed cell death, IUBMB Life 2008;60:661-668.

89. Nguyen DB, Wagner-Britz L, Maia S, Steffen P, Wagner C, Kaestner L, Bernhardt I: Regulation of Phosphatidylserine Exposure in Red Blood Cells, Cell Physiol Biochem 2011;28:847-856.

90. Frasch SC, Henson PM, Kailey JM, Richter DA, Janes MS, Fadok VA, Bratton DL: Regulation of phospholipid scramblase activity during apoptosis and cell activation by protein kinase C delta. J BiolChem 2000;275:23065-23073.

91. Torr EE, Gardner DH, Thomas L, GoodallDM, Bielemeier A, Willetts R, Griffiths HR, Marshall LJ, Devitt A: Apoptotic cell-derived ICAM-3 promotes both macrophage chemoattraction to and tethering of apoptotic cells. Cell Death Differ 2012;19:671-679.

92. Klarl BA, Lang PA, Kempe DS, Niemoeller OM, Akel A, Sobiesiak M, Eisele K, Podolski M, Huber SM, Wieder T, Lang F: Protein kinase C mediates erythrocyte

"programmed cell death" following glucose depletion. Am J Physiol Cell Physiol. 2006;290:C244-253.

93. Cohen CM, Foley SF: Phorbol ester- and Ca^{2+}-dependent phosphorylation of human red cell membrane skeletal proteins. J Biol Chem 1986;261:7701–7709.

94. Raval PJ, Allan D: The effects of phorbol ester, diacylglycerol, phospholipase C and Ca^{2+} ionophore on protein phosphorylation in human and sheep erythrocytes. Biochem J 1985;231:43-7.

95. Deuticke B: Membrane lipids and proteins as a basis of red cell shape and its alterations. In: Red cell membrane transport in health and disease; Bernhardt I, Ellory JC. Eds. Springer Verlag: Berlin, 2003, pp. 27-60.

96. Gedde MM, Davies DK, Huestis WH: Cytoplasmic pH and human erythrocyte shape. Biophys J 1997;72:1234-1246.

97. Rasia M, Bollini A: Red blood cell shape as a function of medium's ionic strength and pH. Biochim Biophys Acta 1998;1372:198-204.

98. Gimsa J, Ried C: Do band 3 protein conformational changes mediate shape changes of human erythrocytes? Mol Membr Biol 1995;12:247-254.

99. Deuticke B: Transformation and restoration of biconcave shape of human erythrocytes induced by amphiphilic agents and changes of ionic environment. Biochim Biophys Acta 1968;163:494-500.

100. Lim GHW, Wortis M, Mukhopadhyay R: Somatocyte-discocyte-echinocyte sequence of the human red blood cell: Evidence for the bilayer-couple hypothesis from membrane mechanics. Proc Natl Acad Sci USA 2002;99:16766-16769.

101. Wesseling MC, Wagner-Britz L, Boukhdoud F, Asanidze S, Nguyen DB, Kaestner L, Bernhardt I: Measurements of intracellular Ca^{2+} content and phosphatidylserine

exposure in human red blood cells: Methodological issues. Cell Physiol Biochem 2016b;38:2414-2425.

102. Kaestner L: Channelizing the red blood cell: molecular biology competes with patch-clamp. Front Mol Biosci 2015;2:46.

103. Haugeland RP: Handbook of fluorescent probes and research products, ed 9. Molecular Probes Inc, 2002.

104. Lipp P, Kaestner L: Detecting calcium in cardiac muscle: fluorescence to dye for. Am J Physiol Heart Circ Physiol 2014;307:H1687–1690.

105. Wang J, Wagner-Britz L, Bogdanova A, Ruppenthal S, Wiesen K, Kaiser E, Tian Q, Krause E, Bernhardt I, Lipp P, Philipp SE, Kaestner L: Morphologically homogeneous red blood cells present a heterogeneous response to hormonal stimulation. PLoS ONE 2013;8:e67697.

106. Bogdanova A, Makhro A, Wang J, Lipp P, Kaestner L: Calcium in red blood cells - a perilous balance. Int J Mol Sci 2013;14:9848–9872.

107. Weiss E, Cytlak UM, Rees DC, Osei A, Gibson JS: Deoxygenation-induced and Ca^{2+} dependent phosphatidylserine externalisation in red blood cells from normal individuals and sickle cell patients. Cell Calcium 2012;51:51–56.

108. Widengren J, Schwille P: Characterization of photoinduced isomerization and back-isomerization of the cyanine dye Cy5 by fluorescence correlation spectroscopy. J Phys Chem 2000;104:6416-6428.

109. Zanetti-Domingues LC, Tynan CJ, Rolfe DJ, Clarke DT, Martin-Fernandez M: Hydrophobic fluorescent probes introduce artifacts into single molecule tracking experiments due to non-specific binding. PLoS ONE 2013;8:e74200.

110. Tiffert T, García-Sancho J, Lew VL: Irreversible ATP depletion caused by low concentrations of formaldehyde and of calcium-chelator esters in intact human red cells. Biochim Biophys Acta 1984;773:143–156.

111. García-Sancho J: Pyruvate prevents the ATP depletion caused by formaldehyde or calcium-chelator esters in the human red cell. Biochim Biophys Acta 1985;813:148–150.

112. Martens J, Wesseling MC, Weickert J, Bernhardt I: Robust automated image analysis of activated red blood cells. Open Biol Sci J 2016. Submitted manuscript.

113. Piomelli S, Seaman C: Mechanism of red blood cell aging: relationship of cell density and cell age. Am J Hematol 1993;42:46-52.

114. Lutz HU, Stammler P, Fasler S, Ingold M, Fehr J: Density separation of human red blood cells on self-forming Percoll gradients: correlation with cell age. Biochim Biophys Acta 1992;1116:1-10.

115. Romero PJ, Romero EA, Winkler MD: Ionic calcium content of light dense human red cells separated by Percoll density gradients. Biochim Biophys Acta 1997;1323:23-8.

116. Aiken NR, Satterlee JD, Galey WR: Measurement of intracellular Ca^{2+} in young and old human erythrocytes using F-NMR spectroscopy. Biochim Biophys Acta 1992;1136:155-60.

117. de Haro C, de Herreros AG, Ochoa S: Protein phosphorylation and translational control in reticulocytes: Activation of the heme-controlled translational inhibitor by calcium ions and phospholipid. Curr Top Cell Regul 1985;27:63-81.

118. Franco RS, Puchulu-Campanella ME, Barber LA, Palascak MB, Joiner CH, Low PS, Cohen RM: Changes in the properties of normal human red blood cells during in vivo aging. Am J Hematol 2013;88:44-51.

119. Ghashghaeinia M, Cluitmans JC, Akel A, Dreischer D, Toulany M, Köberle M, Skabytska Y, Saki M, Biedermann T, Duszenko M, Lang F, Wieder T, Bosman GJ: The impact of erythrocyte age on eryptosis. Br J Haematol 2012;157:606-14.

120. Wesseling MC, Wagner-Britz, Huppert H, Hanf B, Hertz L, Nguyen DB, Bernhardt I: Phosphatidylserine exposure in human red blood cells depending on cell age. Cell Physiol Biochem 2016a;38:1376-1390.

121. Herbert JM, Augereau JM, Gleye J, Maffrand JP: Chelerythrine is a potent and specific inhibitor of protein kinase C. Biochem Biophys Res Commun 1990;172:993-999.

122. Kobayashi E, Nakano H, Morimoto M, Tamaoki T: Calphostin C (UCN-1028C), a novel microbial compound, is a highly potent and specific inhibitor of protein kinase C. Biochem Biophys Res Commun 1989;159:548-553.

123. Bessis M: Corpuscles. Atlas of red blood cell shapes. Springer-Verlag, Berlin 1974.

124. Betz T, Bakowsky U, Müller MR, Lehr CM, Bernhardt I: Conformational change of membrane proteins leads to shape changes of red blood cells. Bioelectrochemistry 2007;70:122-126.

125. Sosale NG, Rouhiparkouhi T, Bradshaw AM, Dimova R, Lipowsky R, Discher DE: Cell rigidity and shape override CD47's "self"-signaling in phagocytosis by hyperactivating myosin-II. Blood 2015;125:542-552.

Acknowledgements

First of all, I would like to express my special gratitude to my supervisor Prof. Dr. Ingolf Bernhardt for giving me the opportunity to work in his research group. The area I was working on is a very interesting field of research and Prof. Dr. Ingolf Bernhardt provided me excellent scientific support and friendly working conditions. He kindly gave me worthfully advises and always had time for answering my questions, constructive critics and discussions.

I am also grateful to Prof. Dr. Claus Jacob for his interest in this work as well as accompanying the entire work being the co-supervisor.

My thanks go also to my colleagues in the research group: Benjamin Hanf, Claudia Hahn, Henry Huppert, Yaser Alkhaled, Lisa Wagner-Britz, Daniel Mörsdorf, Duc Bach Nguyen, Jan Martens, Sascha Herzinger, Laura Hertz, Mira Türknety, Nina Peltokangas, Rebecca Groß, Melanie Zimmer, Mariane Croyè, Yannik Müllers, Louis Lescoeur, Jean-Nicolas Zimmermann, Nagla Mohamed, Salome Asanidze, Judy Mutua, Carolin Werner, Fatima Boukhdoud. I am special grateful to Jörg Riedel for his kindness and for technical support.

I am grateful to the CNPq (program "science without boarders"), from Brazil, for granting me a Ph.D. scholarship.

Especially, I would like to give my deep thanks to my parents for educating, for unconditional support and for encouragement to finish my Ph.D. work, as well as to my brothers for his cares towards me throughout.

Finally, I would like to thank my girlfriend Jessica Zierhut for friendship and support.